THE GROWTH AND DEVELOPMENT OF THE MAJOR PELVIC GANGLION OF THE FEMALE RAT IN NORMAL AND DISEASE CONDITIONS

THESIS SUBMITTED TO THE UNIVERSITY OF LONDON

FOR THE DEGREE

Master of Philosophy

By

DEREK KEITH KAYANJA

Department of Anatomy and Developmental Biology

University College London

JUNE 1998

Acknowledgements

This thesis is dedicated to my parents Professor Frederick and Mrs Beatrice Kayanja

I thank my supervisor, Professor Giorgio Gabella, for giving me direction, for his patience and critical appraisal of my efforts.

For technical support I thank Christine Davis, Peter Trigg, and Mike Corder. Their contribution to the demystification of embedding, sectioning, and computing will not be forgotten.

Much appreciation also goes to Betty Lwanga- Kayanja, and my brothers Mark, Emmanuel and Adrian Kayanja for their continued support throughout this project.

I have been fortunate to work alongside some very pleasant people notably Masoud Alian, Musaed Al-Fayez, Abdulla Al-Dahmash and Heba Mubarak.

'Gakyali Mabaga'

ABSTRACT

The development of the pelvic ganglion was studied in female rats from birth to 90 days (adult) by electron microscopy, by morphometry on plastic sections and by histochemistry on whole-mount preparations.

The pelvic ganglion of the adult female Sprague-Dawley rat had a volume (measured by the Cavalieri method) of 210 million μm^3 and contained a total of 8185 ± 2147 neurons (counted by full reconstruction of three ganglia), which ranged in size from 1100-24500 μm^3 (average 4942). In the newborn, the pelvic ganglion had similar topographical relations with surrounding organs as in the adult, was immersed in loose connective tissue rather than possessing a proper capsule, and had a volume about one quarter that in the adult. The ganglion was made of neurons, non-neuronal cells and blood vessels but it contained notably less collagen and fewer nerve bundles than in the adult; in contrast, SIF cells were abundant. Neuronal sizes ranged from 350 to 2250 μm^3 with an average of 596. The number of neurons was not evaluated at the developmental stages, but other studies have shown that in the female rat neurons are markedly more numerous in the newborn than in the adult. Intermediate stages in ganglion volume and neuronal size growth were found at 3, 7, 14, and 30 days.

The neurons at birth were similar to those of the adult in shape; however, they lacked a glial sheath and had extensive membrane to membrane contacts with each other and with SIF cells. Only few Schwann cells were present and many nerve bundles were devoid of them. The intracellular organelles observed at birth were the same as those in the adult, but some, notably microtubules, were less abundant. Both axo-dendritic and axo-somatic synapses were observed from the time of birth.

The growth of the pelvic ganglion was also investigated in experimental conditions of polyuria. For this, Brattleboro rats, with congenital diabetes insipidus, and their control parent strain Long-Evans, were used. In the adult Brattleboro rat there was hypertrophy of pelvic ganglion neurons and of urinary bladder: bladder weight was increased 4 fold and bladder capacity 3 fold. The muscle coat was increased in extent but not in thickness over the controls, and the muscle cells much enlarged in size. Brattleboro rats studied at 14 days of age were already displaying significant enlargement of bladder and pelvic ganglion over age matched controls.

1. INTRODUCTION

1.1 AUTONOMIC NERVOUS SYSTEM

The autonomic nervous system is the part of the nervous system responsible for innervating mainly the heart, blood vessels and viscera, that is tissues not under voluntary control. Claude Bernard in the nineteenth century wrote 'nature thought it provident to remove important phenomena from the capriciousness of an ignorant will'. The term 'autonomic nervous system' was first proposed by Joseph Langley in 1898. The autonomic nervous system has a similar basic structure in all mammals, including the rat, which is the species studied in this thesis.

The peripheral autonomic nervous system of the rat, like that of other mammals, consists of an extensive array of nerves and ganglia, connected to the central nervous system on one side and the viscera on the other side via two basic pathways, sympathetic and parasympathetic.

Functionally, it consists of two motor neurons placed one after the other (in series) connected by nerves. The first lies either in the brain stem or spinal gray matter, the second is located in a ganglion which may lie next to, within or at a distance from the organ it innervates.

The autonomic nervous system receives input from the target tissue (via visceral sensory neurons) and effects changes in the target tissue via motor (or efferent) neurons. The fact that the autonomic nervous system has both afferent and efferent components was overlooked in the early studies such as those of Langley who described only the motor fibres. In addition to Langley, other researchers who contributed greatly to the understanding of the autonomic nervous system early in this century, include Otto Loewi (1921) who discovered 'Vagusstoff', later known as acetylcholine, and Walter

Cannon (1921) who discovered 'sympathin', later known as noradrenaline. The work of these three people laid the basis for Dale's distinction between cholinergic and adrenergic transmission in the autonomic nervous system.

The autonomic neurons communicate with each other via synapses (a term first suggested by Charles Sherrington in 1897 [published 1906 in the Yale University press]). The question of whether synaptic transmission is chemical or electrical was the subject of much controversy from 1897 to 1952 when crucial physiological evidence, proving by means of intracellular electrodes the existence of chemical synaptic transmission, was finally obtained. The microelectrode recording, showed that the excitatory post-synaptic potential was very much greater than could be accounted for by electrotonic transmission from neuron to neuron, and made certain that the observed amplification is mediated by a chemical step, i.e. that there is chemical synaptic transmission. At around the same time, David Robertson (1953), using the electron microscope and tissues fixed in osmium, embedded in methacrylate, and sectioned with glass knives, showed that presynaptic and post-synaptic membranes were separated by a cleft about 20 nm wide. This evidence was reviewed by Eccles (1959, 1964) who reversed his early position of support of electrical transmission. It is ironic that no sooner had the controversy been resolved in favour of chemical transmission, the first report of authentic electrical transmission in the crayfish giant fibre appeared (Furshpan and Potter, 1957).

The synapses in the autonomic nervous system of mammals are believed to be chemical in nature. In large mammals these synapses are formed mainly on dendrites and not directly on the neuronal cell body (Forehand, 1985; Purves and Lichtman, 1983). In small mammals like the mouse and the rat the picture is different, due to the fact that these animals have relatively few dendrites. In the rat pelvic ganglion the synapses are mainly axo-somatic, whereas in the rat superior cervical ganglion the

synapses are predominately axo-dendritic. In the mouse the autonomic synapses are predominantly axo-somatic.

1.1.1 Structure and Function

The autonomic nervous system contains ganglia which consist of nerve cells and satellite cells which give physical and trophic support to the nerve cells. The ganglia convey impulses originating in the brain or spinal cord to smooth muscles and glands by way of visceral or splanchnic nerves. In addition, other autonomic fibres convey impulses in the opposite direction, namely from the effector organs via white rami communicantes and dorsal root ganglia to the brain stem and spinal cord.

The autonomic ganglia are organised into groups which can be subdivided anatomically according to their location:

a) Paravertebral ganglia; these ganglia form a chain on each side of the vertebral column, and are connected to the spinal nerves via 'white' rami communicantes (these are particularly short in the rat, De Lemos and Pick, 1966).

b) Prevertebral ganglia; these ganglia lying ventral to the abdominal aorta are assembled into the abdominal plexus, which includes the celiac ganglion and superior mesenteric ganglion.

c) Paravisceral ganglia; these ganglia are located in the proximity of the viscera; the main groups are found in the pelvic plexus and the cardiac plexus.

d) Intramural ganglia; these ganglia are only seen microscopically and are located principally in the wall of the intestine and biliary tract.

e) The last group of ganglia is situated in the head and supplies principally the cranial blood vessels, eye, salivary gland, and nasal mucosa. They are part of the parasympathetic pathway of the head and neck (see section 1.1.1.2.).

Another basic distinction in the autonomic nervous system is that of a sympathetic, parasympathetic, and an enteric division.

1.1.1.1 Sympathetic system

The sympathetic division of the autonomic nervous system is that which prepares the body for emergency. It increases heart rate, causes peripheral vasoconstriction, raises blood pressure, increases glandular activity, inhibits peristalsis, closes sphincters and causes redistribution of blood from the skin and gut to the brain and skeletal muscles.

The cell bodies of the sympathetic preganglionic neurons lie in the intermediolateral gray column of the thoracic and upper lumbar spinal cord. The fibres emerge from the spinal cord within the ventral roots (T1-L2) together with somatic motor fibres and reach the paravertebral (sympathetic chains) and prevertebral ganglia.

The sympathetic neurons generally are small (in comparison with somatic neurons) and vary in shape. They have two types of processes, dendrites and axons. These processes are anatomically similar, but possess different electrophysiological and histochemical properties. In general, quantitatively there are usually more dendrites than axons. Sympathetic neurons communicate with each other via synapses, which can be located on the neuronal somata or on their dendrites.

Preganglionic sympathetic neurons are all cholinergic. Whereas post-ganglionic sympathetic neurons are predominantly noradrenergic in nature; however, a small number of them are cholinergic (Yamauchi and Lever, 1971) and several of these cholinergic neurons contain vasoactive intestinal peptide (Landis and Fredieu, 1986).

The sympathetic chains in the rat are bilaterally symmetrical structures extending from the base of the skull to the sacrum, with small horizontal nerves connecting them across the midline (Baljet and Drukker, 1980).

In the neck, the cervical sympathetic chain lies ventral to the prevertebral muscles and transverse processes, and dorsal to the vagus nerve and common carotid artery. It has two clearly defined ganglia, the superior cervical ganglion and the inferior cervical ganglia (the later is fused with the first 3 thoracic ganglia and is known as the stellate ganglion). Occasionally a middle ganglion is present (Baljet and Drukker, 1980; Hedger and Webber, 1976). The superior cervical ganglion supplies the cerebral blood vessels, the pupil, lachrymal glands and salivary glands.

In the thorax the sympathetic chain lies dorsal to the parietal pleura and consists of 10 ganglia in series, the first 3 fused with the inferior cervical ganglion and the most inferior located opposite the tenth intercostal space. The thoracic sympathetic chains give rise to the greater (or major) splanchnic nerves (right and left) each containing approximately 190,000 nerve fibres and 25,000 neurons (Isomura *et al.*, 1985). These nerves enter the abdomen by travelling between medial and lateral diaphragmatic crura and end in the abdominal plexus.

The abdominal sympathetic chains, containing 5-6 ganglia each, are embedded in the psoas muscle (and are therefore retroperitoneal) and issue the lumbar splanchnic nerves which end in the prevertebral plexus (Baljet and Drukker, 1980).

The prevertebral ganglia, make up the abdominal plexus which is a large assembly of ganglia and nerves that lie close to the abdominal aorta and its major branches. In the rat the abdominal plexus has two main parts. Firstly, the celiac plexus which is close to the celiac and superior mesenteric arteries (Gabella, 1995 b), has a more developed left side, and extends dorsally between the adrenal glands and cranial half of the kidneys to form the aorticorenal ganglion (Hamer and Santer, 1981). Secondly, the inferior mesenteric plexus which has two sides that are extensively connected and lie around the cranial portion of the inferior mesenteric artery. The inferior mesenteric ganglion (also known as the hypogastric ganglion, Langworthy 1965) is a swelling on the main nerve

trunk of the plexus, this trunk becomes the hypogastric nerve which terminates in the pelvic plexus.

There is an intermesenteric plexus between the celiac and inferior mesenteric plexuses that issues nerves to the kidneys, uterus and the ovaries or testis.

1.1.1.2 Parasympathetic system

The parasympathetic (or craniosacral) system is concerned with restoring and conserving energy. It slows heart rate, increases glandular activity, increases peristalsis and opens sphincters. Its preganglionic neuron cell bodies of the are located in the brainstem and in the sacral region of the spinal cord, while the post-ganglionic neurons which express acetylcholine as a neuro-transmitter, as a rule lie close to the viscera innervated. The preganglionic fibres are therefore relatively long and the post-ganglionic fibres short.

Axons of the cranial division emerge in the oculomotor, facial, glossopharyngeal and vagus nerves to synapse in ganglia located close to their target organs.

Parasympathetic ganglia of the head and neck include, the ciliary ganglion, composed of approximately 200 neurons in the rat (Wigston, 1983), which lies lateral to the optic nerve and is attached to the first part of the branch the oculomotor nerve for the medial rectus muscle. This ganglion supplies the ciliary muscle and iris of the eye. The otic ganglion in the rat receives preganglionic fibres via a connection with the facial nerve, and has no direct connection with the glossopharyngeal nerve (unlike in man and other mammals). The sphenopalatine ganglion, a major contributor of vasomotor fibres to cerebral blood vessels (Suzuki *et al.,* 1988; Suzuki and Hardebo, 1991), is associated with the facial nerve and issues post-ganglionic fibres to the lacrimal gland, nasal mucosa and hair follicles of the facial skin (Ehinger *et al.,* 1983; Gibbins, 1990). The

submandibular ganglion, in the rat has a total of approximately 4000 neurons (Ng *et al.*, 1992), and is formed by a group of very small ganglia situated within the submandibular gland, and in the connective tissue that invests the gland and its ducts and the lingual nerve (Snell, 1958; Lichtman, 1977). The nodose ganglion, contains approximately 6000 neurons in the rat, it is seen as a distinct swelling on the vagus nerve inferior to the jugular foramen, it forms two nerves, namely the cranial (or pharyngeal) and the superior laryngeal (Greene, 1963). Lastly, the internal carotid ganglion consists of two large groups of ganglion neurons, which lie close to each other at the junction of the internal carotid nerve and the greater superficial petrosal nerve (Suzuki *et al.*, 1988). On the basis of the histochemical features of its neurons this ganglion is considered an aberrant sympathetic ganglion (or a rostral extension of the superior cervical ganglion, Hardebo *et al.*, 1992).

In the thorax there are two main locations of parasympathetic ganglia. The first group, called the cardiac ganglia, are located subepicardially at the base of the aorta and pulmonary artery (King and Coakley, 1958). The total number of neurons found in these ganglia is approximately 4000, of which 50% are located by the cranial border of the interatrial septum, 24% dorsal to the left atrium, 23.5% dorsal to the right atrium, and 2.5% between the aorta and superior vena cava (Pardini *et al.*, 1987). The second group is located along the trachea (and main bronchi) and is called the tracheal ganglionated plexus (Baluk and Gabella, 1989).

In the abdomen the parasympathetic supply comes from two sources. Firstly, the vagus nerve that innervates the oesophagus and stomach. Secondly, from the second, third and fourth sacral segments of the spinal cord. The sacral outlet innervates the urinary bladder, rectum and reproductive organs via the pelvic nerves that end in the pelvic plexus (Langworthy, 1965; Purinton *et al.*, 1973). The largest ganglion in the

pelvic plexus is the pelvic ganglion which is a mixed ganglion containing both parasympathetic and sympathetic neurons, and is described in detail in section 1.3.

1.1.1.3 Enteric nervous system

The gastrointestinal tract is unique because as well as receiving innervation from both the parasympathetic (via vagus and pelvic nerves) and sympathetic (via the mesenteric nerves from the prevertebral ganglia) systems, it has an extensive network of nerve fibres and intramural ganglia. These ganglia function spontaneously even after denervation and are called the enteric ganglia. The enteric ganglia, unlike the superior cervical and pelvic ganglia, do not have a well defined capsule, and their thickness and shape change drastically with contraction and expansion of the wall of the gastrointestinal tract.

The enteric ganglia can be divided (based on their location) into two plexuses;

a) The myenteric plexus, which is located between the circular and longitudinal muscle layers and is therefore intramuscular, is continuous from the oesophagus to the anal canal (for review see Gabella, 1995 b). In the small intestine of the rat there are about 9400 myenteric neurons per square centimetre of serosal surface. The myenteric ganglia in the large intestine are larger and more clearly defined than those of the small intestine.

b) The submucosal plexus, which is found in the submucosa close to the luminal side of the circular muscle, is present in small and large intestine but not in the stomach and its neurons are smaller in size and less numerous than those of the myenteric plexus.

Enteric neurons, have been classified by different workers on the basis of features such as; number of processes and cell size (see review by Gabella, 1979), ultrastructure (Cook and Burnstock, 1976), electrophysiology (Wood, 1981), and neuropeptide

distribution (Furness and Costa, 1980). There are no adrenergic neurons present in the enteric nervous system. However, adrenergic fibres are seen around intramural blood vessels, within the ganglia and layers of muscle (Van Driel and Drukker, 1973). Studies done on neuropeptide distribution in the neurons of the submucosal plexus by Schultzberg *et al.,* (1980) found, 50% positive for Vasoactive Intestinal Peptide (VIP), 20% positive for substance P, and 19% positive for somatostatin.

In addition to providing innervation to the muscles of the gut wall, the enteric nervous system contains afferent neurons projecting to prevertebral ganglia (e.g. guinea pig, Kuramoto and Furness, 1989), and spinal cord (e.g. in rat, Dörffler-Melly and Neuhuber, 1988).

Input from the pelvic ganglion. The enteric nervous system of the large intestine receives its main (in the distal portion and rectum its sole) parasympathetic supply from the pelvic ganglia. The precise intestinal targets of the pelvic neurons are not known although work on dogs by Fukai and Fukuda (1984) revealed many of the target neurons as being in the myenteric plexus. Some sympathetic innervation to these regions of the gut also originates in the pelvic ganglia (Costa and Furness, 1973; Keast *et al.,* 1989).

1.1.2 Development of autonomic nervous system

The neural crest contains the precursor cells which migrate, divide and give rise to neurons and glial cells of cranial and autonomic ganglia, and enteric ganglion cells of the entire gastrointestinal tract (Van Campenhout, 1930 b; Detwiler, 1937; Muller and Ingvar, 1923; Yntema and Hammond, 1947; Nawar, 1956. [See review by Jacobson 1991]).

Sympathetic nervous system

The sympathetic neurons, originate from precursors in the neural crest at a level equivalent to somites 8-28. They migrate to the dorsolateral surface of the aorta to form a primary sympathetic chain. The majority of these sympathetic neurons then migrate laterally along segmental branches of the aorta to form the paravertebral sympathetic chain (Tello, 1925; Van Campenhout, 1931). The neurons that remain in the primary sympathetic chain, migrate ventrally and medially to form prevertebral sympathetic ganglia on the ventral aspect of the aorta.

Parasympathetic nervous system

The parasympathetic nervous system arises from two areas of the neural crest. The neurons of the cranial portion of the parasympathetic system arise from a region of the neural crest equivalent to somites 1-7, while those of the sacral portion migrate from a level of the neural crest below somite 28 (Van Campenhout, 1930 a; Le Douarin and Teillet, 1974; Le Douarin , 1982 review).

Enteric nervous system

The enteric ganglion cells and associated neuroglial cells, like those of the sympathetic and parasympathetic systems, are derived from the neural crest (Andrew, 1971). In the chick embryo the ganglion cells of the digestive tract migrate from the same neural crest levels as those of the parasympathetic system (Le Douarin and Teillet, 1973). The factors that lead to the formation of several functional classes of enteric neuron are not known. However, it has been postulated by Patterson (1978) and Gershon (1981), that these differences are due to local differences in tissue microenvironment and cellular interactions and not the level of the neural crest from which the cells are derived. The reason for this conclusion is that neural crest cells from levels that do not normally contribute to the gut (e.g. at the levels of somites 8-28) do so after transplantation to the vagal level of the neural crest.

1.1.2.1 Development of autonomic ganglia

Most of the work done on development of the autonomic nervous system has been done on avian material, and as a result there is less literature on the development of the mammalian autonomic nervous system than on the avian. Most of the work done on the development of the mammalian autonomic ganglia has centred, because of its size and accessibility, on the superior cervical ganglion (SCG) in preference to other ganglia.

In the rat, on embryonic day 12 the precursors of the cervical sympathetic ganglia form a uniform column along the dorsal surface of the aorta and start to proliferate and coalesce to form the superior cervical and stellate ganglia. By comparison, the ganglia in the thorax form on embryonic day 11. The reason for this discrepancy is that the cervical precursor cells originate from the trunk region of the neural crest and have therefore a longer migratory pathway to cover.

Sympathoblasts in the rat SCG contain catecholamines and tyrosine hydroxylase before they undergo their final mitotic division (Hall and Landis, 1991) to become sympathetic neurons. The final mitotic division occurs between embryonic days 12 and 20 (Hendry, 1977). Developing SCG neurons require the presence of target tissues (Dibner *et al.*, 1977), these target tissues provide nerve growth factor (NGF) which is essential for neuronal survival during embryonic and early post-natal development. In the mouse SCG, NGF-dependent neurons have been documented by Coughlin and Collins (1985) from embryonic day 17. NGF is retrogradely transported from peripheral tissues to the neurons via axons (Korsching and Thoenen, 1988). Treatment with exogenous NGF prevents the normal developmental neuronal cell death, as well as the increased loss of neurons that occurs when the target tissue is removed or the neurons axotomized (Levi-Montalcini and Booker, 1960; Levi-Montalcini, 1964; Hendry and Campbell, 1976; Banks and Walter, 1977; Goedert *et al.*,1978).

The sprouting of a single axon from the neurons occurs soon after the final cell division. The axons grow directly towards the region of emergence of one of the major trunks from the SCG, the speed at which these axons grow can be appreciated by the fact that some processes extend beyond the ganglion into post-ganglionic nerves as early as embryonic day 12. This early sprouting of axons enables early transport of trophic factors (NGF) from the target organ to the neuron. Preganglion axons grow into the ganglion between embryonic days 13-14 (Rubin, 1985 b).

Dendrites (many of which branch repeatedly) are seen on several ganglion neurons on embryonic day 14 (Rubin, 1985 b). Although the appearance of dendrites and preganglionic ingrowth coincide, normal dendritic structure develops even in the absence of preganglionic input (Smolen and Beaston-Wimmer, 1986; Voyvodic, 1987). At birth, rat SCG neurons have on average 2.4 primary dendrites and 1.2 secondary branches (Smolen and Beaston-Wimmer, 1986); this figure increases to 4-14 dendrites in the adult (Purves and Lichtman, 1983). Concomitant with the expansion of the dendritic arbors there is an increase in the NGF content in the target tissues (Snider, 1988).

Synapses in the rat SCG have been identified morphologically on embryonic day 14; however, a response to electrical stimulation can be elicited in the ganglion from embryonic day 13 (Rubin, 1985 c). Since the evidence of synaptic activity precedes the formation of dendrites, it can be concluded that the majority of these early synapses are axosomatic. In the rat SCG about 10% of the adult number of synapses are present at birth, and there is a very large increase in number in the first post-natal week. The adult number is present at three months (Smolen and Raisman, 1980). Trophic factors, notably NGF, play an important role in determining the number of synapses. An

increase in the level of trophic factors leads to an increase in the number of synapses (Schaffer *et al.*, 1983).

1.2 URINARY BLADDER

1.2.1 Structure and function

The function of the urinary bladder is to act as a reservoir for the storage and periodic elimination of urine produced by the kidneys. In the female rat, the bladder lies on the midline of the pelvic cavity, ventral to the uterus in its cranial two thirds, and the utero-vaginal junction and vagina in its caudal third. In the adult female Sprague -Dawley rat (one of the strains of rat studied in this thesis), Gabella and Uvelius (1990) reported the following observations. The bladder weighs on average 70 mg, has a musculature 100-120μm thick (when distended by 0.7 ml of fluid), has a greater diameter in cranio-caudal axis (~ 14 mm) than in the transverse (~ 9.5 mm) or ventro-dorsal (~ 9.0 mm) axis; therefore the ratio between greater and lesser diameter is 1.5. In the normal distended bladder both inner and outer surfaces are smooth.

In the male rat the bladder is located on the midline of the pelvic cavity with its cranial third ventral to the seminal vesicles and its caudal two thirds ventral to the rectum; its lowest third is embedded in the prostate gland. In both sexes the bladder is pierced bilaterally and obliquely along the lower third of its lateral borders by the ureters.

The bladder can be described as having the following layers; an inner mucosal layer, a middle muscular layer and an outer serosal layer. The epithelial lining of the bladder consists of transitional epithelium. When the walls of the bladder are contracted the epithelium is 6-8 cells thick and its superficial cells are rounded or even club shaped.

When the bladder is distended the epithelium is thin and the cells are stretched and flattened (Bloom and Fawcett, 1975). The lumenal surface of the epithelium, has a special cell membrane. This membrane has a unique substructure consisting of hexagonally arranged subunits (Hicks and Ketterer, 1970; Hicks, 1975) which make them a barrier preventing movement of water from urine to interstitial space. The epithelium lies on the lamina propria the two being joined by a thin basal lamina (Bloom and Fawcett, 1975), the lamina propria contains connective tissue, elastic fibre networks and sometimes lymphatic nodules.

The muscular coat of the bladder in man has three layers which intermingle at their margins and cannot be separated from each other (Bloom and Fawcett, 1975). The outer longitudinal layer is best developed on the dorsal and ventral surfaces of the bladder. The middle circular layer is the thickest layer of all. The inner layer consists of sparse longitudinal or oblique strands. In the rat, there is a large component of longitudinal muscle running from cranial to caudal pole on the ventral aspect. Along the dorsal aspect, there is a large sheet like layer of circular muscle. Along the lateral aspects and cranial pole the muscle bundles run without preferred orientation (Gabella and Uvelius, 1990).

1.2.2 Blood supply

In the rat, the blood supply to the bladder comes from branches of the superior and inferior vesical arteries. These arteries are generally branches of the common iliac artery (Baljet and Drukker, 1980). The blood vessels penetrate the muscular coat giving capillaries to the muscle, then form a plexus deep in the mucosal layer. From this plexus small arteries travel towards the epithelium. Upon reaching the epithelium, the arteries give rise to capillaries that run in grooves 3-4 μm deep and about 10 μm wide (Inoue

and Gabella, 1990) on the submucosal aspect of the epithelium, giving off branches that can be seen running between the epithelial cells.

1.2.3 Nerve supply

The bladder has both autonomic and somatic innervation. The somatic innervation is supplied by the pudendal nerve, while the autonomic innervation is from the pelvic and hypogastric nerves via the pelvic ganglion. The innervation of the bladder and other pelvic structures by the pudendal, pelvic and hypogastric nerves has been investigated by several researchers, notably Langworthy (1965) and Purinton *et al.* (1973).

1.2.3.1 Somatic nerve supply.

The Pudendal Nerve is the main somatic nerve supplying the bladder. The Pudendal nerve originates from part of the bigeminal nerve (ventral ramus of the sixth lumbar spinal nerve) and part of the ventral ramus of the first sacral nerve (Baljet and Drukker, 1980). It may also receive branches from the lumbosacral trunk near the origins of the perineal nerves.

The pudendal nerve in the rat consists of slightly more than 4000 axons of which two thirds are unmyelinated (Hulsebosch and Coggeshall, 1982), and 84% of these axons are sensory. This nerve also contains 4% post-ganglionic sympathetic fibres and 12% motor or preganglionic axons (Hulsebosch and Coggeshall, 1982). Sensations from a full urinary bladder, experienced prior to micturition, are carried by the ascending tracts located in the posterior white columns of the spinal cord (Snell 1987).

1.2.3.2 Autonomic nerve supply of the bladder

The preganglionic autonomic innervation of the rat bladder arrives in the pelvis via the pelvic and hypogastric nerves; these nerves carry fibres which synapse on neurons in the Major Pelvic Ganglion (MPG). The neurons of the MPG then send post-ganglionic

nerves to the bladder directly and via the nerve plexus in the mesometrium of the uterus. This ganglion and its branches are described in detail in section 1.3 below.

1.2.3.3 Distribution of nerve fibres in the bladder.

Several authors have shown that there are adrenergic axons in the bladder nerves, and that these nerve fibres are mainly distributed to the trigone region of the bladder. The remainder of the detrusor receives the majority of its efferent innervation from cholinergic axons (Elbadawi and Schenk, 1966; Schulman *et al.,* 1972; Raezer *et al.,* 1973; Dixon and Gosling, 1974). These findings agree with the clinical observation that generally sympathetic action causes relaxation of the bladder wall and contraction of the sphincter vesicae, and parasympathetic action causes contraction of the detrusor muscle and relaxation of the sphincter (Snell, 1987).

In the adult female rat, all the nerve fibres seen originate outside the bladder as no intramural ganglion neurons are seen (Gabella and Uvelius, 1990). However, in the new-born female rat, up to 200 neurons are seen in the wall of the bladder (Alian and Gabella, 1996), implying that some of the fibres innervating the bladder originate in intramural ganglia.

The actual innervation of the individual bladder muscle fibres, is achieved via a neuromuscular junction (region of specialized contact between axon and muscle cell). These junctions can be identified by four features (Gabella, 1995 a); firstly the axon has a varicosity packed with vesicles, secondly the axolemma is exposed by a 'window' in the Schwann cell sheath, thirdly the distance between the two membranes is between 10 and 100 nm, and lastly the intercellular gap contains no fibrils and only a single basal lamina.

1.3 MAJOR PELVIC GANGLION

In general the autonomic neurons supplying the pelvis can be distributed as follows: Firstly, in discrete ganglia with two or three accessory ganglia (e.g. rat and mouse). Secondly, along the autonomic nerves in the pelvis and near the serosal surface of the bowel and bladder (e.g. cat, dog, rabbit). Thirdly, in between the two previous sites e.g. in the male guinea pig, where the pelvic ganglia form ventral and dorsal clusters which supply the bladder and reproductive system (ventral cluster), and the distal portion of the large intestine and the rectum (dorsal cluster) (Costa and Furness, 1973). In the female, guinea pig the two clusters are not as well defined as in the male, but the majority of the ventral neurons are located along the antero-lateral walls of the vagina in the region of the cervix and are therefore paracervical.

Nomenclature

The name of this ganglion has been debated since as early as 1895 when in response to it being called the hypogastric plexus, Langley and Anderson stated "there is a certain absurdity in applying the term 'hypogastric' to a plexus in the pelvic basin".

The name of this ganglion still varies between authors. In the female rat, it is known variously as:

a)'uterine cervical' ganglion by Fleming (1928), Lehmann and Stange (1953), Baljet and Drukker (1980);

b) 'pelvic' ganglion by Langworthy (1965), Foroglou and Winckler (1973), Gabella (1990), Santer and Symons, (1993);

c) 'paracervical' ganglion by Kanerva (1971), Papka and McNeil, (1993);

d) 'major pelvic' ganglion by Purinton *et al.,* (1973).

The animal studied in this thesis is the rat, which has on each side of the pelvic cavity one main ganglion and two or three accessory ganglia. Referring to this ganglion as a plexus is not an accurate description as it implies a network of nerves without stating

that it contains neurons. I have therefore chosen the name 'major pelvic ganglion' (MPG).

The ganglion has only two nerve inputs, namely, the pelvic and hypogastric nerves (Purinton *et al.,* 1973) (the composition of these nerves is discussed in section 1.3.1 below), but has several outputs to the pelvic organs. The presence of two distinct inputs and several outputs, have long made this ganglion an ideal model for the study of ganglionic activity regulating pelvic viscera.

The MPG was described in the male by Langworthy in 1965 (after application of methylene blue), as a three dimensional structure "lying in the mesenteric fold related to the bladder, ureter, seminal vesicle, seminal duct, and rectum", and, in the female, as being finer and more gracile and smaller than in the male, lying in the mesenteric fold related to the bladder, ureter, vagina and rectum. Purinton *et al.,* (1973), reported the ganglion in the rat as being "located in the lateral ligament of the bladder lateral to the prostate in male and the vagina in female". Purinton and fellow workers also noted that the ganglion was larger and more distinct in the male rats (2 mm by 4 mm in diameter) compared to the female rats (2 mm by 2 mm in diameter). More recently the ganglion has been described in the female rat by Baljet and Drukker (1980). They described it has as a flat triangular structure, located lateral to the junction between uterus and vagina, caudal to the terminal segment of the ureter and close to the vaginal artery (or one of the vaginal arteries) branching off the internal iliac artery (this artery is sometimes referred to as the hypogastric artery Greene, 1963).

1.3.1 Preganglionic supply

The MPG, is a unique autonomic ganglion as it receives both parasympathetic and sympathetic input.

1.3.1.1 Pelvic Nerve

The pelvic nerve in the rat usually arises as a direct branch of the ventral ramus of the first sacral nerve, but sometimes it is a branch of the pudendal nerve (Baljet and Drukker, 1980). Some earlier workers described it as arising from the last lumbar (L6) and the first sacral (S1) spinal nerves (Purinton *et al.,* 1973). It usually consists of two separate bundles of nerve fibres (Baljet and Drukker, 1980), and runs along the urogenital artery (Purinton *et al.,* 1973), pelvic artery (Hulsebosch and Coggeshall, 1982) or branches of the internal iliac artery (Baljet and Drukker, 1980), mainly ventrally and reaches the dorsolateral aspect of the MPG.

The pelvic nerve has approximately 5,000 axons and is generally regarded as parasympathetic (Purinton *et al.,* 1973, Baljet and Drukker, 1980). However, it also carries post-ganglionic sympathetic fibres as well as sensory fibres (Hulsebosch and Coggeshall, 1982) to the MPG. The composition of the fibres of this nerve is: 34% sensory, 49% parasympathetic preganglionic and 17% sympathetic post-ganglionic axons. Only 12% preganglionic fibres going to the pelvic ganglion are myelinated. A few myelinated axons are present in the post-ganglionic nerves.

1.3.1.2 Hypogastric Nerve

The hypogastric nerve carries the bulk of the sympathetic input to the major pelvic ganglion. It originates, as the caudal continuation of the inferior mesenteric ganglion. This nerve is retroperitoneal and runs medial to the external iliac artery then posterior to the ureter, where it branches into the main and accessory hypogastric nerves (Gabella, 1995 b). The main branch reaches the cranial pole of the ganglion while the accessory branch travels to the uterine artery near its origin from the superior vesical artery (Baljet and Drukker, 1980).

This nerve has on average 1600 axons (Hulsebosch and Coggeshall, 1982), the majority of which are sympathetic. It has a relatively small component of sensory fibres (compared with the pudendal and pelvic nerves). The composition of the axons in this nerve is as follows: 58% sympathetic post-ganglionic, 34% sympathetic preganglionic and 8% sensory axons (Hulsebosch and Coggeshall, 1982).

1.3.1.3 Sensory projections of pelvic and hypogastric nerves.

Both the pelvic and hypogastric nerves carry sensory fibres to the lumbar and sacral primary afferent neurons, from the organs in the pelvis. The pelvic nerve was found to be 34% sensory and the hypogastric 8% sensory (Hulsebosch and Coggeshall, 1982).

Studies on the sensory fibres of the pelvic and hypogastric nerves show that many of them contain one or more peptides such as substance P (SP) and calcitonin gene-related peptide (CGRP) (Dail and Dziurzynski, 1985; Senba and Tohyama, 1989; Papka, 1990). According to Keast (1995) two types of SP and CGRP fibres are found in the rat. The first type, consists of bundles of smooth axons which appear to cross the ganglion without branching. The second type of fibres form varicose clusters around some ganglion neurons; however, no synaptic connections have as yet been seen between these fibres and ganglion neurons, although the close proximity of the varicosities (of the fibres) to the neurons suggests that synapses exist.

1.3.2 Postganglionic nerves

The ganglion issues efferent nerves to the ureters, urethra, vas deferens, seminal vesicles, prostate, vagina, cervix, bladder, uterus and the lower bowel (distal colon and rectum).

The largest trunk in the male is that innervating the penis and urethra and contains several hundred ganglion neurons (Dail *et al.*, 1989). In the female the largest branch

arising from the caudal aspect of the ganglion innervates the clitoris after giving branches to the rectum, vagina and urethra. There is extensive crossing over of fibres in the midline on the ventral surface of the cervix and vagina.

At least 8 small nerves supply the bladder divided into two groups by the ureter; those anterior to the ureter supplying the ventral aspect of the bladder, those posterior to the ureter supply the dorsal aspect of the bladder.

1.3.3 Ganglion structure

The structure of the major pelvic ganglion, is similar to that of other autonomic ganglia (with the exception of the enteric ganglia) in that it has a capsule, intraganglionic blood supply, neurons surrounded by a basal lamina and glial cells, connective tissue, and extensive neuropil (Dail *et al.*, 1975; Kanerva and Hervonen, 1976; Kawatani *et al.*, 1989; Wang *et al.*, 1990; Gabella *et al.*, 1992).

The capsule of the rat pelvic ganglion is made up of connective tissue laid down by specialized fibroblasts (Bunge *et al.*, 1989). It can be divided into three layers; a thin epineurium, a thick perineurium, and a delicate endoneurium. Occasionally the capsule sends septa between groups of neurons (Gabella *et al.*, 1992) dividing the ganglion into regions. The capsule of the major pelvic ganglion is not as thick as that found in other autonomic ganglia, e.g. the superior cervical ganglion.

In adult rats the pelvic ganglion neurons are sheathed by a capsule of glia cells whose nuclei are visible by light microscopy (Gabella *et al.*, 1992). A large range of pelvic ganglion neuron sizes are seen. Keast (1995) states that these neurons fall into two groups: those with a diameter of 40-60 μm which are noradrenergic, and those with a diameter of 15-25 μm which are non-noradrenergic. Gabella *et al* (1992) describe the neurons of adult female Sprague-Dawley has having maximal profiles ranging from

150-1250 μm^2 (corresponding to diameters of 14–40 μm). Amongst the larger pelvic ganglion neurons are neurons that possess large cytoplasmic vacuoles (Pawlikowski, 1961; Becker, 1968; Dali *et al.,* 1975; Gabella *et al.*, 1992); it is not known whether these vacuoles are fixation artifacts, an indication of degenerative change, or an indicator of high neurosecretory activity. The larger pelvic ganglion neurons may also contain two nuclei (Gabella *et al.*, 1992).

In the rat most (two thirds) of pelvic ganglion neurons have no dendrites (Foroglou and Winckler, 1973; Tabatabai *et al.,* 1986; Keast *et al.,* 1989; Rogers *et al.,*1990) and therefore resemble many parasympathetic neurons (Purves and Hume, 1981). Following retrograde filling of neurons with Lucifer yellow, it has been found that rat pelvic ganglion neurons that have dendrites have between 1-4 per cell, with an average of 1.5 (Tabatabai *et al.,* 1986). The number of dendrites present in the rat pelvic ganglion, differs from that of the rat superior cervical ganglion where cells have an average of 6.3 dendrites, studies on cat pelvic ganglion have found the neurons possess on average 6.9 dendrites (Tabatabai *et al.,* 1986).

Pelvic ganglia also contain 'small intensely fluorescent' (SIF) cells, as found in sympathetic ganglia (Becker, 1972; Kanerva and Teräväinen, 1972; Dail *et al.,* 1975; Baker *et al.,* 1977). These cells were first mentioned in the rat superior cervical ganglion (SCG) by Eränkö and Härkönen (1963); however, the term 'SIF' cells was proposed by Norberg *et al.,*(1966). SIF cells are smaller than ganglion neurons and have a diameter of 10-15 μm. They contain vesicles which store noradrenaline, or dopamine or serotonin. SIF cells are generally found in clusters varying from a few cells up to about 50 cells, at the surface of the ganglion, around blood vessels or near nerve bundles. A few of these cells possess processes (10-20 μm long) which extend into neighbouring cells or blood vessels (Becker, 1972; Dail *et al.,* 1975). However, the

functional significance of these processes is at present unclear. SIF cells are able to form synapses with other SIF cells as well as with ganglion neurons (Becker, 1972; Dail *et al.,* 1975).

1.4 BLADDER MUSCLE HYPERTROPHY.

Visceral smooth muscle increases in volume when the flow of the lumenal contents is chronically partially obstructed. Smooth muscle hypertrophy occurs in several medical conditions, for example in the bladder of men with is prostatic enlargement. Over the years experimental techniques have been developed to induce smooth muscle hypertrophy in the ureter, bladder and small intestine of laboratory animals. The amount of hypertrophy depends upon the type of experimental procedure, the species of animal, the age of the animal, and the organ being studied. In smooth muscle hypertrophy the general structure of the muscle and its relations with other tissue does not change. However, the individual muscle cells do change significantly. Work done by Gabella and Uvelius (1990), has shown that hypertrophic muscle cells have an irregular profile with deep indentations of the cell membrane and a reduction in the surface to volume ratio. The contents of the cell also show significant changes: the nucleus appears crenated, mitochondria increase in number, and the sarcoplasmic reticulum has increased spatial density.

The urinary bladder becomes enlarged and grows in weight when the organ is chronically overdistended by urine retention, typically with a partial outlet obstruction. The volume of the musculature increases (as described above), mainly due to increase in the muscle cell size. In man it is found in benign prostatic hypertrophy in aged males (Gilpin *et al.,* 1985), and it is simulated in experimental animals by a surgical reduction of the lumen of the urethra.

Concomitant with bladder muscle hypertrophy there is marked enlargement of the pelvic ganglion neurons innervating the bladder, known as neuronal hypertrophy, (Steers *et al.,* 1990, Gabella *et al.,* 1992). Similar but less intense degrees of neuronal hypertrophy in adult rats are seen in the pelvic ganglion neurons following contralateral ganglionectomy (Gabella and Uvelius, 1992) and in streptozotocin induced diabetes mellitus (Nadelhaft *et al.,* 1993).

All The experiments above give a consistent picture, i.e. distension regardless of stimulus leads to muscle hypertrophy and neuronal hypertrophy. It must, however, be pointed out that all this work was done on adult rats over relatively short periods of time.

The animals used in this work to explore the effect of polyuria from birth, are the Brattleboro rats. The Brattleboro rat is a strain of Long Evan's rats that have familial hypothalamic diabetes insipidus, and arose by spontaneous mutation. They were first reported in 1964 in laboratories in Brattleboro Vermont (Valtin and Schroeder, 1964). Diabetes insipidus leads in these animals to greatly increased urinary output, 24-hour urine flow averages about 70% of body weight (Valtin and Schroeder 1964, Valtin *et al.,* 1965).

The Brattleboro rats lack the hormone vasopressin as well as its corresponding neurophysin carrier (Pickering *et al.,* 1982). The lack of vasopressin leads to impairment of resorption of water in the distal tubuli of the kidneys, giving rise to polyuria. In the Brattleboro rat the neurons of the supraoptic and paraventricular nuclei (where the precursor for vasopressin is normally formed) are hypertrophied (Sokol and Valtin, 1982), and the cells that produce vasopressin lack normal secretory granules (Valtin *et al.,* 1978). A single base deletion (delta G) in the vasopressin gene leads to a frameshift in the vasopressin gene. The result of this is expression of a vasopressin precursor with an entirely different C-terminus, which is unable to enter the secretory

pathway, thereby preventing vasopressin biosynthesis (Sonnemans *et al.*, 1996). However, oxytocin production is not impaired in these animals.

1.5 NEURONAL COUNTING METHODS

Accurate and consistent counts of neurons are very useful in neurobiology, but they are at a premium because of the difficulty, labour and uncertainty associated with the methods available. In principle it is always possible to determine the true number of neurons by collecting all the sections and then identifying and counting every single neuron, especially when the outline of the nervous structure in question is sharp, as is usually the case with a peripheral ganglion. In practice, this approach is of little use, because the vast amount of work involved appears unjustified; however, the approach is useful, even if applied to a very limited extent, to produce an absolute value against which the accuracy of methods based on sampling can be tested. In the following thesis the results of full reconstruction of the pelvic ganglion with the counting of each and every neuron will be compared with two sampling methods: the method of sampling small areas of the ganglion to determine neuronal density and hence estimate number, and the disector method. The disector is a method for producing an unbiased estimate of the number of cells present in a structure, thus removing the need to collect serial sections from the entire structure. The basic principle of the disector method for particle number counting (neuronal cell bodies in the case of a ganglion) is to determine numbers per unit volume. This numerical density is then multiplied by the total volume of the structure giving the cell number estimation. This method was developed and first employed by Sterio (1984), discussed by Pakkenberg and Gunderson (1988) and more recently by Pover and Coggeshall (1991). The aim of this part of the thesis was to develop a sampling method for an accurate estimate of the

number of neurons in the pelvic ganglion of the rat or in similar autonomic ganglia. In order to establish the accuracy of the sampling methods used the exact number of neurons present will be established by complete reconstruction of the ganglia.

2. MATERIALS AND METHODS

2.1 ANIMALS

1) Female rats were used throughout this work.

2) The development of the pelvic ganglion and the number of neurons in mature ganglia were studied in rats of the Sprague-Dawley strain. They were obtained from the Central Unit Biological Services at University College London, where they had been bred from a strain of Sprague-Dawley originally supplied by Charles River Ltd (UK). For work on development of normal animals the following ages were used: 0 (newborn), 3, 7, 14, 30 and 90 (young adult) days.

The serial section work was carried out on 3 adult Sprague-Dawley rats of about 200 grams body weight.

3) The work on bladder hypertrophy and neuronal hypertrophy was carried out on Long-Evans non-diabetic rats (controls) and Brattleboro rats (diabetes insipidus). Both of these were obtained from Dr. Lansdown in the Department of Comparative Biology, Charing Cross Hospital, London. Two ages were studied in each group, 14 days (body weight approx. 34 grams) and 96 days (body weight approx. 200 grams).

2.2 MICROSCOPY

2.2.1 Anaesthetic

All material used in this work was obtained from recently dead or terminally anaesthetized animals. For irreversible anaesthesia, Sodium Pentobarbitone (Sagatal; Rhone Merieux Ltd. UK) was administered intra-peritoneally at a dosage of 60 mg per Kg of body weight.

2.2.2 Cannulation and Perfusion of Washing Solution

When the anaesthetic had abolished the corneal reflex and all skin pain reflexes, and respiration had ceased, the animal's chest was shaved and a V shaped incision made through the skin from xiphoid process to axilla with a scalpel. The flap of skin was reflected cranially exposing the rib cage. The rib cage was opened along the lines of the skin incision using scissors and reflected cranially and clamped to secure it in position.

The heart was clamped through its tip with a cardiac clip, and via a small incision a bulb ended cannula (zero gauge in adults and 12 gauge in young animals) was inserted into the left ventricle and up into the aortic arch. The right auricle was then cut open to allow drainage of blood and perfusing solutions. Initially the blood was washed out by transcardial perfusion carried out using manual pressure applied to a 50 ml syringe connected to the cannula via a three way tap. The perfusion fluid consisted of Krebs solution (Bülbring, 1955) composed of: 0.11 M NaCl; 6 mM KCl; 15 mM $NaHCO_3$; 2.3 mM $CaCl_2$; 1.2 mM $MgCl_2.6H_2O$; 1.2 mM $C_6H_{12}O_6$, containing sodium nitrite (0.1%) (to cause vasodilatation and counteract vasoconstriction) and heparin (1%) (to help prevent blood coagulation).

Perfusion was continued till no blood was seen in the effluent; in general this followed perfusion of 1 ml per gram body weight in the adult animals. In the newborn animals a minimum of 30 ml of perfusion fluid was used, 1 ml per gm body weight was added to this for the animals older than 1 day.

2.2.3 Perfusion Fixation

This technique was used to fix material for both light microscopy and electron microscopy.

2.2.3.1 Perfusion System

The fixative was placed in a 250 ml pyrex glass flask (with side connector for tubing) at a height of 102 cm above the operating table, connected via a 5 mm diameter tube to a three-way tap which attached to the perfusion cannula. Immediately after the washing out of the blood with Krebs solution, the three-way tap was turned to allow the fixative to flow through the cannula. The pressure developed by the perfusion system was 102 cm of water.

The animals of 14 days or younger were perfused using a 50 ml syringe with pressure applied manually.

2.2.3.2 Perfusion Fixatives

For both light and electron microscopy, fixation was achieved with a solution of 4 or 5% glutaraldehyde + 1% formaldehyde in 100 mM sodium cacodylate at room temperature and at a pH of 7.4. The volume of fixative used was 150-400 ml and the perfusion lasted 2-4 minutes.

2.2.4 Immersion Fixation

This technique was used to fix material for some of the semi-thin sections and for acetylcholinestrase histochemistry. In both cases the material was first dissected out of the animal as described in 2.2.5. For acetylcholinestrase histochemistry the tissue was

fixed in 10% buffered formalin at 5 degrees Celsius. For semi-thin sectioning the material (depending on its age) was fixed by immersion in a mixture of 3-5% glutaraldehyde and 1-2% paraformaldehyde in 100 mM Na cacodylate.

2.2.5 Dissection

The abdomen of the animal was opened by a midline incision from xiphoid process to and through the pubic symphysis; cuts were then made bilaterally from the mid-point of the first incision to the spinal column. A cut was made through the rectum 2-3 cm from the urogenital diaphragm, through the esophagus and the mesentery, and the gut was removed in one single piece. Then a deep incision was made in the midline through bladder, vagina, uterus, and rectum dividing the block of pelvic viscera into two halves.

Each of them was then removed from the animal, pinned onto a plate and put under a dissecting microscope. All the fat in the angle between the ureter, vaginal and rectal walls was removed, exposing and leaving intact the pelvic plexus. For resin embedding the ganglion was dissected out of its bed of connective tissue, pinned out on a piece of Sylgard (Dow Corning, Wiesbaden, Germany) in a known orientation and processed as described in 2.2.7.

In order to study the various nerve connections of the ganglion by the cholinesterase method the ganglion was left attached to bladder, vagina, rectum and uterus and the whole block of tissue histochemically stained.

2.2.6 Cholinesterase Histochemistry

To visualize the pelvic ganglion and its pre- and post-ganglionic nerves, the tissue was stained histochemically for the enzyme acetylcholinesterase, using the method of

Karnowski and Roots (1964) modified from Baker *et al.,* (1986). The principle of this histochemical method is the hydrolysis of acetylthiocholine (a more stable compound than acetylcholine) by acetylcholinesterase into acetic acid and thiocholine. The released thiocholine reduces ferricyanide to ferrocyanide, the latter compound being insoluble and brown coloured (due to the presence of Cu^{2+}) thus identifying the site of acetylcholinesterase (AChE) activity in the tissue.

The tissue was fixed in 10% buffered formalin for one hour (at 5 ^{o}C), then washed in Krebs solution. The tissue was left overnight at 5 ^{o}C in Krebs solution containing hyaluronidase (Sigma Ltd, UK) 0.33 mg per 100 ml (used to increase permeability of tissue) and tetra-isopropyl-pyrophosphoramide (ISO-OMPA) (Sigma Ltd, UK) at a final concentration 10^{-4} M (for inhibition of non-specific or pseudo-cholinesterase).

The tissue was then incubated with constant agitation in the acetylcholinesterase medium (65 ml 0.1M acetate buffer at pH 5.0 with 1.5% Triton X-100; 10 ml 0.15M sodium citrate; 10 ml 30 mM copper sulphate; 10 ml 5 mM potassium ferricyanide; 6.84 mg iso-OMPA; 5 ml distilled water; 50 mg acetylthiocholine iodide) for 8 to 48 hours with changes to fresh medium every 2 hours for the first 8 hours and every 8 hours thereafter. During incubation the specimens were regularly examined and dissected to increase exposure of the tissue to the incubation medium.

On completion of the incubation the tissue was washed in distilled water for 1 hour and then fixed and stored at room temperature in 10% buffered formalin, prior to mounting under glass in 70% glycerol.

2.2.7 Embedding

The dissected material obtained as described in 2.2.5 (whether for thin or semi thin sections) was stored in fresh fixative overnight, then washed in cacodylate buffer, post-fixed in 2% osmium tetroxide in cacodylate buffer for 60 minutes in the dark, washed in cacodylate buffer three times then in distilled water three times. The tissue was then block-stained with an aqueous saturated solution of uranyl acetate for 30 minutes and then washed three times in distilled water. Dehydration of the material was achieved by placing it in graded ethanols as follows (at room temperature in a fume cupboard): 10 minutes in 50% ethanol (with change to fresh ethanol after 5 minutes), 10 minutes in 70% ethanol (with change to fresh ethanol after 5 minutes and removal of pins), 10 minutes in 90% ethanol (with change to fresh ethanol after 5 minutes), 20 minutes in absolute dried ethanol (with change to fresh ethanol after 5 and 10 minutes).

After dehydration the material was placed in propylene oxide for 10 minutes (with change to fresh propylene oxide after 5 minutes). The material was then placed in a mixture of 10% resin (composition; 51 g araldite, 49 g dodecenyl succinic anhydride, 1.5 ml dibutyl phthalate and 3 ml benzyldimethylamine BDMA) and 90% propylene oxide for one hour (removing the cover of the container after 30 minutes), followed by 50% resin and 50% propylene oxide for one hour and finally left in 90% resin and 10% propylene oxide overnight at room temperature. The material was placed in 100% resin for 24 hours (change to fresh resin after 12 hours) and then placed in fresh resin in the oven at 70 ^{o}C for 3 days.

2.2.8 Microtomy

2.2.8.1 Semi-thin Sections

Semi-thin sections were cut on a Reichert OMU2 microtome. Serial sections of 1-2 μm thickness were cut with wet glass knives (a diamond knife in the case of the total reconstruction) orientated transversely to the main preganglionic trunk (pelvic nerve), starting from the region of the ganglion nearest to the bladder. The sections were floated off on water and collected with an eyelash and deposited on a drop of distilled water on glass slides.

2.2.8.2 Thin Sections

Thin sections about 100 nm thick (with pale gold interference colour) were cut on a Reichert OMU2 microtome with a wet glass knife; they were floated off on water and collected on copper grids. All sections were cut orientated transversely to the main preganglionic trunk (pelvic nerve).

2.2.9 Staining

2.2.9.1 Semi-thin Sections

The glass slides (2.2.8) where dried on a hot plate at a temperature of 55 ^{o}C; when dry the slides were stained with toluidine blue (1% aqueous solution) for 15-60 seconds (depending on type of tissue and section thickness) at 55^{o}C. Excess stain was then removed by washing the slides with 50% ethanol after which they where dried at 55 ^{o}C and then mounted in araldite under a coverslip.

2.2.9.2 Thin Sections

The copper grids were then placed section side down on 3% uranyl acetate (in 50% ethanol) for no more than 5 minutes, washed in distilled water (for 1.5 minutes), and placed for less than 2 minutes section side down in a petrie dish on lead citrate (in the presence of sodium hydroxide pellets), there after they were washed in distilled water for 4 minutes.

2.2.10 Photography

2.2.10.1 Whole-mount Preparations

The whole-mount tissue mounted on plain glass slides was photographed with a stereo dissecting microscope equipped with a fibre optic light source. Photographs of the tissue were taken with objective lens 1.6x, 2x, and 4x, using a Nikon camera loaded with Ilford HP 5 film rated at 400 ASA. The resulting negatives where printed at a magnification of 5x on Ilford multigrade photographic paper. The magnifications on the final prints were 14.4x, 18x, and 36x respectively.

2.2.10.2 Semi-thin Sections

The semi-thin sections were photographed with a Zeiss photomicroscope equipped with phase contrast optics (with an intermediate lens magnification of 1.25x and an eye piece magnification of 3.2x). Objectives of 16x, 25x and 40x were used and an Ilford PAN F film rated at 50 ASA was used. The negatives were enlarged 5x to obtain prints of a total magnification of 320x, 500x, and 800x respectively.

2.2.10.3 Thin Sections

When the grids were dry they were examined and photographed in a Philips 400 electron microscope on Kodak 3/4 inch by 4 inch EM film 4489. The film was developed with Kodak D19 for 7 minutes at 20^{o}C, fixed in Amfix black and white high speed fix for 5 minutes, then washed for 20 minutes in running water at room temperature. The resulting negatives printed on Ilford multigrade paper.

2.3 MORPHOMETRY

2.3.1 Quantitative Study

Serial sections were used in the quantitative study. In three cases the entire ganglion was cut from pelvic nerve to post-ganglionic bladder nerves. The sections were collected individually and placed on drops of water 10 to a slide.

Each series of sections comprised 1100-2000 sections, and included a portion of the pre- and post-ganglionic nerves.

2.3.2 Ganglion Size

2.3.2.1 Ganglion Length

In order to determine the length of the ganglion it was necessary to have an operational definition of the first and last sections of the ganglion. The beginning of the ganglion was defined as the first section containing no less than 20 neurons, and the end of the ganglion the last section containing no less than 20 neurons.

The length of the ganglion was therefore estimated by counting the number of sections between 'first' and 'last' section, and multiplying the number of sections by the thickness of each section in micrometres.

2.3.2.2 Average Sectional Area

In order to estimate the average sectional area of the ganglion, the area of individual serial sections cut transversely through the ganglion was measured (in μm^2) at intervals of 100 μm. The figures obtained were averaged and the resulting figure was called the average sectional area of the ganglion (μm^2).

2.3.2.3 Ganglion Volume

The ganglion volume was estimated by calculating the product of the average sectional area of the ganglion and the length of the ganglion (the so called Cavalieri method).

2.3.3 Neuronal Parameters

2.3.3.1 Neuronal Size

Neuronal size was defined as the cross sectional area of the largest sectional profile of a neuron serially sectioned (in μm^2). In order to estimate this, the neurons were individually numbered on the photographs, each being given a number that was used for all profiles of the same neuron.

The largest profile of each neuron was identified and the section in which it appeared noted; this profile together with its nucleus was then traced in pencil from the original negative, by use of a microfilm reader that projected the image onto drawing paper at a final magnification of 1750 x. Profile areas where measured with a digitising tablet connected to a personal computer.

2.3.3.2 Neuronal Volume

Neuronal volume was estimated first by using the neuronal size (μm^2) to determine the radius of the neuron. This was achieved by assuming for the sake of simplicity the neuronal profiles to be circular and applying the equation area = πr^2 . Then, from the radius the neuronal volume was calculated as $V = 4/3\pi r^3$.

2.3.3.3 Neuronal Number by Total Reconstruction

The total neuronal number in the adult female Sprague -Dawley rat pelvic ganglion was determined from three ganglia (from three different rats) which were serially sectioned through their full length, at 1 micrometre thickness.

Every fourth section was photographed and printed. Then every neuron was labeled and numbered on all the micrographs in which it appeared. (The collection of total neuronal number data was done in collaboration with Edward Bliss, a fellow research student).

2.3.3.4 Neuronal Number By Partial Reconstruction.

With the exception of the three ganglia described in the previous section and the work on the disector, the neuronal number was estimated by a method involving partial

reconstruction. In this case, from each ganglion three equidistant 'short series' of 200 μm were selected and the total number of neurons in each was counted. The profile area of the ganglion at each short series, multiplied by the thickness of the short series, gave the volume of the short series. From the number of neurons present within the short series, and the volume of the ganglion the total number of neurons per ganglion was calculated on the basis of its volume.

2.3.3.5 Neuronal Number by Disector Method.

On the sections produced for the total reconstruction (2.3.3.3), the disector method was applied (Sterio 1984). The basic principle of this method is to determine the number of particles per unit volume (numerical density); this is then multiplied by the total volume of the structure giving the cell number estimate.

A disector is a short series of sections covering a given distance ('height' of the dissector) chosen so as to be as large as possible but shorter than the diameter of the particles to be counted (in this case the neuronal diameter). The first section in the 'mini-series' is termed the 'reference' section; the last section in the is the 'look-up' section. The number of sections in between the 'reference' and 'look-up' is chosen depending on the size of the particles being counted; the number should be sufficiently small that no particle can be included in the dissector without appearing in either the 'reference' or the 'look-up' section or in both (if that were the case the particle would be missed by the count). The number of 'tops' in each dissector is counted; a 'top' being a neuronal profile that is seen in the reference section but not in the look-up section. The volume of the disector is then calculated (area of the reference section multiplied by the height of the disector). The number of tops in each disector is then divided by the volume of each disector, resulting in the average numerical density. As already

described, the final estimation of ganglion cell number is obtained by multiplying the numerical density by the total volume.

This method was applied to a selection of the same sections produced in the true number counts. Disector pairs were taken at 100μm intervals throughout the entire length of the ganglion, and the height of the dissector was 8μm.

Along with the disector pair comparisons undertaken at each of the 100μm intervals, the section area was also measured. The average of these cross-sectional areas was calculated and this multiplied by the length of the ganglion to calculate its volume.

2.3.4 Definition of Parameters

Body weight; The weight of the animal at the time of death, before the removal of any organs.

Bladder weight; The weight of the unfixed empty bladder, immediately after removal from the animal.

Kidney weight; The weight of the kidneys removed from the animal and dissected clean of any surrounding tissue. The weight is given as one figure, which is the average of the two kidneys from the particular animal.

Bladder capacity; The amount of fluid that could be put into the bladder till it was taut.

Bladder wall thickness; The thickness of the entire wall of the distended bladder from mucosal surface to serosal surface.

3. POST-NATAL DEVELOPMENT OF THE PELVIC GANGLION

3.1 GROSS ANATOMY OF POST-NATAL GANGLION (0, 7, 14 AND 90 DAYS)

The gross anatomy of the pelvic plexus in the postnatal female rat was studied using a Zeiss dissecting microscope. In order to clearly visualize the pelvic ganglion and its pre- and post-ganglionic nerves, the tissue was stained histochemically for the enzyme Acetylcholinesterase, using the method of Karnowski and Roots (1964) modified from Baker *et al.,* (1986); this method is described in detail in section 2.2.6 above.

3.1.1 Birth

The pelvic ganglion at birth was a triangular structure (figure 3.01) with each of its three borders measuring approximately 0.8 mm (800 micrometres). It was located on the lateral surface of the cranial portion of the vagina in the region of the uterine cervix as in the adult. The ganglion was embedded in connective tissue loosely attached to the muscle layer of the vaginal wall and had a well defined hole in it through which blood vessels passed (figure 3.01).

The most dorsal aspect of the ganglion was pierced by a nerve consisting of two or three well defined bundles (figure 3.01) identified as the pelvic nerve, (the main preganglionic parasympathetic nerve to the ganglion). Approximately midway along the cranial border of the ganglion a thin nerve was seen entering the ganglion and identified as the hypogastric nerve. The hypogastric nerve sometimes had a small swelling on it approximately 3 mm before it entered the ganglion this; was named the hypogastric ganglion.

The cranial border of the ganglion gave rise to three or four small nerves that ran cranially and supplied the ureter, the mesometrium of the uterus (this branch was relatively larger than in the adult), and the proximal portion of the rectum.

The caudal border of the ganglion gave rise to the largest nerve that the ganglion issued (the genital nerve) as well as other nerves of varying size. The genital nerve was approximately 0.11 mm (110 micrometres) in diameter at the point it emerged from the ganglion, and tapered to 0.05 mm (50 micrometres) before dividing into approximately 11 branches that went to supply the ventral and lateral aspects of the anal canal and the clitoris and vulva. Along its length the genital nerve gave branches to the lateral aspect of the rectum and the dorsal aspect of the vagina. The other nerves given off by the caudal border of the ganglion were: The paravaginal nerves that were small, occasionally paired and branched repeatedly to form a plexus in the outer layer of the vaginal wall, occasionally giving branches to the dorsal aspect of the urethra. And the rectal nerves which branched repeatedly upon emerging from the ganglion and supplied the rectum.

The ventral border of the ganglion gave rise to the nerves that supplied the bladder, these could be divided into three groups: the first group ran to the bladder neck and supplied the ventral portion of the bladder as in the adult; this group also supplied the area of the bladder on the opposite side of the midline. The second group passed along the ventral surface of the ureter to supply the lateral aspect of the bladder wall. The third group of nerves ran along the dorsal aspect of the ureter, the largest of these supplied the anterior aspect of the uterus; the rest of this group of nerves supply the dorsal aspect of the bladder wall. In the newborn female rat, unlike in the adult, the nerves from the ventral aspect of the ganglion supplied intramural ganglia in the wall of the bladder (figure 3.02).

3.1.2 Seven days

The pelvic ganglion at seven days was a triangular structure as at birth (figure 3.03). Its longest border was approximately 0.11 mm (1100 micrometres) long, and its shortest 0.83 mm (830 microns). It was located as at birth on the lateral surface of the cranial portion of the vagina in the region of the uterine cervix. The ganglion was embedded in connective tissue more firmly attached to the muscle layer of the vaginal wall than at birth.

The pelvic nerve made up of up to 4 separate bundles entered the ganglion at its most dorsal point. The hypogastric nerve entered the ganglion between one third and half of the way up the cranial border of the ganglion.

The cranial border of the ganglion gave rise to three or four small nerves that ran cranially travelling both above and below the ureter (figure 3.03) to supply the ureter, the mesometrium of the uterus and the proximal portion of the rectum.

The caudal border of the ganglion issued the following nerves: a) the genital nerve which was approximately 0.12 mm (120 micrometres) in diameter at the point it emerged from the ganglion; b) the paravaginal nerves which were much more developed than at birth, and the largest had a diameter of 40 micrometres at the point it emerged from the ganglion. They ran parallel to the long axis of the vagina (as at birth) and gave branches to the plexus in wall of the vagina, the anterior aspect of the rectum, and posterior aspect of the urethra; c) the rectal nerves, they were more prominent than at birth and occasionally had small ganglia along their length (figure 3.03), branched repeatedly upon emerging from the ganglion and terminated in the plexus in the wall of the rectum.

The ventral border of the ganglion gave rise to the nerves that supplied the bladder; these could be divided into three groups as at birth. The first group ran to the bladder neck and supplied the ventral portion of the bladder; this group as in the adult

occasionally had small ganglia along their length (figure 3.03). The second group passed along the ventral surface of the ureter to supply the lateral aspect of the bladder wall. The third group of nerves ran along the dorsal aspect of the ureter and supplied the dorsal aspect of the bladder wall and the ventral surface of the uterus. Nerves from the ventral aspect of the ganglion supplied intramural ganglia in the wall of the bladder as at birth but the intramural ganglia were less numerous than at birth.

3.1.3 Fourteen days

The pelvic ganglion at 14 days was a triangular structure (figure 3.04), with numerous cord like nerves emerging from it. It was located on the lateral surface of the cranial portion of the vagina in the region of the uterine cervix as in the adult. The ganglion was embedded in connective tissue attached to the muscle layer of the vaginal wall.

The pelvic nerve, the main preganglionic parasympathetic nerve to the ganglion, entered the ganglion at its dorsal pole as in earlier stages. The hypogastric nerve entered the ganglion in the middle of its cranial border; this nerve occasionally had a small swelling 1 - 2 millimetres from the body of the pelvic ganglion (figure 5.4) named the hypogastric ganglion.

The cranial border of the ganglion as in other stages gave rise to three or four nerves that ran cranially and supplied the ureter, the mesometrium of the uterus and the proximal rectum.

The caudal border of the ganglion gave rise to several nerves: a) the genital nerve; this was the largest of the nerves from this area of the ganglion and travelled caudally to innervate the vulva and clitoris, giving off small nerves to the rectum and vagina along its course; b) the paravaginal nerves; they were only slightly smaller than the genital nerve (figure 3.04), were occasionally paired, and supplied the plexus in the outer layer

of the vaginal wall (occasionally giving branches to the posterior portion of the urethra); The rectal nerves; these were smaller then the vaginal nerves and branched soon after they emerged from the ganglion and supplied the rectum.

The ventral border of the ganglion gave rise to the nerves that supplied the bladder, and these could be divided into three groups. The first group were up to 50 micrometres in diameter, ran to the bladder neck and supplied the ipsilateral portion of the ventral surface of the bladder, as well as part of the contralateral area of the bladder. The second group passed along the ventral surface of the ureter to supply the lateral aspect of the bladder wall. The third group of nerves ran along the dorsal aspect of the ureter to supply the uterus, and dorsal aspect of the bladder wall. At 14 days very few intramural ganglia were seen in the wall of the bladder compared with earlier stages.

3.1.4 Ninety days

The main component of the pelvic plexus in the young adult female Sprague-Dawley rat was a large ganglion, the major pelvic ganglion, located on the lateral surface of the cranial portion of the vagina in the region of the uterine cervix (figures 3.05 and 3.06). The ganglion was embedded in a dense, non-elastic fascia tightly attached to the muscle layer of the vaginal wall, making it difficult to dissect out.

The ganglion measured 0.75- 1.5 mm along its cranio-caudal axis, and 2-3 mm along its dorso-ventral axis. The ganglion was widest at its ventral pole and tapered to its narrowest at its dorsal pole, and therefore could be described as triangular in profile. Left and right ganglia had mirror like symmetry (figures 3.05 and 3.06).

At the dorsal end of the ganglion a nerve, the pelvic nerve (the main preganglionic parasympathetic nerve to the ganglion), consisting of two or three well defined bundles (figures 3.05 and 3.06) entered the ganglion. Approximately midway along the cranial border of the ganglion, a thin nerve was seen entering the ganglion (figures 3.05 and

3.06); this was identified as the hypogastric nerve, which arises from the inferior mesenteric ganglion and is the main preganglionic sympathetic input to the pelvic ganglion. The hypogastric nerve sometimes presented a small swelling approximately 3 mm before it entered the ganglion, and this was named the hypogastric ganglion.

The cranial border of the ganglion gave rise to three or four small nerves that ran cranially and supplied the mesometrium of the uterus, the ureter, and the proximal portion of the rectum.

The caudal border of the ganglion gave rise to many nerves of varied size, divided into groups according to the structures they innervated: rectal nerves, nerves to clitoris (genital nerve), and paravaginal nerves. The rectal nerves were the smallest of the nerves exiting the caudal border of the ganglion and ran parallel to the long axis of the rectum, and branched repeatedly. The nerve to the clitoris was the largest nerve issued by the caudal border of the ganglion, it travelled caudally along the junction of rectum and vagina, and it gave branches to the anterior surface of the rectum (figures 3.05 and 3.06), and the posterior surface of the vagina before reaching the perineum. The paravaginal nerves were issued from the most ventral portion of the caudal border of the ganglion, these nerves were numerous, small, and branched repeatedly to form a plexus in the outer layer of the vaginal wall.

The ventral border of the ganglion gave rise to the nerves to the bladder, which could be divided into three groups. The first group ran to the bladder neck and supplied the ventral portion of the bladder; this group also supplied the area of the bladder on the opposite side of the midline. The second group passed along the ventral surface of the ureter to supply the lateral aspect of the bladder wall. The third group of nerves ran along the dorsal aspect of the ureter to supply the dorsal aspect of the bladder wall (this group of nerves were less distinct than the previous two); these nerves also gave branches to the anterior aspect of the uterus. From the ventral aspect of the ganglion two

to four nerves were issued that supplied small accessory ganglia, and these accessory ganglia supplied nerves to the ventral and lateral aspects of the bladder.

3.2 HISTOLOGY OF DEVELOPING PELVIC GANGLION (BIRTH TO 90 DAYS)

The histology of the pelvic ganglion in rats from birth to 90 days was studied on semi-thin sections of plastic embedded material, examined by light microscopy (as described in sections 2.2 & 2.3).

3.2.1 At birth

The major pelvic ganglion, when sectioned on a frontal plane was a compact structure with an ovoid profile. It had a well-defined outline and an incomplete capsule. In the ganglion it was possible to recognize neurons, blood vessels and small amounts of connective tissue and neuropil (figure 3.07A)

3.2.1.1 Neurons

The ganglion neurons had a smooth surface and were mostly ovoid in sectional profile (figure 3.07B). The ganglion neurons were packed together (figure 3.07B); however, there was clear demarcation between the individual neurons. Neuronal profiles mostly were nucleated. The nucleus was relatively large, set at one side of the cell, commonly occupied more than half of the cell profile, and contained 1 or 2 nucleoli.

Non-neuronal nuclei close to the surface of the neurons were interpreted as glial cell nuclei, but details of the glial sheath were unclear by light microscopy; the glial cells were studied in detail in the transmission electron microscope (see chapter 5).

No binucleate or vacuolated neurons were seen in any of the preparations.

3.2.1.2 Size of neurons

Neuronal size, meaning the area of the largest profile of the neuron, determined by studying a series of consecutive sections through the neuron, was measured in square micrometres in 500 neurons. The size of the largest neuron was 208 μm^2, this corresponds to a diameter of approximately 16.3 micrometres. The lower end of range of neuronal sizes, though not easy to define owing to the difficulty in differentiating very small neurons and other cell types, was determined by measuring the size of the smallest cell identified as a neuron this gave a value of 50 μm^2, this value corresponds to a diameter of 8 micrometres.

The average neuronal size for the three ganglia varied from 77 μm^2 to 100 μm^2, the mean being 85.4 μm^2 (table 1).

Neuronal volume was estimated by assuming the neurons to be spherical and following the method outlined in section 2.3.3.2. The average neuronal volume for the three ganglia ranged from 508 μm^3 to 747 μm^3 the mean value for the three ganglia was 596 μm^3 (table 1).

Table 1.

Body weight, Neuronal size of Newborn Female Sprague-Dawley rats.

Animal	Body Weight (gms)	Average Neuronal size (μm^2)	Average Neuronal volume (μm^3)
S-D. 61	6.25	77.1	508.0
S-D. 62	6.74	79.6	533.1
S-D. 63	6.11	99.5	747.6
Mean	**6.37**	**85.4**	**596.0**

Graph one

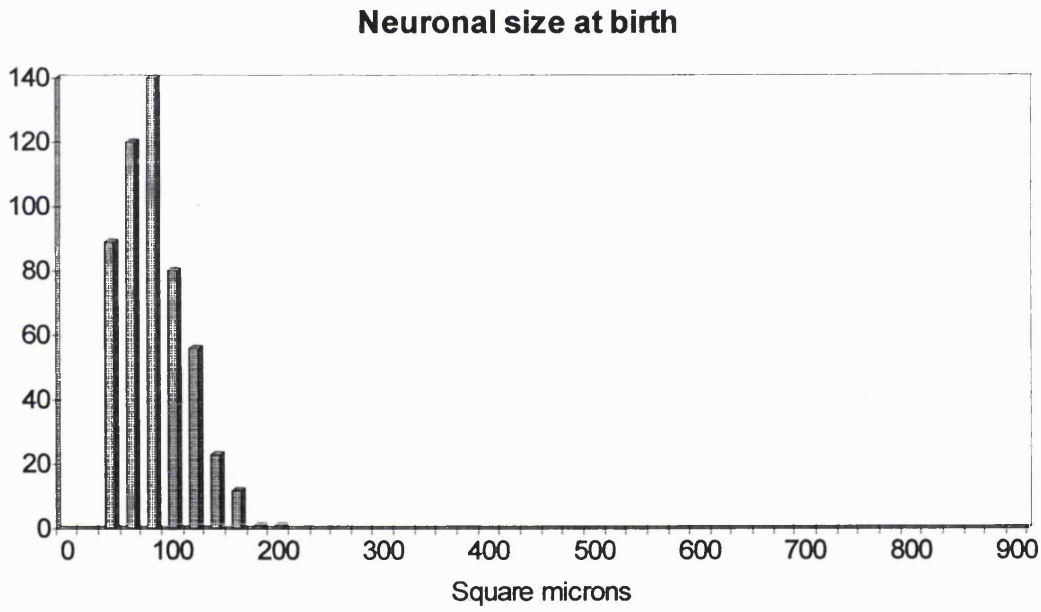

Y axis = Number of neurons (N = 500), X axis = area in square micrometres of the largest profile of each serially-sectioned neuron.

3.2.1.3 Nerve fibres

At birth no myelinated nerve fibres were seen. Structures believed to be unmyelinated nerve fibres with small groups of Schwann cell nuclei were seen, and these fibres were studied in greater detail in the electron microscope (see section 5.6).

3.2.1.4 Capsule

A thin layer of connective tissue lay around the ganglion, forming its capsule, which was, however, incomplete in some areas (figure 3.07A). Outside the capsule was a matrix of loose connective tissue, which was in direct contact with the components of the ganglion where the capsule was absent.

The capsule was formed by fibroblasts with clearly visible nuclei and their processes.

Aggregations of connective tissue and fibroblasts were seen in the ganglion between some of the neurons and partially surrounding some blood vessels, but they did not form proper laminar structures partitioning the ganglion. Occasionally these aggregations of connective tissue were continuous with the connective tissue of the capsule.

The capsule, unlike that of the adult ganglion, could not be divided into distinct layers.

3.2.1.5 Other cells

There were other cells in the ganglion; the most distinct feature of these cells was their nuclei as their cytoplasm was not clearly visible.

Other nuclei, probably of glial cells, were seen very close to the surface of the ganglion neurons; they were approximately one sixth of the size of neuronal nuclei, and generally either rod shaped or triangular. The cytoplasm surrounding these nuclei was not clear in the light microscope, but was investigated by electron microscopy (see Chapter 5).

Other nuclei probably of Schwann cells, were seen in groups of two or three in structures believed to be unmyelinated nerve fibres. These were investigated by electron microscopy (see chapter 5).

Other nuclei, probably of fibroblasts, were seen surrounded by a rim of cytoplasm with well defined processes in two locations, firstly within the ganglion between some of the neurons and around some blood vessels (figure 3.07B), and secondly around the ganglion where their cell bodies and processes made up the ganglion capsule.

Other nuclei of cells different from glia and fibroblasts and tentatively termed SIF cells, were relatively large, surrounded by well defined cell bodies with small amounts of cytoplasm, and were seen around the edge of the ganglion and around some small blood vessels. These nuclei and their cell bodies were examined by electron microscopy (see chapter 5).

Other nuclei, probably of endothelial cells, were seen in the cells forming the lining the blood vessels that ran through the ganglion.

3.2.1.6 Blood vessels

The ganglion at birth had a blood supply delivered by small intra-ganglionic blood vessels. Three types of blood vessel were clearly seen. Firstly, those that were lined only by endothelial cells which were identified as capillaries. Secondly, those with a layer of muscle cells (figure 3.07B) around the lining of endothelial cells, which were termed arterioles. Thirdly, vessels more than twice the size of capillaries, lined by endothelial cells, without a layer of muscle cells termed venules. Most of the blood vessels seen in the ganglion appeared round or oval in sectional profile, implying that they ran perpendicular to the plane of the section; blood vessels, therefore, ran along the dorso-ventral axis of the ganglion.

A branch of the obturator artery was seen, with its accompanying vein, running along the outside of the ganglion (figure 3.07B) and giving branches to the ganglion.

Red blood cells were occasionally seen inside some of the blood vessels in the ganglion (figure 3.07B).

3.2.1.7 Size of ganglion

The length of the ganglion, was determined by serially sectioning the ganglion from its dorsal to its ventral 'end'. The length along the dorso-ventral axis of the ganglion in three newborn rats was 441, 560, and 640 μm, respectively, the average being 547 μm (Table 2).

The average ganglion sectional area at birth, ranged from 65,765-110,959 μm^2 for the three animals, with an average value of 89,746μm^2 (Table 2, n=3).

The volume of the ganglion, calculated by using the Cavalieri method, mean ganglion volume of the three newborn female Sprague-Dawley ganglia was calculated as 48.3 million cubic micrometres (Table 2).

Table 2.

Body weight, and pelvic ganglion volume of newborn Sprague-Dawley rats.

Animal	Body Weight (gms)	Ganglion length (μm)	Average Ganglion cross section area (μm^2)	Ganglion volume (millions of μm^3)
S-D. 61	6.25	441	92,513	40.7
S-D. 62	6.74	560	110,959	62.0
S-D. 63	6.11	640	65,765	42.1
Mean	**6.37**	**547**	**89,746**	**48.3**

3.2.2 Three days

The structure of the major pelvic ganglion three days after birth was similar to that at birth. However; the components of the ganglion were less tightly packed together, the capsule was more complete and there was more neuropil and connective tissue.

3.2.2.1 Ganglion neurons

The ganglion neurons at three days were not as closely packed together as at birth (figure 3.08A). The ganglion neurons as at birth had a smooth surface and were ovoid in sectional profile. Most of the neurons had glial cell nuclei very closely associated with them (figure 3.08B), but details of the glial sheath were unclear by light microscopy.

The neurons had relatively more cytoplasm than those at birth, and had a large nucleus containing 1-2 nucleoli (figure 3.08B) generally located at one end of the cell. No binucleate or vacuolated neurons were seen in any of the preparations.

3.2.2.2 Size of neurons

Neuronal size was determined by measuring the largest sectional area of the neuron (as at birth). The neuronal size varied from 50 μm^2 to 368 μm^2, this corresponds to a range in diameters of 8 - 22 μm .The average neuronal size for the three ganglia had a mean value of 138 μm^2 (table 3). The neurons at three days had an average size 62% larger than at birth.

Neuronal volume was estimated as at birth. The average neuronal volume for the three ganglia ranged from 931.3 μm^3 to 1525.6 μm^3 the mean value for the three ganglia was 1233.5 μm^3 (table 3).

The neuronal volume is 107% larger than at birth ($P<0.001$).

Table 3

Body weight, Neuronal size of Three-day-old female Sprague-Dawley rats.

Animal	Animal Weight (gms)	Average Neuronal size (μm^2)	Average Neuronal volume (μm^3)
S-D. 51	10	115.4	931.3
S-D. 52	10	160.1	1525.6
S-D. 53	10	139.7	1243.5
average	**10**	**138.4**	**1233.5**

Graph Two

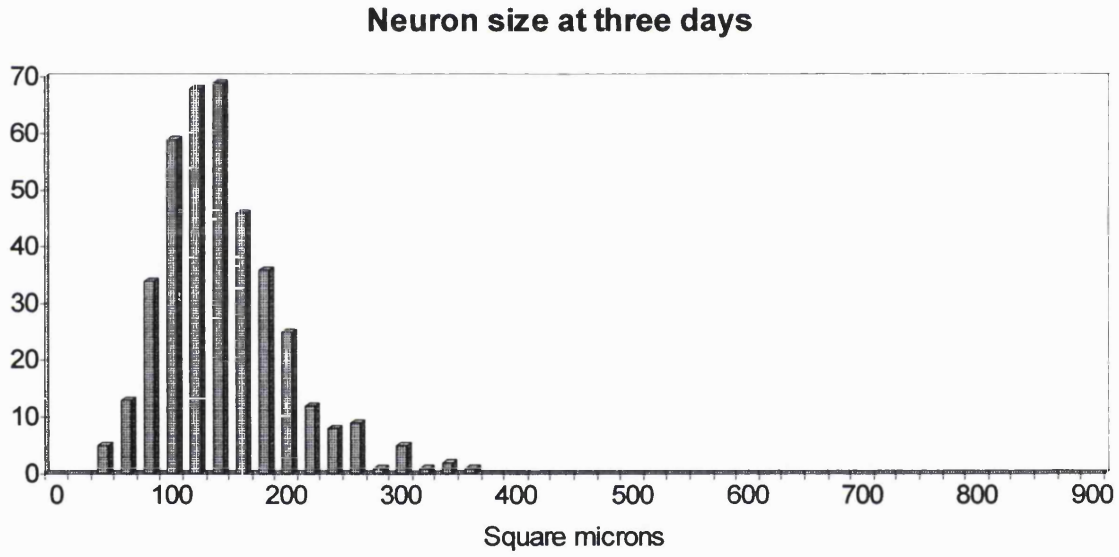

Y axis = Number of neurons (N = 500), X axis = area in square micrometres of the largest profile of each serially-sectioned neuron.

3.2.2.3 Nerve fibres

No myelinated nerve fibres were seen in the pelvic ganglion at three days, but groups of Schwann cell nuclei were seen in structures believed to be bundles of unmyelinated nerve fibres.

3.2.2.4 Capsule

The capsule was more extensive than at birth though not completely continuous (figure 3.08A). The capsule was composed of fibroblasts and their processes, cell bodies of the fibroblasts three days after birth were more flat than those at birth, and the processes of these cells were longer than those at birth (figure 3.08B). The capsule had regions where it was more than one cell thick, but could not be divided into distinct layers. The aggregations of fibroblasts and their processes could be seen within the ganglion, partially surrounding some neurons and blood vessels (as at birth), but the ganglion was not divided into distinct unit or areas.

3.2.2.5 Other cells

Glial cells were seen located very close to the surface of most ganglion neurons, by light microscopy there was no clear demarcation between the cytoplasm of the neuron and that of the glial cell.

Schwann cell nuclei were seen in small groups of 2-5 structures that were believed to be unmyelinated nerve fibres (figure 3.08B).

Fibroblasts and their processes were seen in two locations as at birth, firstly within the ganglion between some of the neurons and around blood vessels, and secondly around

the ganglion where their flattened cell bodies and processes made up the ganglion capsule (figure 3.08B).

SIF cells lay in groups of up to 15 cells near the edges of the ganglion, and in groups of up to 5 along side blood vessels.

Endothelial cells were seen lining the blood vessels that ran through the ganglion. Red blood cells were only seen within blood vessels (as at birth).

3.2.2.6 Blood vessels

The ganglion at three days, had an intra-ganglionic blood supply similar to that at birth. The blood vessels seen in the ganglion, were identified as capillaries (figure 3.08B) venules and arterioles, and ran in the same dorso-ventral plane as at birth.

3.2.2.7 Size of ganglion

The length of the ganglion at three days, was determined in the same manner as that at birth. The length along the dorso-ventral axis of the ganglion in 3 three day old rats was 565, 760, and 875 μm, respectively, the average being 733 μm (Table 4).

The average ganglion sectional area at three days, ranged from 70,804 - 117,935 μm^2 with an average value of 91,500 μm^2 (Table 4, n=3).

The volume of the ganglion was calculated by the Cavalieri method. The mean ganglion volume of the 3 three day old female Sprague-Dawley ganglia was calculated as 64.6 million cubic micrometres (Table 4). The ganglion volume is 34% larger than at birth ($P<0.001$).

Table 4

Body weight, and pelvic ganglion volume of three-day-old Sprague-Dawley rats.

Animal	Body Weight (gms)	Ganglion length (μm)	Average Ganglion cross section area (μm^2)	Ganglion volume (millions of μm^3)
S-D. 51	10	760	85,761	65.1
S-D. 52	10	565	117,935	66.7
S-D. 53	10	875	70,804	61.9
Average	**10**	**733**	**91,500**	**64.6**

3.2.3 Seven days

The major pelvic ganglion at seven days, appeared ovoid in sectional profile as at birth and at three days. The ganglion had well defined borders, with a capsule that was much more extensive than in the earlier stages, but still incomplete. The ganglion was composed of neurons, blood vessels, connective tissue, and neuropil (figure 3.09A).

3.2.3.1 Ganglion neurons

The ganglion neurons at seven days were not as tightly packed together as at birth and had a relatively large quantity of neuropil between them. The ganglion neurons (as at birth and three days) had a smooth surface and were ovoid in sectional profile. Most of the neurons had one or more glial cell nuclei very closely associated with them, but details of the glial sheath were unclear by light microscopy. The neurons had nuclei (generally containing 1-2 nucleoli per profile) generally located at one end of the cell, and relatively large amounts of cytoplasm, in this respect they differed from the neurons at birth but were very similar to those at three days. No binucleate or vacuolated neurons were seen at seven days.

3.2.3.2 Size of neurons

The neuronal size varied from $70\mu m^2$ to 449 μm^2; this corresponds to the diameter of the neurons varying from 9.5 - 24 μm. The average neuronal size for the three ganglia varied from 154 μm^2 to 179 μm^2, the mean being 164 μm^2 (table 5); the average neuronal size at seven days was twice as that at birth.

Neuronal volume was estimated using the same technique as in the earlier stages. The average neuronal volume for the three ganglia ranged from 1441.2 μm^3 to 1802.6 μm^3

the mean value for the three ganglia was 1582.3 μm^3 (table 5). The volume of the neurons had increased by 165% from birth ($P<0.001$).

Table 5

Body weight, Neuronal size of Seven-day-old female Sprague-Dawley rats.

Animal	Body Weight (gms)	Average Neuronal size (μm^2)	Average Neuronal volume (μm^3)
S-D. 41	11	158.8	1503.2
S-D. 42	12	154.1	1441.2
S-D. 43	12	179.2	1802.6
Average	**12**	**164.0**	**1582.3**

Graph Three

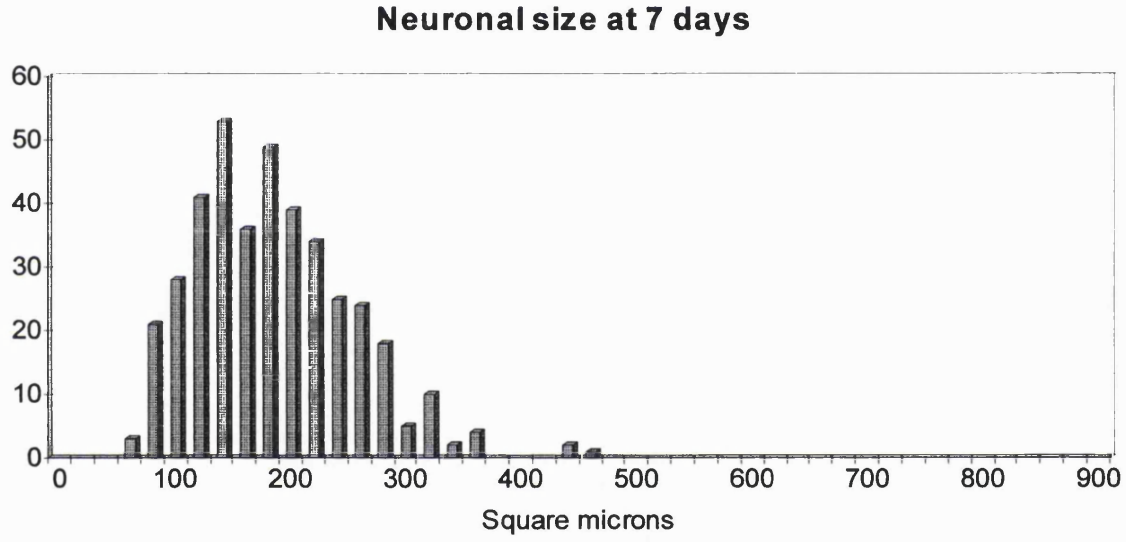

Y axis = number of neurons (N = 500), X axis = area in square micrometres of the largest profile of each serially-sectioned neuron.

3.2.3.3 Nerve fibres

No myelinated nerve fibres were seen in the pelvic ganglion at seven days, but structures believed to be small unmyelinated nerve fibres were seen in the ganglion, and unmyelinated nerves were seen running along the outside of the ganglion.

3.2.3.4 Capsule

The capsule of the pelvic ganglion at seven days was more developed than that at birth in that it has larger fibroblasts with longer processes, but it was not very different from that at three days. The capsule at seven days could be seen connected to laminar aggregations of fibroblasts within the ganglion; these laminar structures (or septa) however, did not completely enclose the groups of neurons around which they lay.

3.2.3.5 Other cells

Glial cell nuclei were seen located close to ganglion neurons as at birth and three days, and there appeared to be more neurons associated with glial cells than in any of the earlier stages.

Schwann cell nuclei were seen grouped together in structures within the ganglion thought to be unmyelinated fibres, and in small nerves that ran along side the ganglion.

Fibroblasts and their processes were seen in two locations as in the three day old ganglia, firstly within the ganglion between some of the neurons, and secondly around the ganglion where their cell bodies and processes made up the incomplete ganglion capsule.

Groups of cells termed SIF cells were seen (as at three days) around the edges of the ganglion and blood vessels.

Endothelial cells were seen lining the blood vessels that ran through the ganglion as at three days and at birth.

3.2.3.6 Blood vessels

Numerous small capillaries lined by endothelial cells and occasionally containing red blood cells, were seen running through the ganglion as at birth and three days (figure 3.09A and B). Arterioles and venules were also seen though they were less numerous than the capillaries.

3.2.3.7 Size of ganglion

The length of the ganglion at seven days was determined by the same method as at three days and birth. The length along the dorso-ventral axis of the ganglion in three, seven day old rats was 595, 660, and 820 μm, respectively, the average being 692 μm (Table 6).

The average ganglion sectional area at seven days, ranged from 105,227- 141866 μm^2 with an average value of 123,090 μm^2 (Table 6, n=3).

The volume of the ganglion was calculated by using the Cavalieri method. The mean ganglion volume of the three, seven-day-old female Sprague-Dawley ganglia was calculated as 84 million cubic micrometres (Table 6). The volume of the ganglion at seven days was 73% larger than at birth ($P<0.001$).

Table 6

Body weight, and pelvic ganglion volume of seven-day-old Sprague-Dawley rats.

Animal	Body Weight (gms)	Ganglion length (μm)	Average Ganglion cross section area (μm^2)	Ganglion volume (millions of μm^3)
S-D. 41	11	820	105,227	86.2
S-D. 42	12	660	122,176	80.6
S-D. 43	12	595	141,866	84.4
Average	**12**	**692**	**123,090**	**83.7**

3.2.4 Fourteen days

The major pelvic ganglion at fourteen days, is ovoid in shape and covered by a thin, continuous capsule. The ganglion was composed of neurons, blood vessels, connective tissue, and neuropil (figure 3.10).

3.2.4.1 Ganglion neurons

The ganglion neurons at fourteen days had a smooth surface. These neurons consistently had one or two glial cell nuclei, which were so closely placed to them, that it was not possible under the light microscope see any clear demarcation between the two cells. The glial sheath details were not seen clearly under the light microscope, but the interneuronal distances were larger than in any of the other stages so far described, and appeared to be filled with a none staining translucent material which was probably the glial sheath.

The ganglion neurons generally had a nucleus, with 1-2 nucleoli, placed towards the edge of the cell, with a thin rim of cytoplasm between it and the cell membrane. The neurons had relatively larger amounts of cytoplasm compared to nucleus than in any of

the earlier stages of development. Binucleate neurons were seen (figure 3.11) though they were not counted. No vacuolated neurons were seen.

3.2.4.2 Size of neurons

Neuronal size was determined as in earlier stages. The neuronal size varied from 87 μm^2 to 479 μm^2, corresponding to neuronal diameters varying from 10.5 - 24.6 μm, The average neuronal size for the three ganglia varied from 245 μm^2 to 267 μm^2, the mean being 256 μm^2 (table 7). The average neuronal size at 14 days is 200% larger than at birth.

Neuronal volume, the average neuronal volume for the three ganglia ranged from 2874.5 μm^3 to 3311.6 μm^3 , the mean value for the three ganglia was 3089.3 μm^3 (table 7). This volume was approximately five times the volume at birth.

Table 7

Body weight, Neuronal size of fourteen-day-old female Sprague-Dawley rats.

Animal	Animal Weight (gms)	Average Neuronal size (μm^2)	Average Neuronal volume (μm^3)
S-D. 31	36	268.6	3311.6
S-D. 32	36	244.5	2874.5
S-D. 33	36	256.1	3081.9
Average	**36**	**256.4**	**3089.3**

Graph Four

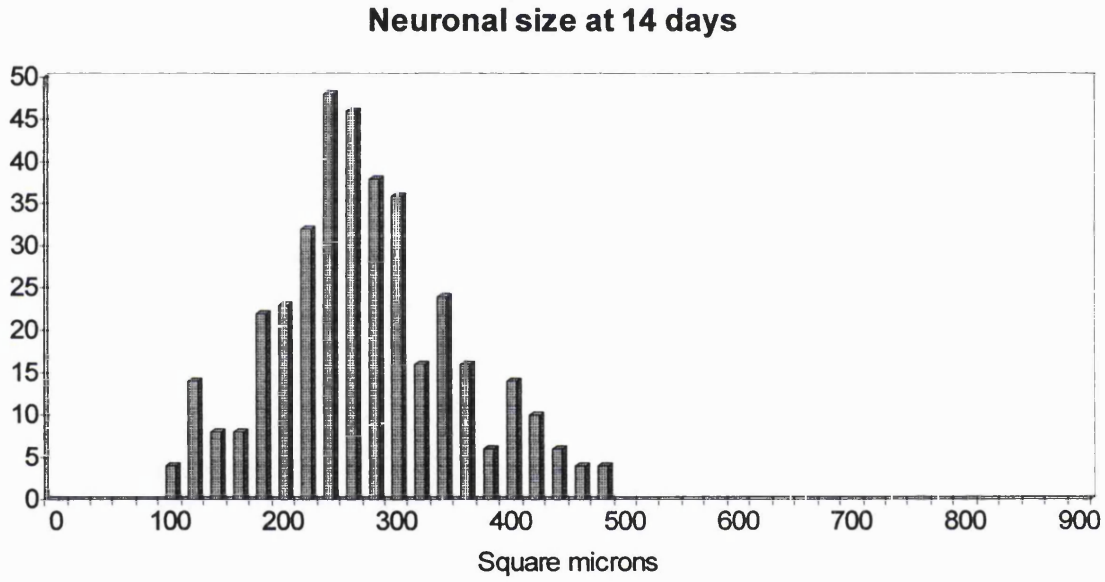

Y axis = number of neurons (N = 500), X axis = area in square micrometres of the largest profile of each serially-sectioned neuron.

3.2.4.3 Nerve fibres

Both myelinated and unmyelinated fibres were seen in the fourteen-day-old ganglia. The myelinated axons were seen, along with Schwann cell nuclei, in small well-defined nerves (figure 3.11) that ran in the ganglion. The unmyelinated fibres were not as clearly seen but were located in structures that were well defined small nerves and had Schwann cell nuclei (figures 3.11).

3.2.4.4 Capsule

The capsule of the pelvic ganglion at fourteen days was thin and continuous (figure 3.10). It was composed of fibroblasts sometimes single or in layers of up to three cells and their processes. The fibroblasts had flattened cell bodies, containing nuclei and cytoplasm and the processes of some of the fibroblasts were several times the length of their cell bodies. The fibroblasts lay very close together and the it was not always possible to differentiate the outlines of their processes. The capsule at fourteen days sent well-defined septa of fibroblasts and their processes into the ganglia and these septa completely separate groups of neurons. The groups of neurons separated by the septa gave rise to postganglionic nerves.

3.2.4.5 Other cells

Glial cell nuclei were seen very close to ganglion neurons generally there were one to two glial cell nuclei associated with one neuron. The cytoplasm of the cell body of the glial cell was not seen clearly under the light microscope.

Schwann cell nuclei were seen in small groups in myelinated nerve fibres, small nerves that ran along the outside of the ganglion and in structures within the ganglion termed unmyelinated fibres.

Cells termed SIF cells were seen in groups of up to 20, distributed around the edges of the ganglion and around blood vessels (figure 3.11).

Fibroblasts and their processes were seen in the capsule, in the septa dividing neurons into groups and around some blood vessels. Endothelial cells were seen lining the blood vessels that ran through the ganglion as at seven days, three days and at birth.

3.2.4.6 Blood vessels

Numerous small capillaries lined by endothelial cells, were seen running through the ganglion as at birth, three days and seven days. And a number of venules and arterioles were also observed.

3.2.4.7 Size of ganglion

The length of the ganglion at fourteen days was determined by the same method as in the earlier stages. The length along the dorso-ventral axis of the ganglion in three, fourteen day old rats was 690, 765, and 825 μm, respectively, the average being 760 μm (Table 8).

The average ganglion sectional area at fourteen days, ranged for the three ganglia from 98,769 - 131,925 μm^2 with an average value of 115,892 μm^2 (Table 8, n=3).

The mean ganglion volume (using the Cavalieri method) of the three, fourteen day old female Sprague-Dawley ganglia was calculated as 87.7 million cubic micrometres (Table 8). The ganglion volume approximately doubled from birth.

Table 8

Body weight, and pelvic ganglion volume of fourteen day old Sprague-Dawley rats.

Animal	Body Weight (gms)	Ganglion length (μm)	Average Ganglion cross section area (μm^2)	Ganglion volume (millions of μm^3)
S-D. 31	36	765	98,769	75.5
S-D. 32	36	825	116,981	96.5
S-D. 33	36	690	131,925	91.0
Average	**36**	**760**	**115,892**	**87.7**

3.2.5 Thirty days

The major pelvic ganglion of the one month old female Sprague-Dawley rat, consisted of neurons (surrounded by glial cells), blood vessels, connective tissue, nerve fibres (myelinated and unmyelinated), and non-neuronal cells (e.g., SIF cells & fibroblasts) covered by a thin continuous capsule of connective tissue (figure 3.12).

3.2.5.1 Ganglion neurons

The ganglion neurons had a smooth surface and were ovoid in sectional profile. The neurons one month after birth had the same appearance as those in the adult ganglia but were smaller in size. Each neuron had a covering (sheath) of glial cells, the nucleus of the glial cells was clearly seen under the light microscope, but the glial sheath was difficult to visualize and separate from the neuronal cell membrane.

Each neuron had at least one pale nucleus placed either centrally or at one side of the cell, the nuclei contained 1 or 2 nucleoli (figure 3.13). Some of the larger neurons were binucleate, but no vacuolated neurons were seen.

3.2.5.2 Size of neurons

Neuronal size was determined as in the earlier stages of development. The size of the neurons in the three ganglia varied from 100 μm^2 to 880 μm^2, the corresponding to a range in neuronal diameters of 11.3 - 33.5 μm. The average neuronal size for the three ganglia varied from 295 μm^2 to 328 μm^2, the mean being 310 μm^2 (table 9).

Neuronal volume was estimated by using the technique described above (3.2.1.2) for the ganglion at birth. The average neuronal volume for the three ganglia ranged from 3805.3 μm^3 to 4461.9 μm^3 the mean value for the three ganglia was 4114.5 μm^3 (table 9).

Table 9

Body weight, Neuronal size of one-month-old female Sprague-Dawley rats.

Animal	Animal Weight (gms)	Average Neuronal size (μm^2)	Average Neuronal volume (μm^3)
S-D. 21	82	308.5	4076.2
S-D. 22	87	294.8	3805.3
S-D. 23	90	327.7	4461.9
Average	86	310.3	4114.5

Graph Five

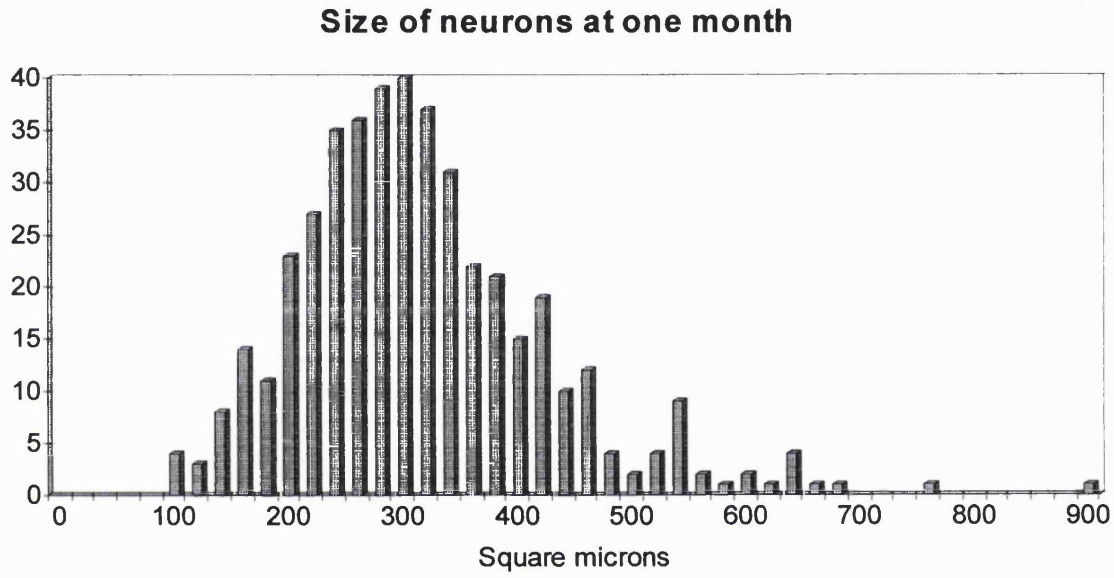

Y axis = number of neurons (N = 500), X axis = area in square micrometres of the largest profile of each serially-sectioned neuron.

3.2.5.3 Nerve fibres

The one-month-old pelvic ganglion had several groups of nerve fibres, with clear demarcation from the neighboring ganglion structures, travelling through it. The vast majority of these fibres were myelinated, the myelinated nerve fibres contained several Schwann cells the nuclei of which were clearly seen in the light microscope (figure 3.13). Smaller unmyelinated fibres were also present in the one month old ganglion these contained Schwann cell nuclei but there axons were not clearly visible in the light microscope.

3.2.5.4 Capsule

The capsule of the pelvic ganglion was composed of connective tissue, continuous and enclosed the whole ganglion. The capsule was formed by closely placed, overlapping layers of thin, flat, fibroblast processes arranged in a concentric fashion around the ganglion. Occasionally, small fibroblast cell bodies with nuclei and very small amounts of cytoplasm were seen. The capsule varied in thickness from 3 micrometres to less than one micrometres. The capsule of the one month old pelvic ganglion was continuous with the septa of connective tissue that separated groups of neurons, and continuous with the covering of the nerves that left the ganglion.

3.2.5.5 Other cells

Glial cells were seen closely associated with neurons but their cytoplasm was not very clear in the light microscope, however each neuron had around it a region of non-staining translucent material believed to be the glial sheath

Schwann cell nuclei were seen in the myelinated and unmyelinated nerve fibres travelling within the ganglion (picture 3.13), the processes of the Schwann were not clearly seen in the light microscope.

Fibroblasts were observed as in earlier stages within the ganglion, where their nuclei could be seen in the septa separating groups of neurons, and around the ganglion where their processes made up the ganglion capsule.

Cells termed SIF cells were seen in clusters of 5 -20 around blood vessels and towards the edge of the ganglion.

Flattened cells lining the blood vessels that ran through the ganglion, were as in earlier stages identified as endothelial cells. The nuclei of the endothelial cells were seen as small swellings in the profile of the endothelial cells.

Red blood cells were seen inside some of the blood vessels in the ganglion, however; as in earlier stages, no red blood cells were seen outside the blood vessels.

3.2.5.6 Blood vessels

The one-month-old ganglion possessed its own intra-ganglionic blood supply composed of arterioles, venules and capillaries. All the blood vessels ran along the dorso-ventral axis of the ganglion, as in earlier stages and in the adult.

3.2.5.7 Size of ganglion

The length of the ganglion at one month was determined by the same method as in the earlier stages. The length along the dorso-ventral axis of the ganglion in three, one month old rats was 671, 850, and 980 μm respectively, the average being 833 μm (Table 10).

The average ganglion sectional area at one month, ranged from 128,556 - 136,263 μm^2 with an average value of 132,519 μm^2 (Table 10, n=3).

The mean ganglion volume of the three, one-month-old female Sprague-Dawley ganglia (calculated by the Cavalieri method) was 109.7 million cubic micrometres (Table 10).

Table 10

Body weight, and pelvic ganglion volume of one-month-old Sprague-Dawley rats.

Animal	Body Weight (gms)	Ganglion length (μm)	Average Ganglion cross section area (μm^2)	Ganglion volume (millions of μm^3)
S-D. 21	82	671	136,263	91.2
S-D. 22	87	850	132,739	112.8
S-D. 23	90	980	128,556	126.0
Average	**86**	**833**	**132,519**	**109.7**

3.2.6 90 days (young adult)

The major pelvic ganglion consisted of neurons (surrounded by satellite cells), blood vessels, connective tissue, nerve fibres (myelinated and unmyelinated), and non-neuronal cells such as SIF cells and fibroblasts, and was enveloped by a thin continuous capsule of connective tissue (figure 3.14).

3.2.6.1 Capsule

The capsule was composed of a layer of connective tissue which was continuous and enclosed the whole ganglion. The capsule measured on average 5 micrometres in thickness, and although it was not always possible to divide the capsule into separate layers, the capsule of the ganglion was continuous with the covering of the nerves that left the ganglion.

The capsule was formed by closely placed, overlapping layers of thin, flat fibroblast cells and their processes arranged in a circular fashion around the ganglion. Occasionally, small fibroblast cell nuclei with a thin rim of cytoplasm were seen.

The capsule of the pelvic ganglion sent processes or septa into the body of the ganglion separating groups of neurons; occasionally the septa completely surrounded a group of neurons and several micrometres later (i.e. further down the series of sections), this area of the ganglion would give rise to a post-ganglionic nerve.

Collagen was not easily visualized under the light microscope due to the limitations of its magnification.

3.2.6.2 Ganglion neurons

The ganglion neurons had a smooth surface and were mostly ovoid in sectional profile, with an occasional single, large, straight process interpreted as an axon seen emerging from the cell body. Each neuron had a covering (sheath) of glial cells; the

nucleus of the glial cells was clearly seen under the light microscope (figure 3.15), but the glial sheath was difficult to visualize and separate from the neuronal cell membrane.

Neurons were either surrounded by neuropil (figure 3.15), or lay close to one another with very clear intercellular borders (figure 3.15).

Most neurons had one nucleus, round, pale, usually centrally placed; observed in serial sections, each nucleus contained 1 to 4 nucleoli. Some of the larger neurons were binucleate (figure 3.16) they constituted on average 1.88 % of the total neuronal population (Table 11).

Some neurons had large vacuoles in their cytoplasm (figure 3.16), which tended to displace the other contents. The vacuolated neurons were occasionally binucleate (figure 3.17). No counts were done on vacuolated neurons.

Table 11. Population Of Binucleate Neurons in adult female Sprague-Dawley rats

Animal	No. of Binucleate neurons	% of total population
S-D.01	123	1.19
S-D.02	178	2.50
S-D.03	118	1.95
Average	**140**	**1.88**

3.2.6.3 Other cells

Groups of cells smaller than ganglion neurons, with small amounts of cytoplasm, located around the edge of the ganglion and around small blood vessels, were identified as SIF cells. They lay near neurons but not in direct contact with them.

Fibroblasts were observed both within the ganglion, where their nuclei could be seen in the septa separating groups of neurons (figure 3.15), and around the ganglion where their processes made up the ganglion capsule.

Schwann cell nuclei were seen in the nerve fibres travelling within the ganglion, but the processes of the Schwann were not obvious in the light microscope.

Endothelial cells were seen as flattened cells lining the blood vessels; their nuclei formed a swelling in the profile of the cell.

3.2.6.4 Blood vessels

Numerous small blood vessels lined only by endothelial cells were seen travelling through the ganglion (figure 3.14), and were identified as capillaries. In addition to the capillaries, but less numerous and slightly larger, were small round muscular blood vessels identified as arterioles; blood vessels the same size as arterioles but with thinner walls were identified as venules. Most of the blood vessels seen in the ganglion appeared round or oval in sectional profile, implying that they ran perpendicular to the plane of the section; since the ganglion was being sectioned from bladder pole to pelvic nerve, the vessels therefore ran along the dorso-ventral axis of the ganglion. The few blood vessels profiles observed to be irregular or elliptical in shape were probably regions where they changed direction, or branched.

A large artery was seen to travel on the outside of the ganglion accompanied by a vein. These were sometimes stripped off during dissection of the ganglion; this artery is a branch of the obturator artery, a branch of the internal iliac artery.

3.2.6.5 Nerve fibres

The pelvic ganglion had several discrete groups of nerve fibres travelling through it, the vast majority of these fibres were myelinated (figure 3.15), the nerve fibres contained axons and several Schwann cell nuclei.

3.2.6.6 Size of ganglion

The length of the adult ganglion, was determined by serially sectioning the ganglion from the entrance of the pelvic nerve (starting with the first section with at least 20 neurons) to the last section containing no fewer than 20 neurons at the post ganglionic end of the ganglion. In three ganglia, the length ranged from 978 micrometres to 1,708 micrometres, the mean length being 1,362 micrometres (Table 12).

The average ganglion sectional area, ranged from 152,000 to 165,000 square micrometres the mean being 158,000 square micrometres (Table 12, n=3).

The volume of the ganglion was calculated by multiplying the length of the ganglion by its mean sectional area (the so-called Cavalieri method). The mean ganglion volume of the three adult female Sprague-Dawley ganglia was calculated as 213 million cubic micrometres (Table 12).

Table 12. Length, sectional area and volume of the pelvic ganglion of adult female Sprague-Dawley rats

Animal	Approx. animal weight (gms)	Ganglion length (μm)	Average ganglion cross section area (μm^2)	Ganglion volume (millions of μm^3)	Average neuronal sectional area (μm^2)	Average neuronal volume (μm^3)
S-D. 01	200	1,708	151,639	259.0	343.4	4,786.5
S-D.02	200	1,400	156,214	218.7	361.6	5,172.5
S-D. 03	200	978	164,928	161.3	347.2	4,865.6
Average	**200**	**1,362**	**157,594**	**213.0**	**350.7**	**4,941.5**

3.2.6.7 Size of neurons

Neuronal size was determined by measuring the largest sectional area of the neuron, from a series of consecutive sections including the full extent of the cell body. The size of the neurons ranged from 131- 1023 micrometres (n = 500, see graph 6), giving a

range of diameters of 13 to 36 micrometres. Neuronal volume was estimated by using the neuronal size (μm^2) to determine the radius of the neuron. This was achieved by assuming the neuronal profiles to be circular and applying the equation area = πr^2. Then the value obtained for the radius was placed in the equation; volume = $4/3\pi r^3$ (the neuron was assumed, for sake of simplicity to be spherical). The range of volumes was 1124 - 24500 cubic micrometres.

The average neuronal sectional area for the three ganglia varied from 343 – 361 μm^2, the mean being 351 μm^2 (table 13).

The average neuronal volume for the three ganglia ranged from 4787 μm^3 to 5173 μm^3 the mean value for the three ganglia was 4941 μm^3 (table 13).

Table 13. Neuronal sectional area and volume in 90 day female Sprague-Dawley rats.

Animal	Approx. animal weight (gms)	Average neuronal sectional area (μm^2)	Average neuronal volume (μm^3)
S-D. 01	200	343.4	4,786.5
S-D.02	200	361.6	5,172.5
S-D. 03	200	347.2	4,865.6
Average	**200**	**350.7**	**4,941.5**

Graph 6. Maximal sectional area of neurons in the adult female Sprague-Dawley rat major pelvic ganglion.

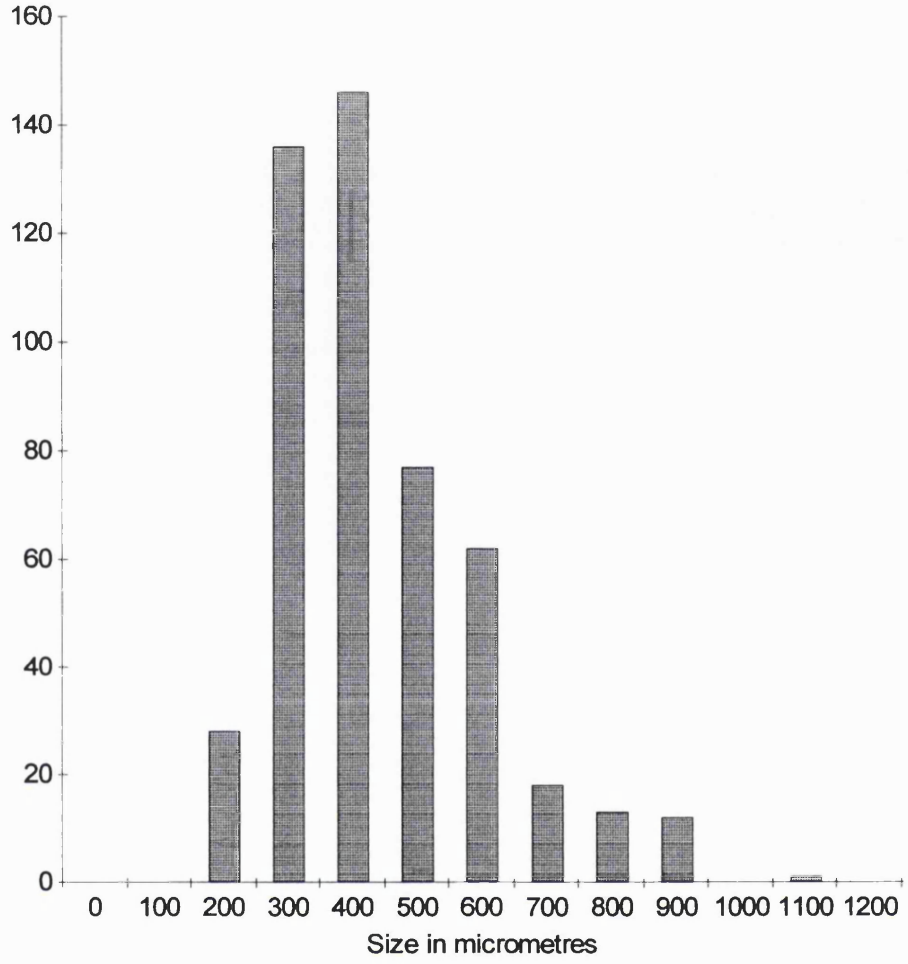

Y axis = number of neurons (N = 500), X axis = area in square micrometres of the largest profile of each serially-sectioned neuron.

Graph 7

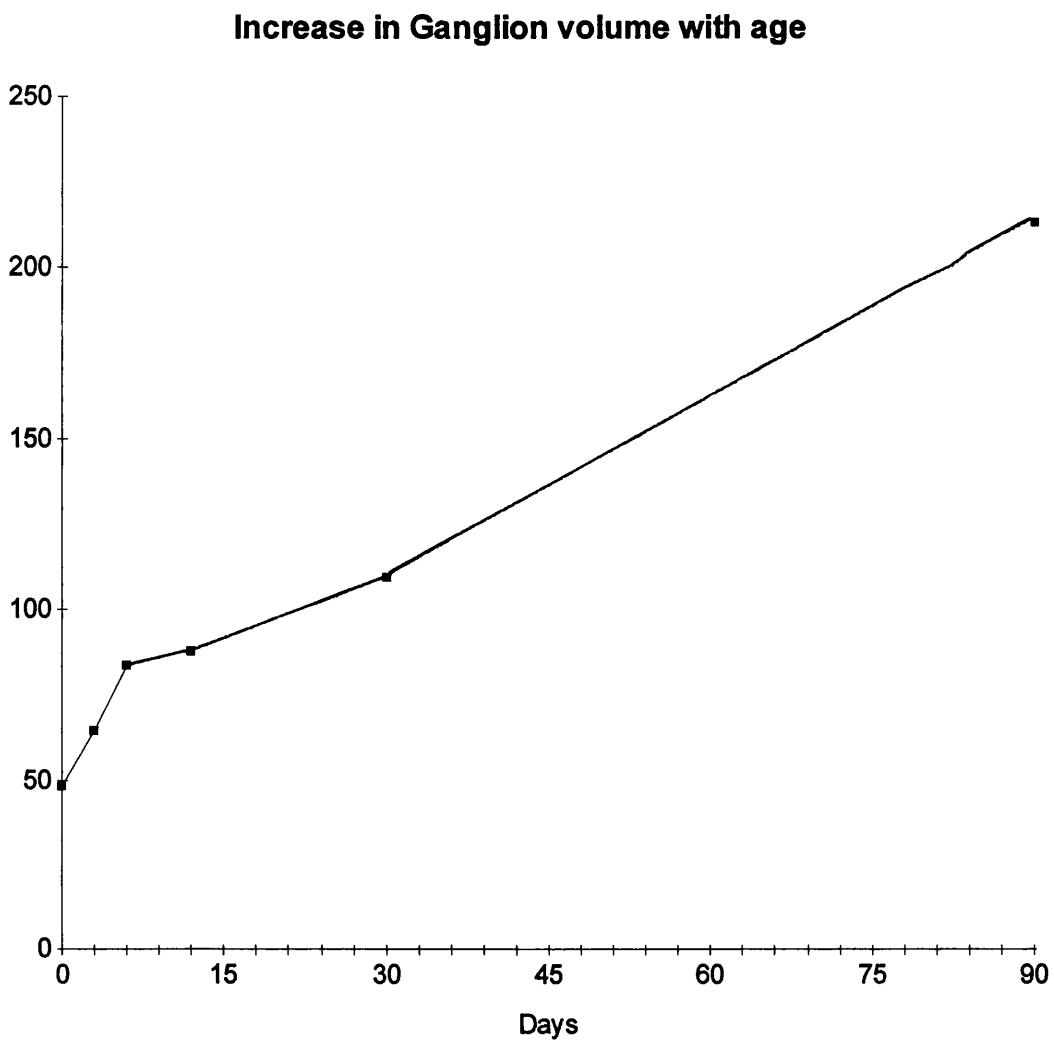

Y axis = Volume of Ganglia in Millions of Cubic Micrometres, X axis = animal age in days.

Graph 8

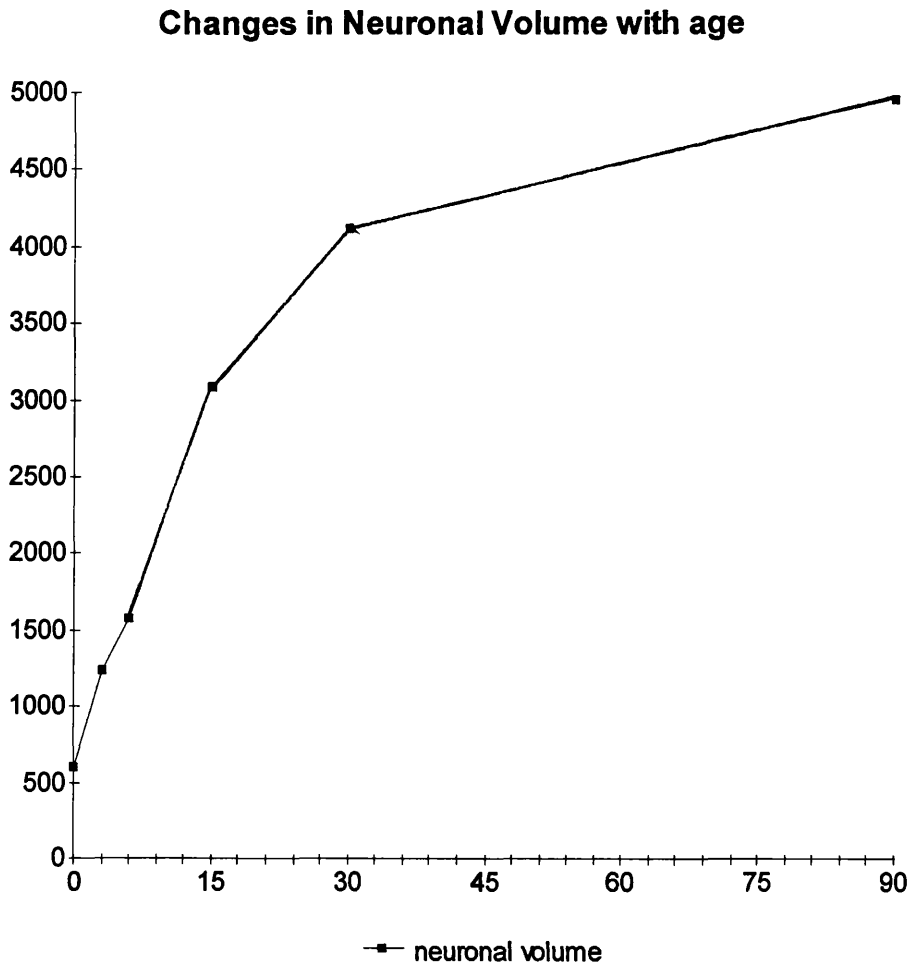

Y axis = Cell volume in cubic micrometres, X axis = animal age in days.

Figure 3.01

Pelvic ganglion and its anatomical relations at birth (stained with the acetylcholinesterase method).

B, bladder; R, rectum; V, vagina; P, pelvic ganglion; pn, pelvic nerve; gn, genital nerve; pv, paravaginal nerves; nu, nerve to anterior of uterus; h, hole for passage of blood vessels; dn, dorsal bladder nerves; an, anterior bladder nerves; ig intramural ganglia.

Magnification x 36

Scale bar = 1 millimetre

Figure 3.02

Urinary bladder at birth

B, bladder; g, intramural ganglion.

Magnification x 36

Scale bar = 1 millimetre.

3.01

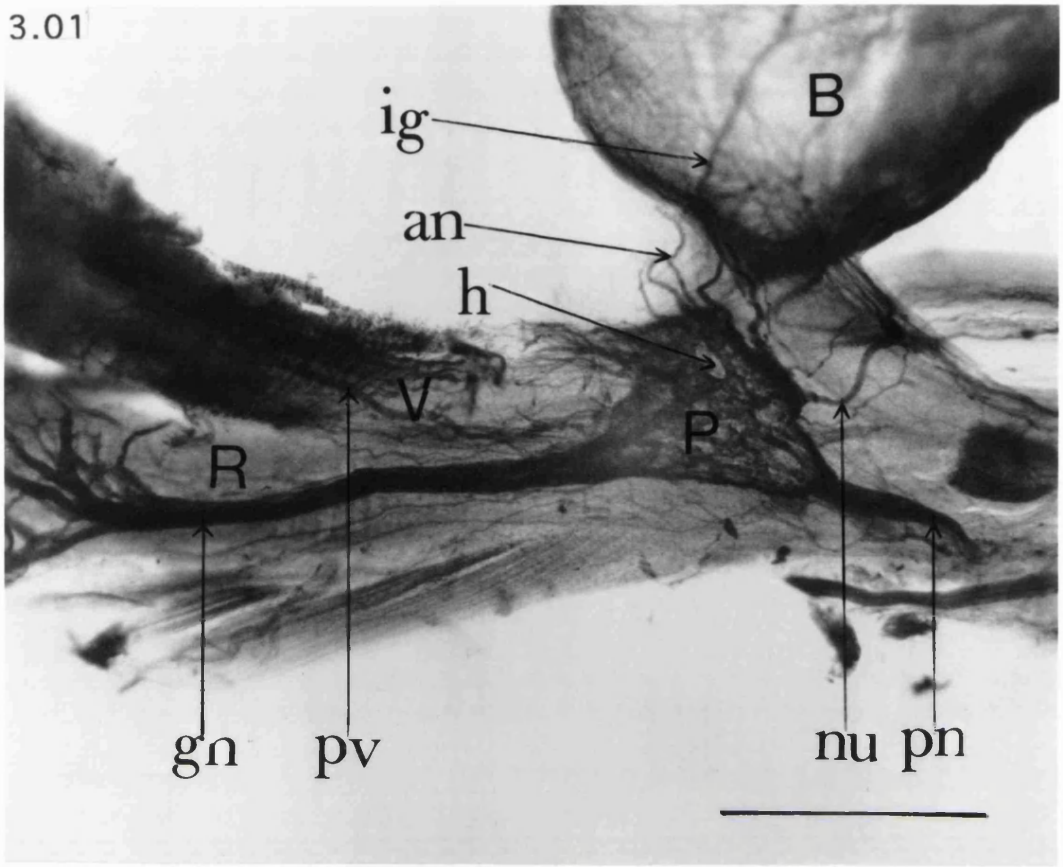

3.02

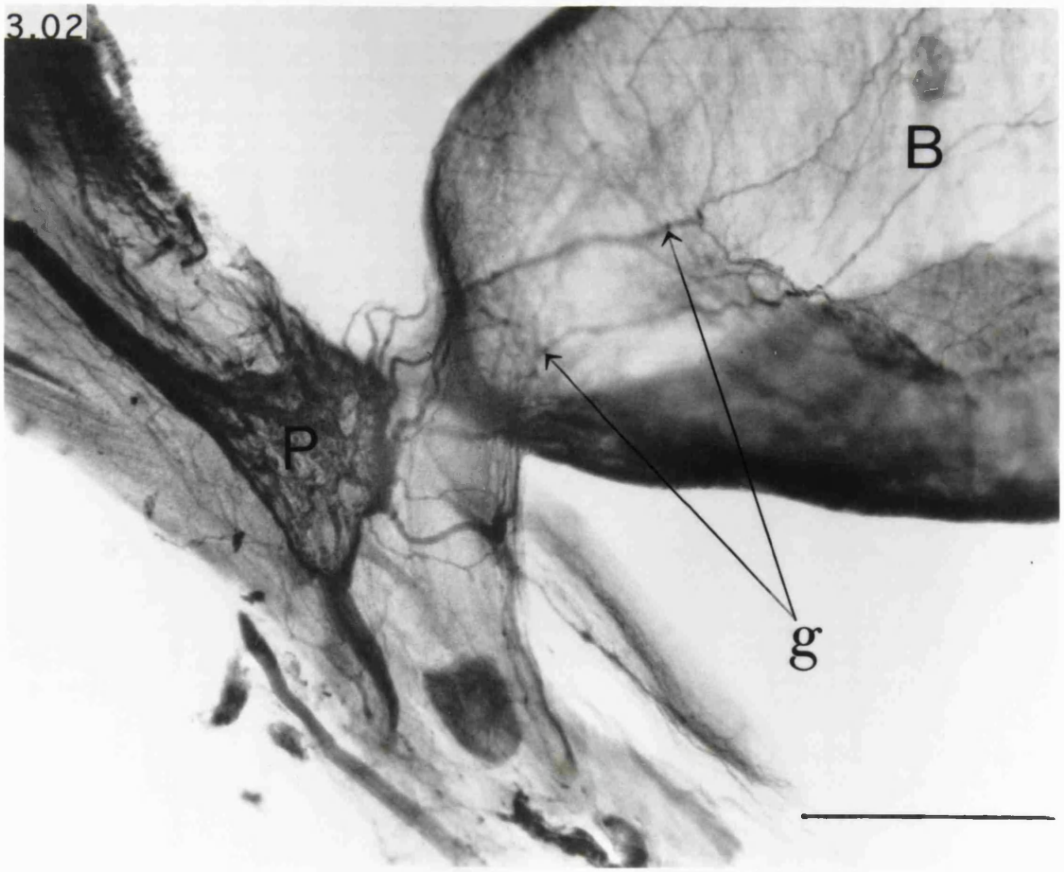

Figure 3.03

Pelvic ganglion and its anatomical relations at seven days (stained with the acetylcholinesterase method). Showing: B, bladder; U, uterus; V, vagina; R, rectum; G, pelvic ganglion; pn, pelvic nerve; hn, hypogastric nerve; an, anterior bladder nerves; dn, dorsal bladder nerves; gn, genital nerve; pv, paired paravaginal nerves; rn, rectal nerves; ag, accessory ganglion along anterior bladder nerve; ar, accessory ganglion along rectal nerve.

Magnification x 36

Scale bar = 1 millimetre

Figure 3.04

Pelvic ganglion and its anatomical relationships at fourteen days (stained with acetylcholinesterase method). Showing: G, pelvic ganglion; pn, pelvic nerve; hn, hypogastric nerve; hg, hypogastric ganglion; gn, genital nerve; pn, paravaginal nerves; an, anterior bladder nerves; dn, dorsal bladder nerves. Magnification x 36

Scale bar = 1 millimetre.

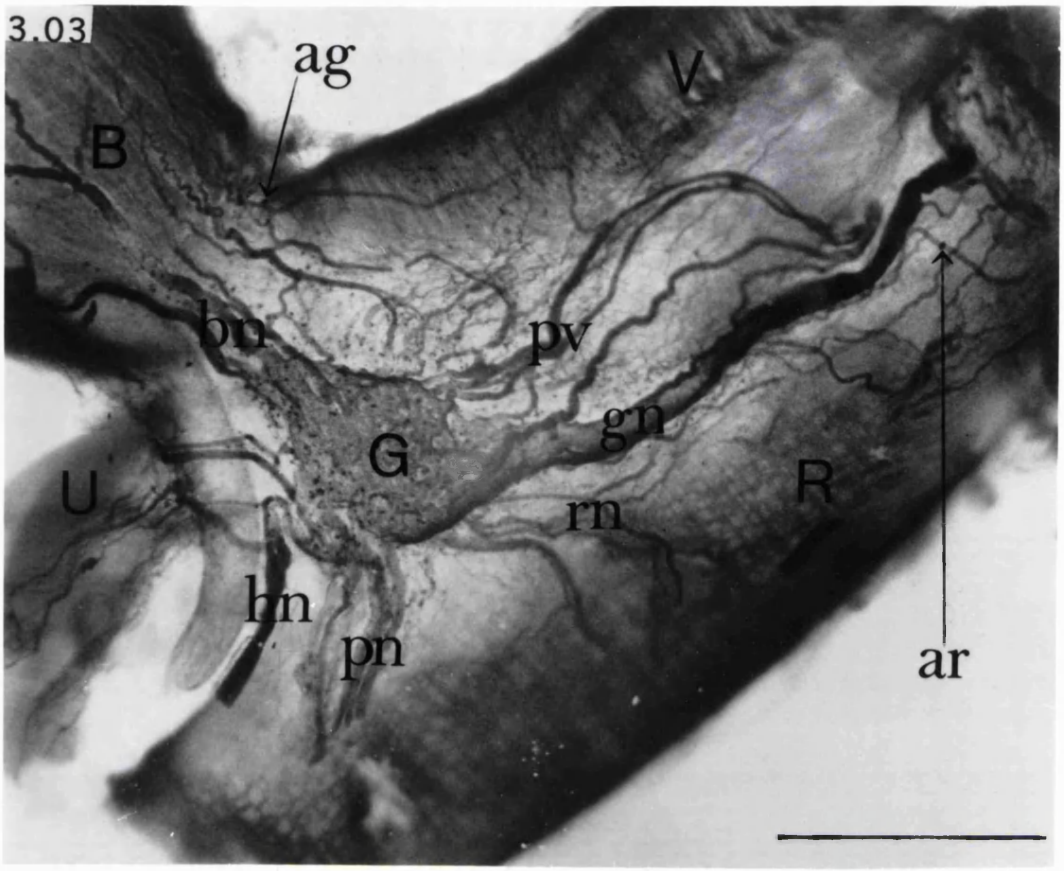
3.03
ag
V
B
bn
pv
gn
G
U
R
rn
hn
pn
ar

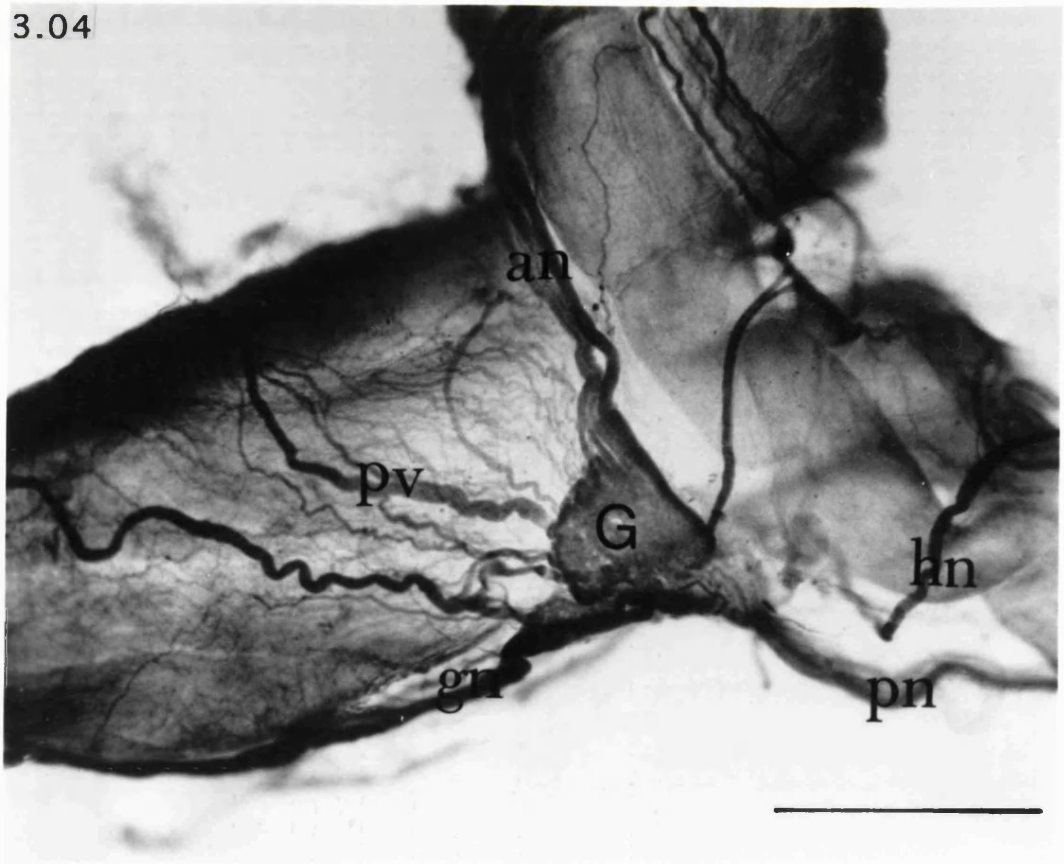
3.04
an
pv
G
hn
gn
pn

Figures 3.05 and 3.06

Adult Female rat major pelvic ganglion (acetylcholinesterase staining).

3.05 Left ganglion,3.06Right ganglion.

G, ganglion; pn, pelvic nerve; H, hypogastric nerve; rn, rectal nerves;

pv, paravaginal nerves; gn, genital nerve; an, anterior bladder nerves;

B, bladder; V, vagina; R, rectum.

Magnification x 18

Scale bar = 1 millimetre.

3.05

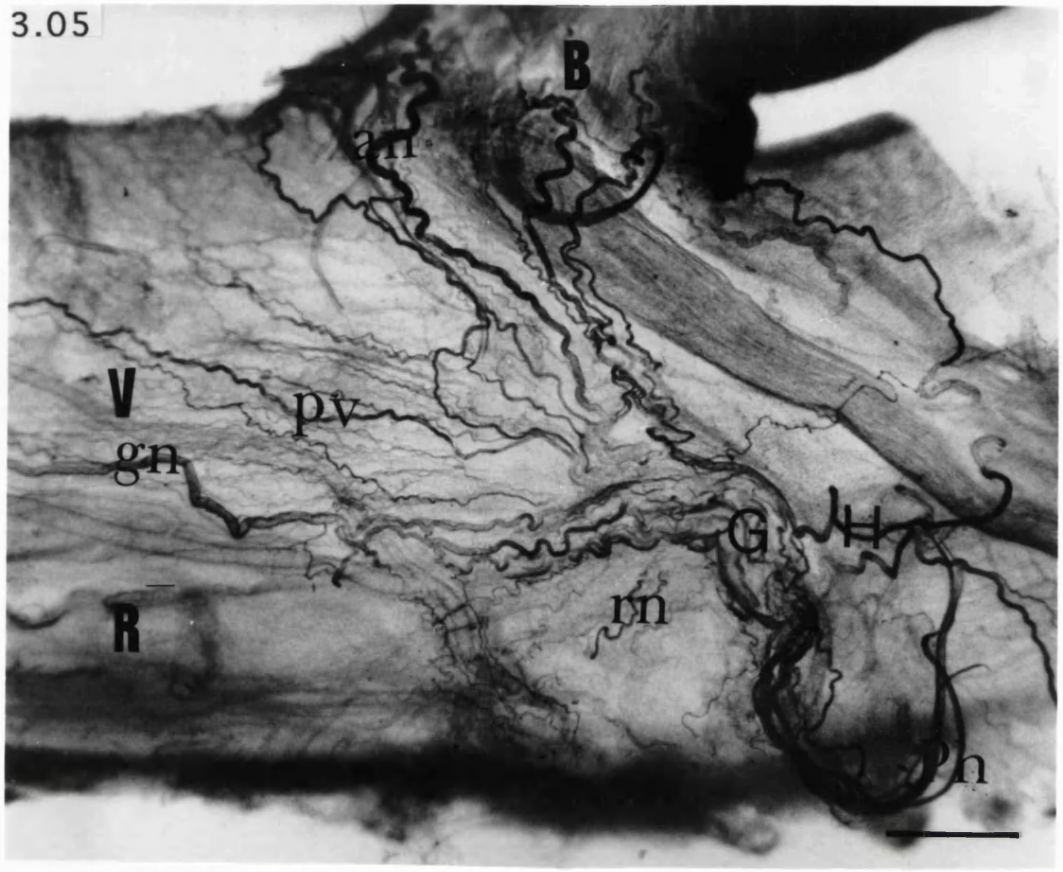

3.06

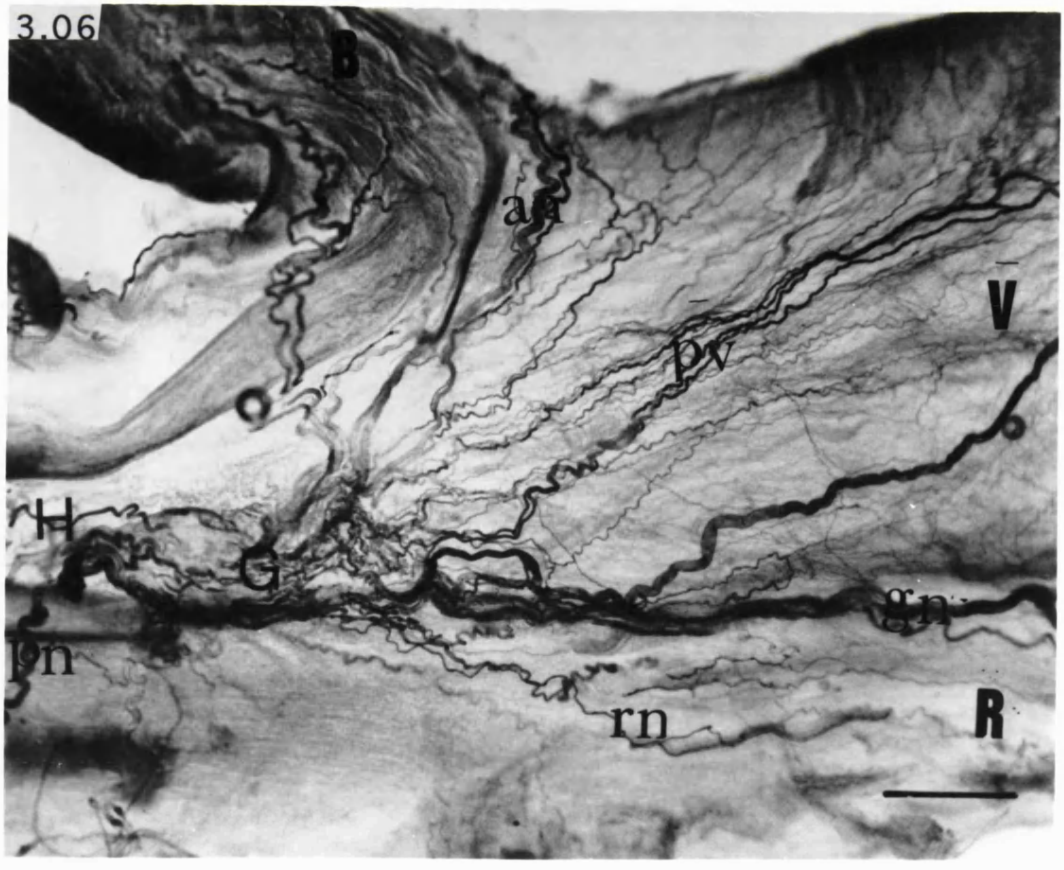

Figure 3.07A

Photomicrograph of a newborn female Sprague-Dawley rat major pelvic ganglion. The micrograph shows: N, ganglion neuron; C, ganglion capsule; B, blood vessel.

Magnification x 250

Scale bar = 100 μm

Figure 3.07B

Photomicrograph of a newborn female Sprague-Dawley rat major pelvic ganglion. The micrograph shows: N, ganglion neuron; B, intraganglionic arteriole; b, extra-ganglionic blood vessel containing a red blood cell; S, incomplete septum of fibroblast processes; g, glial cell nucleus.

Magnification x500

Scale bar = 100 μm

3.07A

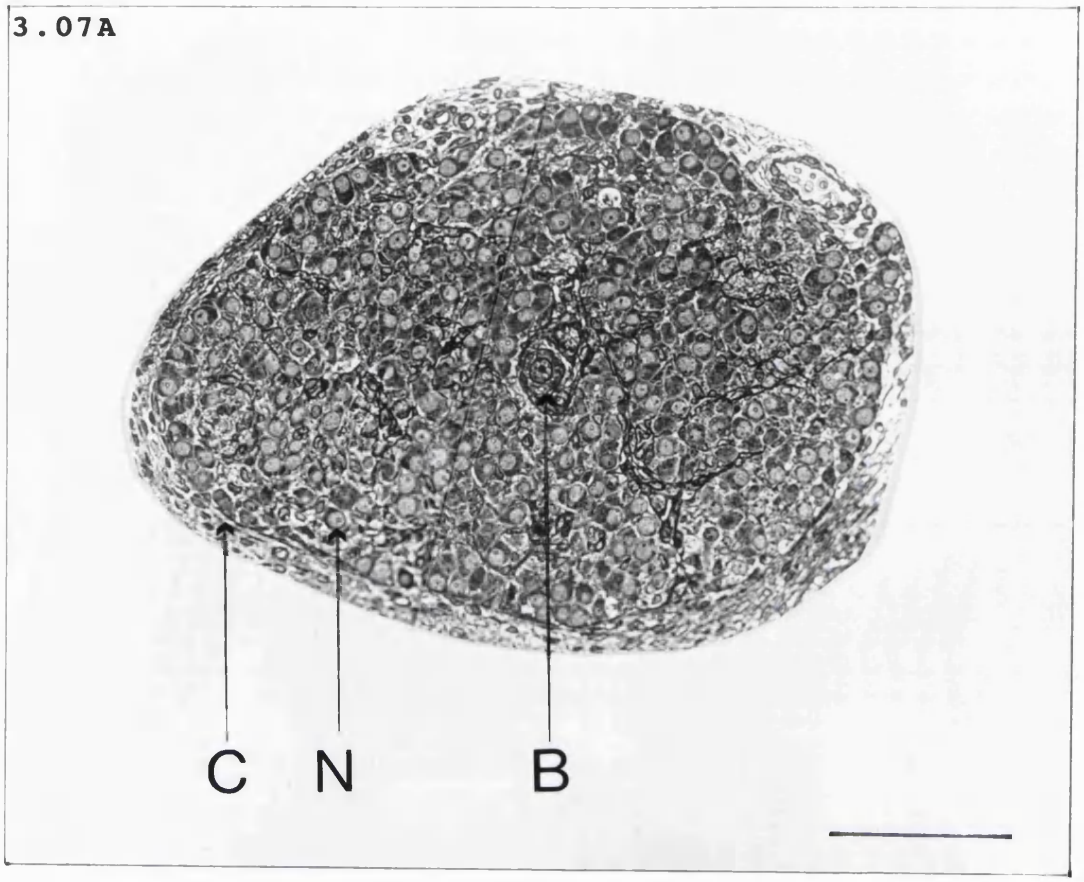

3.07B

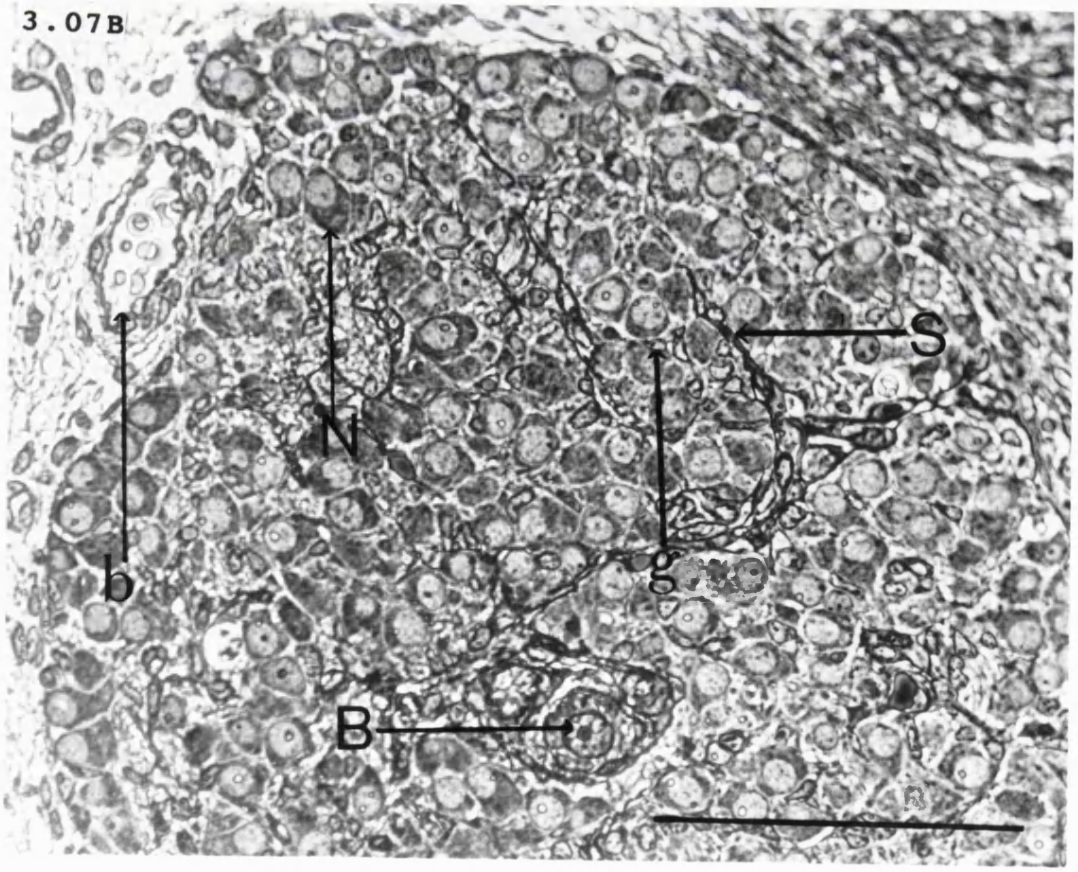

Figure 3.08A

Photomicrograph of a three day old female Sprague-Dawley rat major pelvic ganglion. The micrograph shows: C, capsule; N, ganglion neuron; B, blood vessel.

Magnification x 350

Scale bar = 100 μm

Figure 3.08B

Photomicrograph of a three day old female Sprague-Dawley rat major pelvic ganglion. The micrograph shows: N, neurons; B, blood vessels; g, glial cell nucleus; s, Schwann cell nucleus; f, fibroblast nucleus; S, SIF cell.

Magnification x 500

Scale bar = 100 μm

3.08A

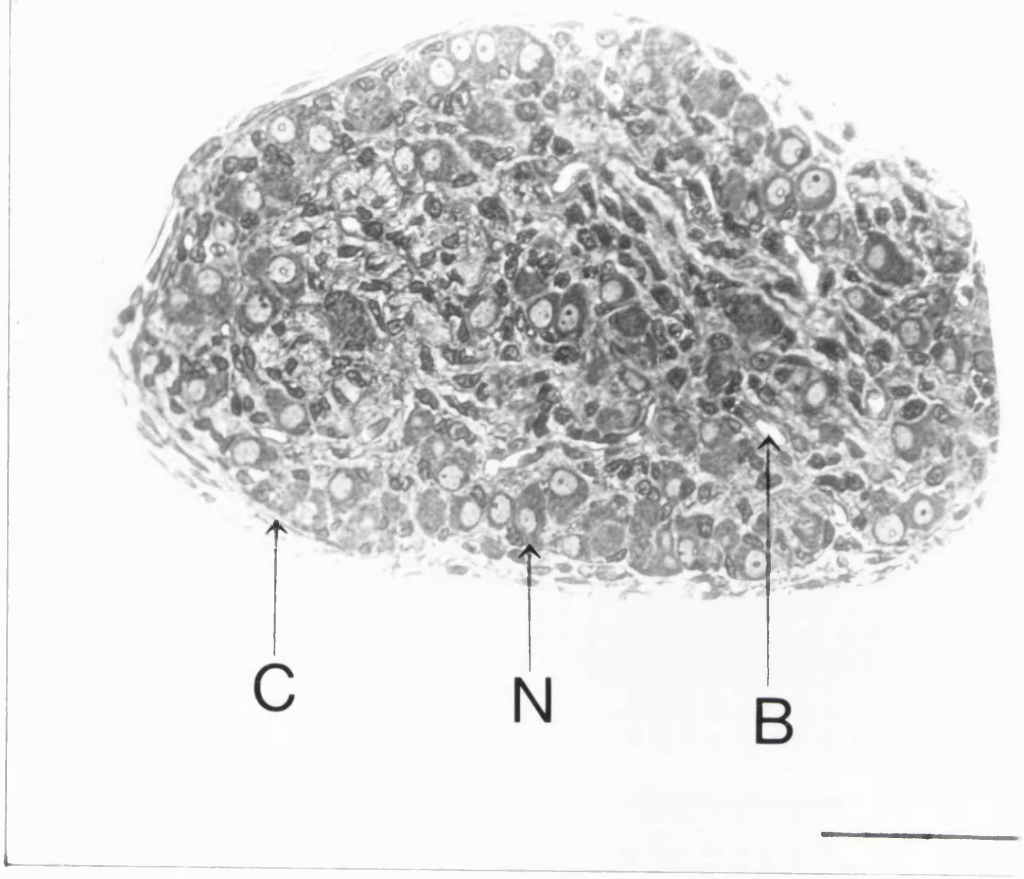

3.08B

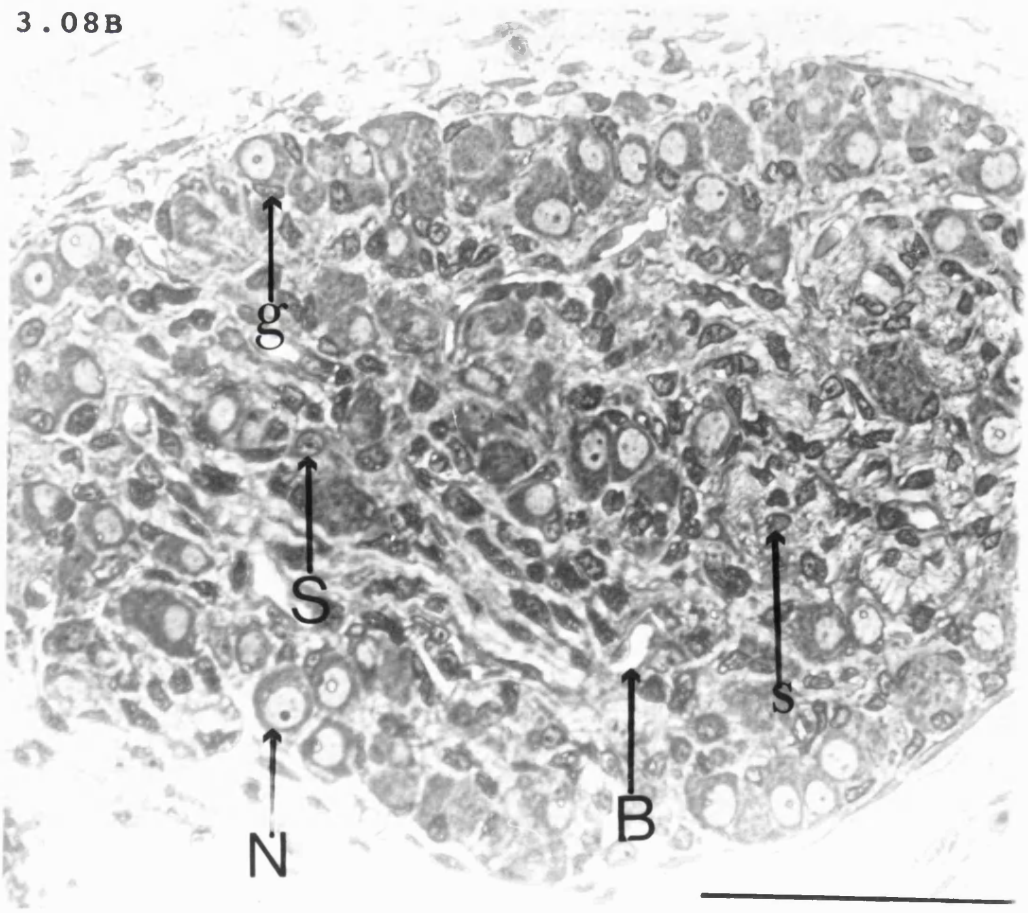

Figure 3.09A

Photomicrograph of seven-day-old female Sprague-Dawley rat major pelvic ganglion. The micrograph shows: N, neuron; C, capsule; B, blood vessel.

Magnification x 250

Scale bar = 100 μm

Figure 3.09B

Photomicrograph of seven-day-old female Sprague-Dawley rat major pelvic ganglion. The micrograph shows: N, ganglion neuron; B, blood vessel; g, glial cell nucleus.

Magnification x 500

Scale bar =100 μm

3.09A

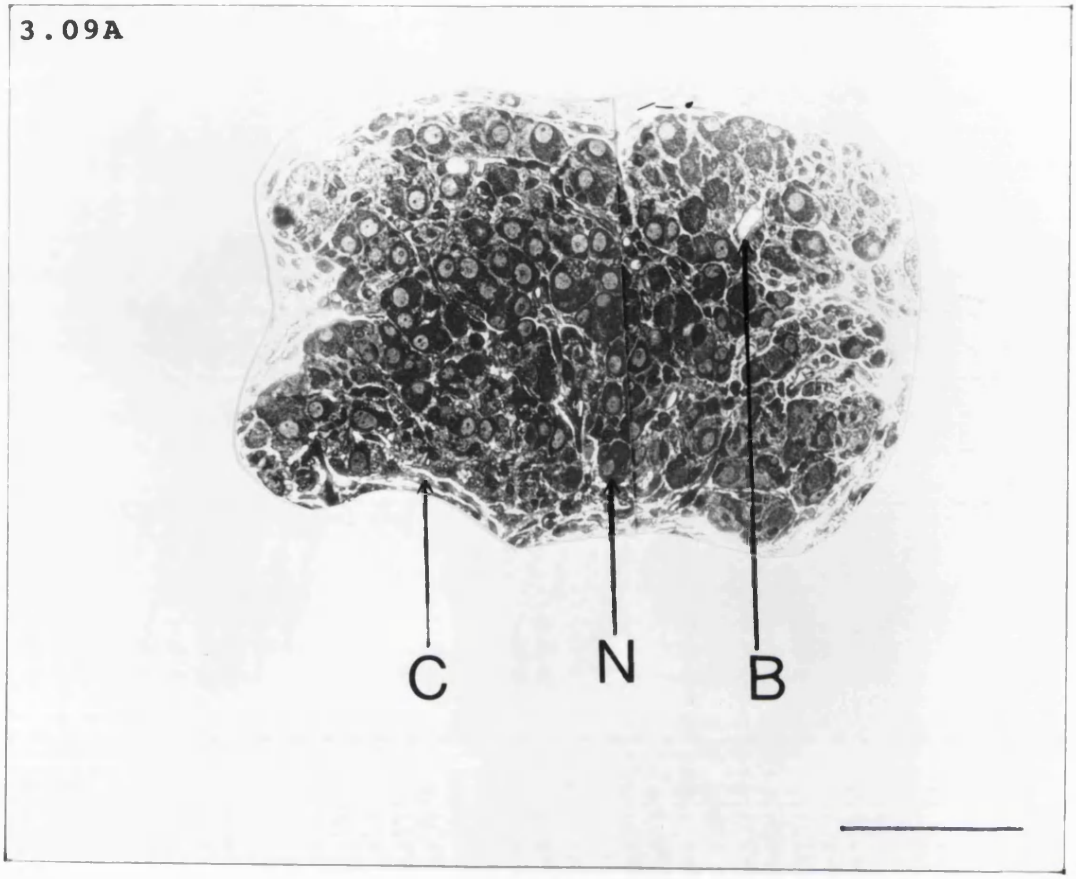

3.09B

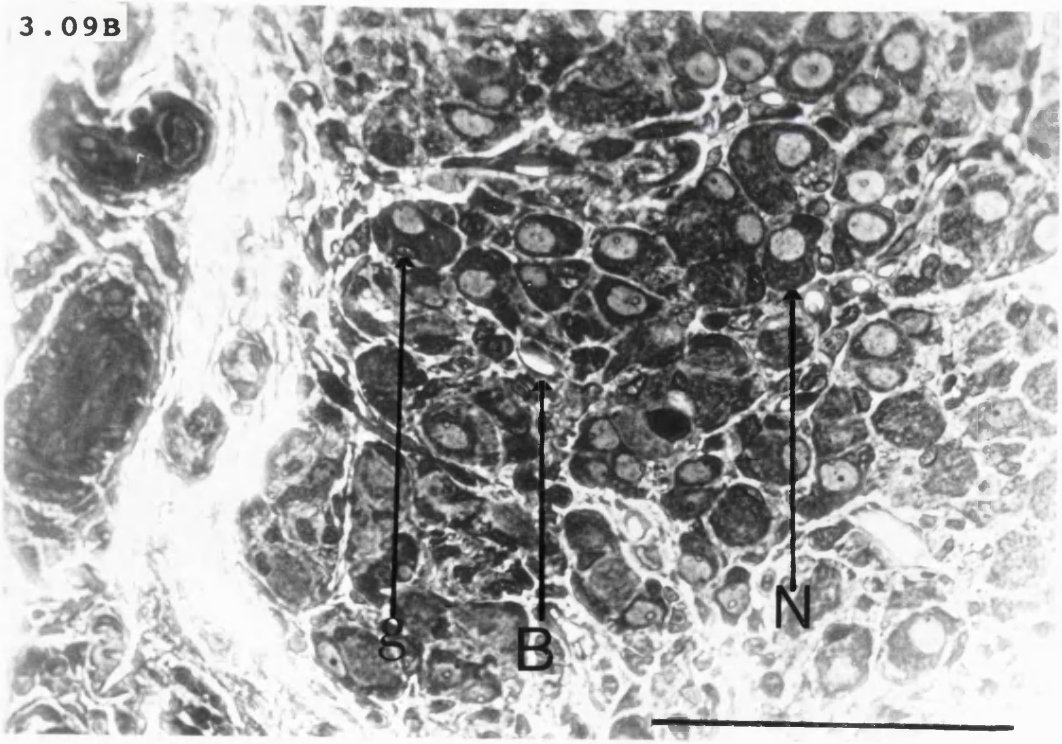

Figure 3.10

Photomicrograph of a 14-day-old female Sprague-Dawley rat major pelvic ganglion. The micrograph shows: N, ganglion neuron; C, ganglion capsule. n, capsular fibroblast.

Magnification x 250

Scale bar = 100 μm

Figure 3.11

Photomicrograph of a 14-day-old female Sprague-Dawley rat major pelvic ganglion. The micrograph shows: N, ganglion neuron; C, ganglion capsule; B, blood vessel; g, glial cell nucleus; bn, binucleate neuron; m, myelinated fibre; S, SIF cell.

Magnification x 500

Scale bar = 100 μm

3.10

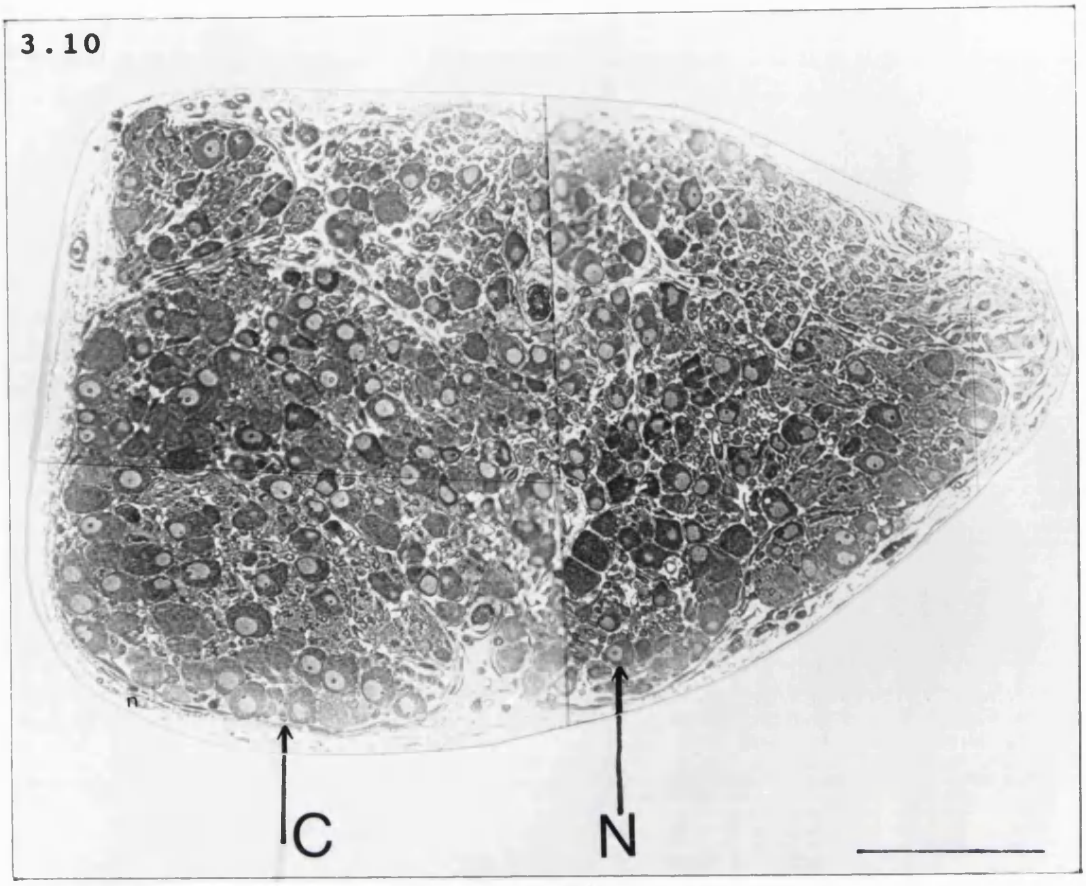

3.11

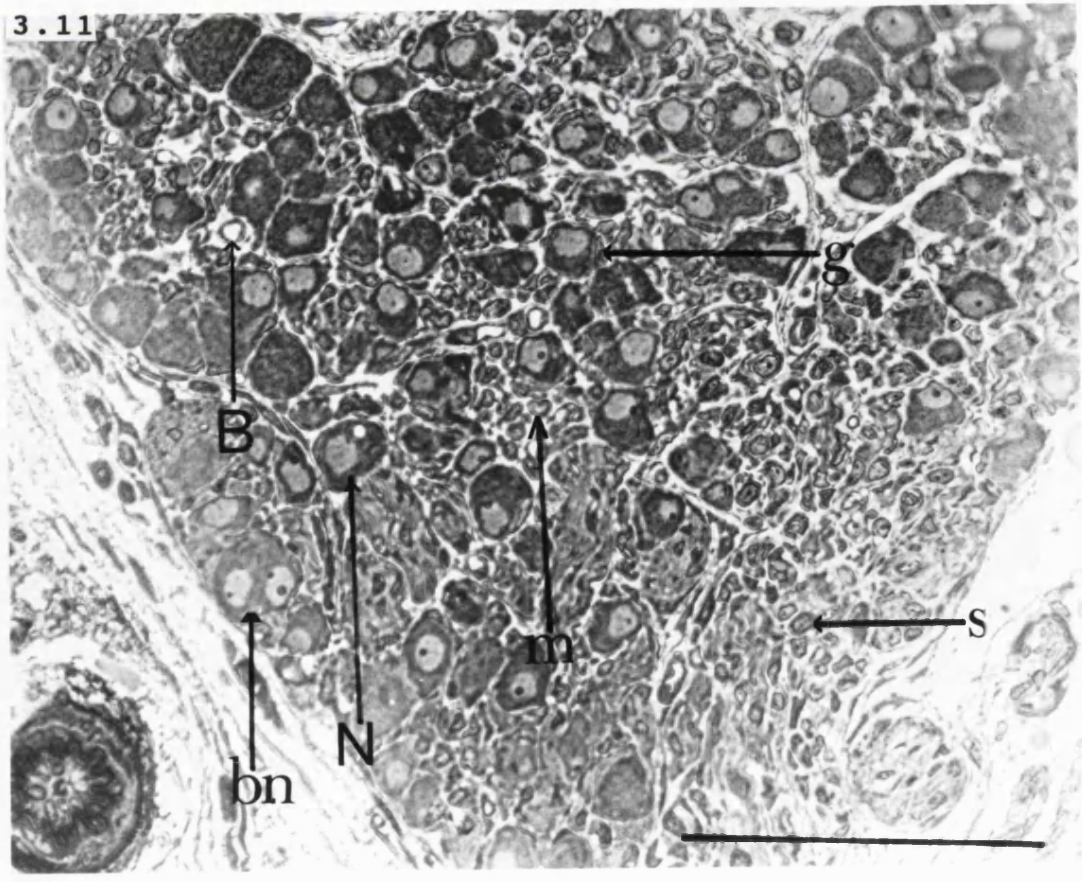

Figure 3.12

Photomicrograph of a thirty-day-old female Sprague-Dawley rat major pelvic ganglion. The micrograph shows: C, capsule; N, neuron; b, blood vessel; n, nerve bundle.

Magnification x 250

Scale bar = 100 μm

Figure 3.13

Photomicrograph of a thirty-day-old female Sprague-Dawley rat major pelvic ganglion. The micrograph shows: N, ganglion neuron; C, ganglion capsule; s, Schwann cell nucleus; g, glial cell nucleus.

Magnification x 500

Scale bar =100 μm

3.12

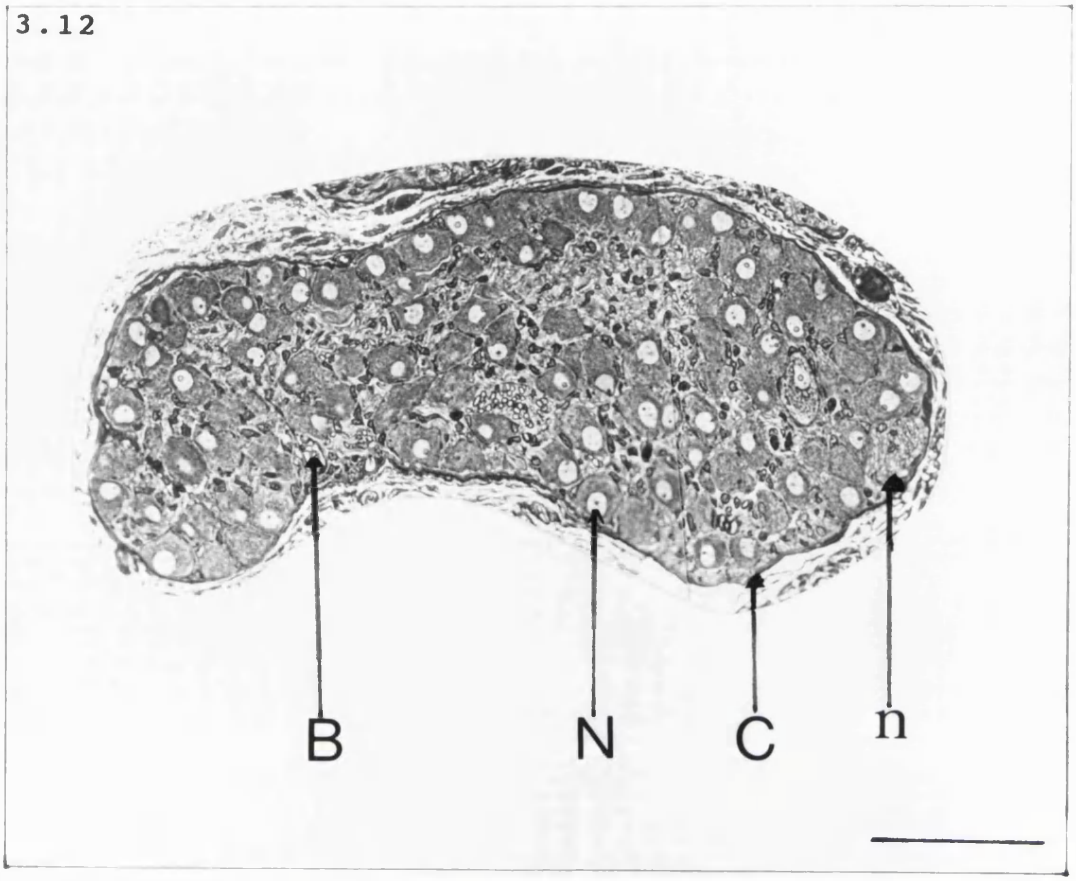

3.13

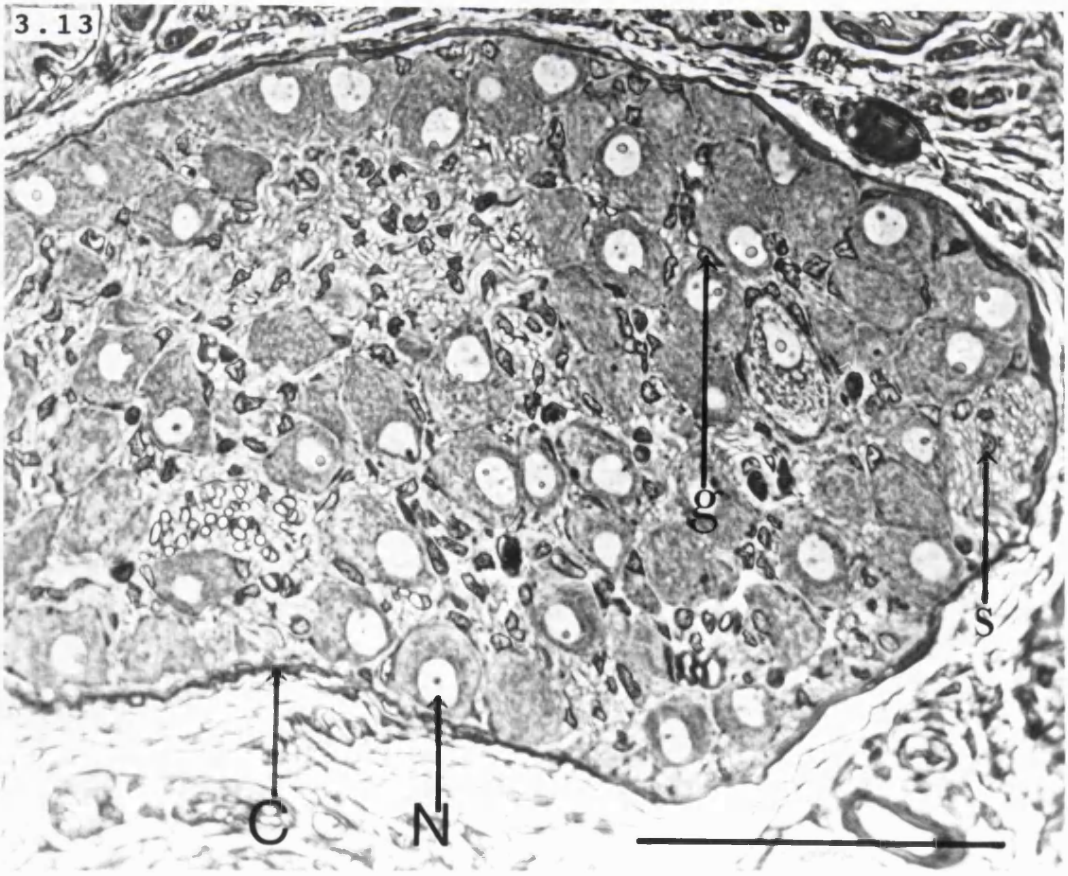

Figure 3.14

Photomicrograph of an adult female Sprague-Dawley rat major pelvic ganglion. The micrograph shows: N, ganglion neuron; C, ganglion capsule; B, blood vessel.

Magnification x 250

Scale Bar =100 μm

Figure 3.15

Photomicrograph of an adult female Sprague-Dawley rat major pelvic ganglion. The micrograph shows: N, ganglion neuron; g, glial cell; B, blood vessel; SC, SIF cell; m, myelinated fibres; f, fibroblast nucleus; e, endothelial cell nucleus.

Magnification x 800

Scale bar = 10 μm.

3.14

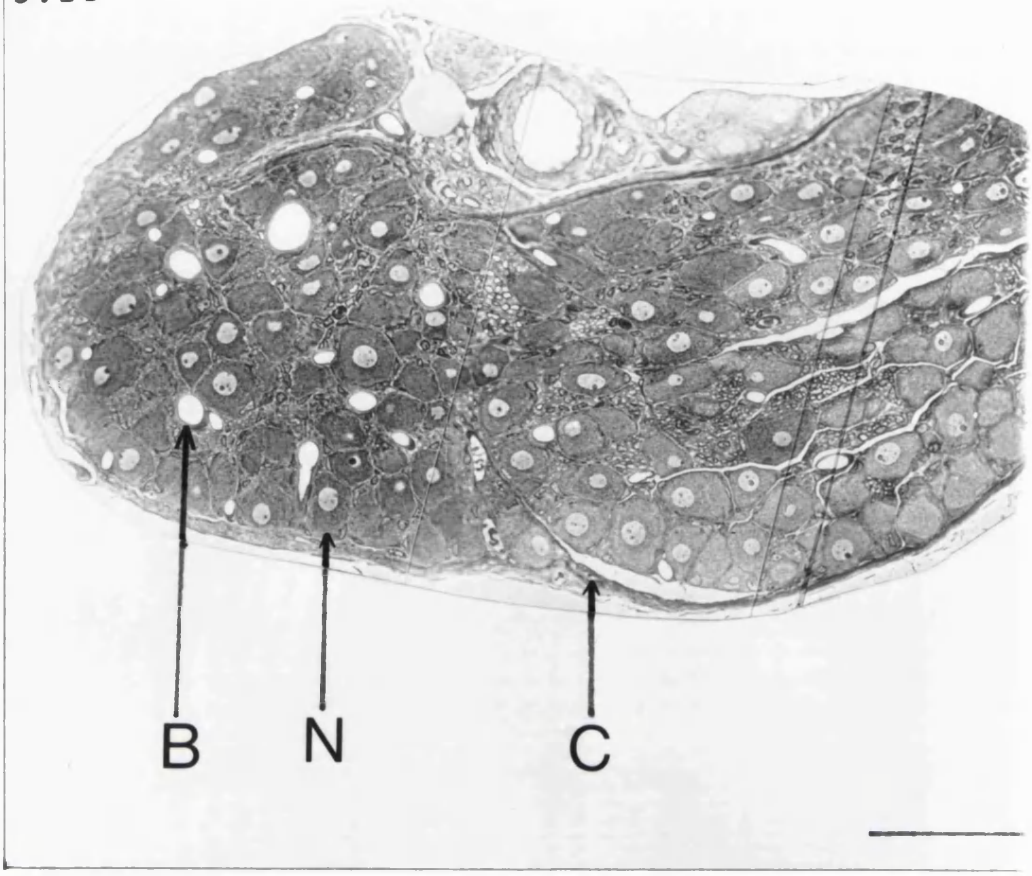

3.15

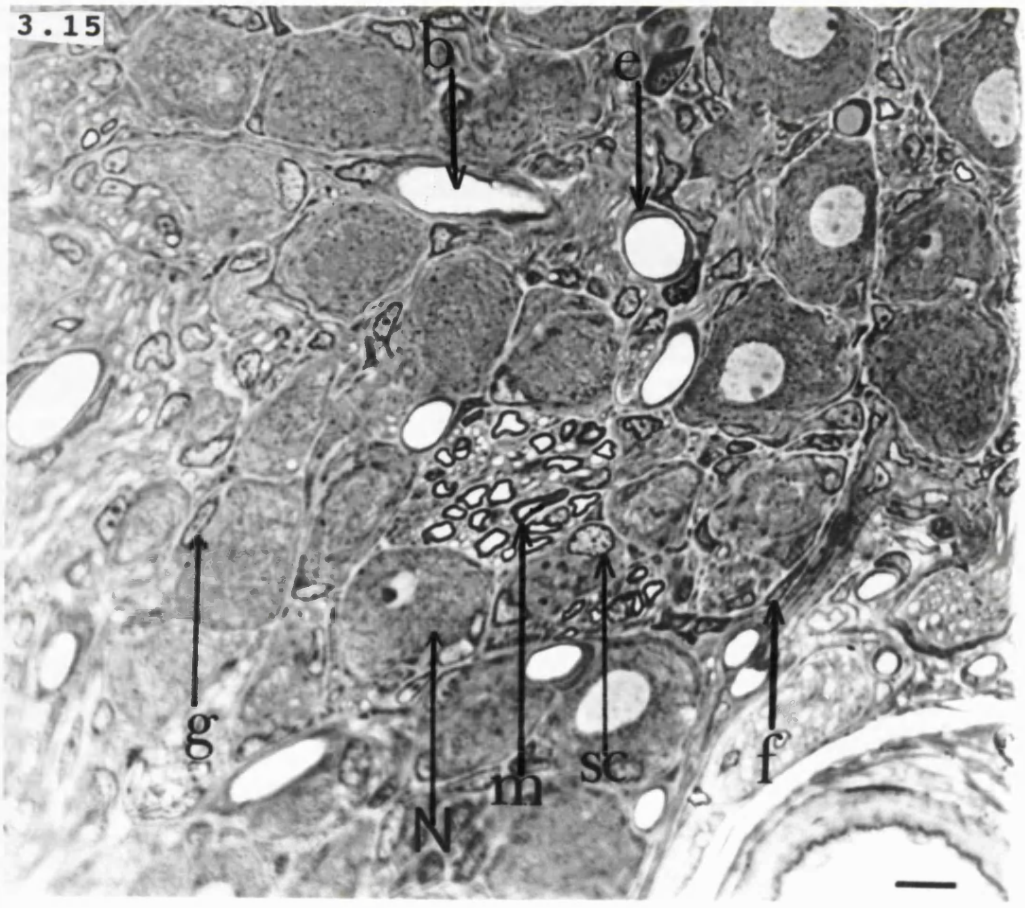

Figure 3.16

Photomicrograph of an adult female Sprague-Dawley rat major pelvic ganglion.

The micrograph shows: B, binucleate neuron; V, vacuolated neuron.

Magnification x 800

Scale bar = 10 μm.

Figure 3.17

Photomicrograph of an adult female Sprague-Dawley rat major pelvic ganglion.

The micrograph shows: BV, binucleate vacuolated neuron; M, myelinated nerve fibre.

Magnification x 800

Scale bar = 10 μm.

Figure 3.18

Photomicrograph of an adult female Sprague-Dawley rat major pelvic ganglion.

The micrograph shows: B, blood vessel; N, ganglion neuron; g, glial cell nucleus; M, myelinated fibres.

Magnification x 800

Scale bar = 10 μm.

Figure 3.19

Photomicrograph of an adult female Sprague-Dawley rat major Pelvic ganglion.

The micrograph shows: N, neuron; C, capsule; SC, SIF cell.

Magnification x 800. Scale bar = 10 μm.

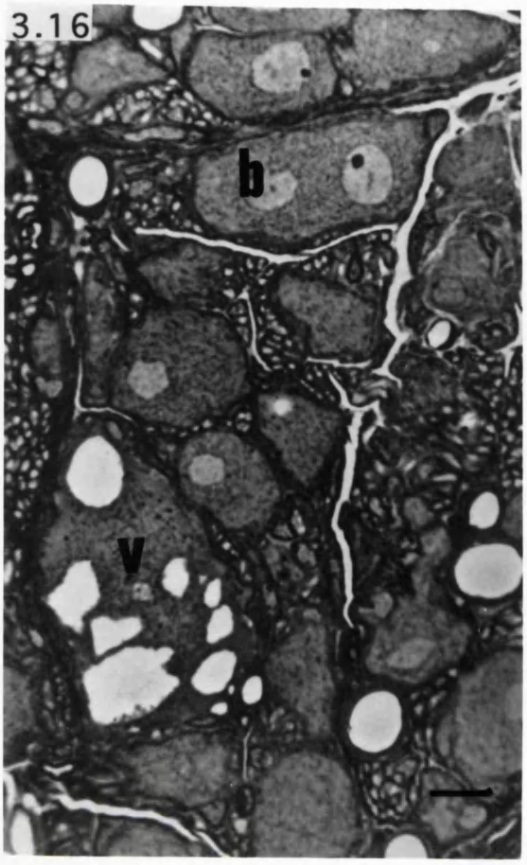
3.16
b
v

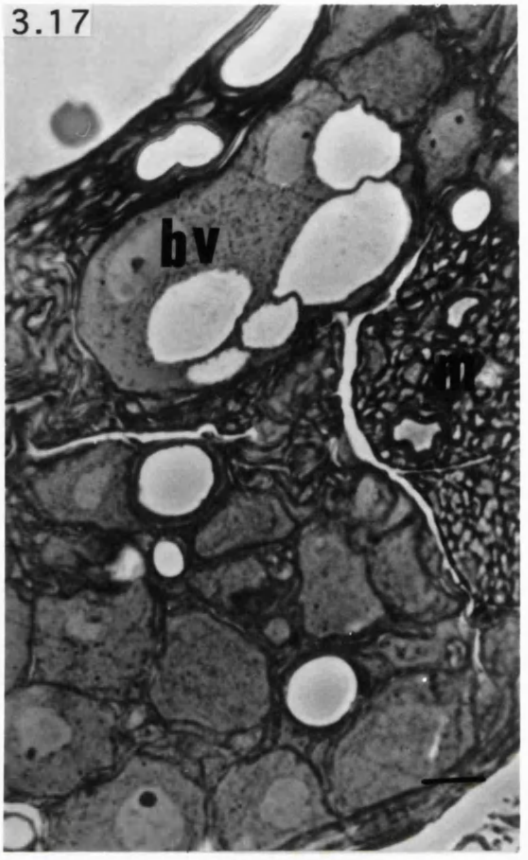
3.17
bv
n

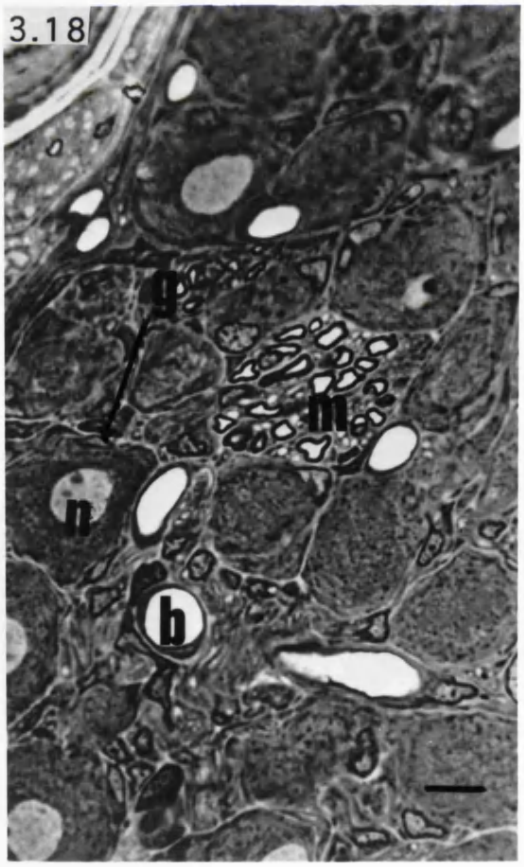
3.18
g
m
n
b

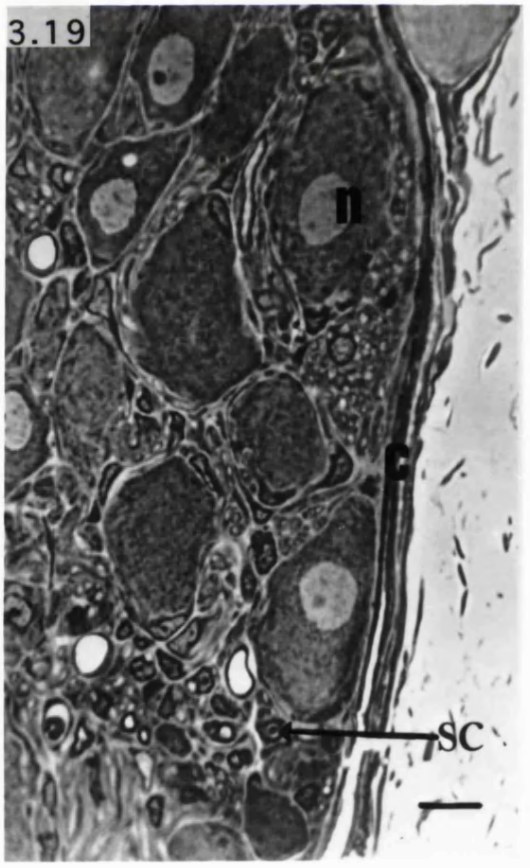
3.19
n
f
SC

3.3 DISCUSSION

This study has shown that the basic anatomical relations of the major pelvic ganglion seen in the adult rat are already present at birth. In addition, a characteristic feature of this ganglion, i.e. that it receives two distinct nerve inputs and projects to many targets, was also present at birth.

The most obvious structural difference between the ganglion at birth and in the adult is its size (volume). The size of the ganglion increases four-fold during the first three months of life. This increase in ganglion size implies an increase in the number or the size of the cellular components of the ganglion. This study has shown that the neurons of the major pelvic ganglion increase eight-fold in average size in the first three months of life. There is therefore a discrepancy between the size increase of the neurons and that of the ganglion as a whole.

One possible explanation for this discrepancy is based on changes in the total number of neurons. There are only few studies on the number of neurons in the rat pelvic ganglion, but recently Bliss (1997) has described a substantial post-natal reduction in the number of pelvic neurons in the female rat (but not the male rat). The counts show about 12,000 neurons at day one and about 7000 neurons in the adult (see also chapter 4), and this by itself could account for the ganglion growing less than its component neurons. Bliss also presented some data suggesting that the loss of neurons in the female ganglion was due, in part at least, to programmed cell death (apoptosis). Fall in the number of neurons during post-natal life is observed in other autonomic ganglia e.g. the superior cervical ganglion. Work done on the superior cervical ganglion by Hendry and Campbell (1976) and more recently by Wright *et al* (1983) showed that there is a loss of 40% of the neurons in the first postnatal week. This decrease in number of neurons in

the superior cervical ganglion, was associated with the presence of degenerating cells. Therefore, both in the superior cervical ganglion and in the major pelvic ganglion, it seems likely that the reduction in neuronal number in the first two weeks of life is due to programmed cell death (apoptosis).

Another factor to consider is the possible migration of neurons during ganglion maturation. At birth there are no accessory ganglia recognizable under the dissecting microscope, whereas in the adult there are 1-3 accessory ganglia, which, however, in the female rat are very small and sometimes absent. In contrast, there is a small number of ganglion neurons located within the wall of the bladder, but these are present in the first two weeks of life and are no longer observed in the adult (Alian and Gabella, 1996).

These anatomical arrangements, and the fact that ganglion neurons are also found scattered within the nerve trunks, make it difficult to produce accurate figures on neuron numbers. However, in the rat by far the largest population of pelvic neurons is located within the major pelvic ganglion. When discussing the post-natal change in ganglion volume, and the fact that its growth is less substantial than that of the neurons, one should also consider the growth of the ganglionic neuropil, blood vessels and connective tissue. In fact, however, all these three components are very poorly developed in the ganglion at birth; in the adult ganglion they occupy a substantially larger proportion of the sectional area than they do in early life.

Histologically, this study has shown that glial cells, are present in the major pelvic ganglion from birth, although no counts were carried out to establish to what extent new glial cells are formed post-natally. The glial cell wrapping (insulation) of the ganglion neurons is incomplete or absent at birth, but develops in the first two weeks of life. This finding leads to the impression that the young neurons rely on trophic support from their extracellular environment during the early stages of postnatal life. During the second post-natal week there is a shift of trophic support from the extracellular environment to

a specialized microenvironment provided by a complete glial cell capsule. Glial cells, were also notably absent from nerve fibres travelling through the ganglion at birth (see also section 5.9), but were observed after the first two weeks of life. Whether appearance of glial cells in nerve fibres and the complete encapsulation (by glial cells) of neurons, is due to redeployment or division of the glial cells in the first two weeks of life is unclear. It is an important question, which will require further investigation.

SIF cells were observed at all stages studied. They were located around blood vessels and at the edge of the ganglion. The location of the SIF cells, may indicate their dependence on some blood-borne factors. And it has been suggested by some workers, notably Wright (1995), that these blood borne factors are glucocorticoids. In terms of quantity, the SIF cells appeared more abundant at birth than in the adult there appeared to be a dilution (or reduction). Counts were not carried out, in view of the considerable inter-individual variability, and therefore it is unclear whether there is a true loss of SIF cells, a dilution or a migration away from the ganglion (as work done by Doupe *et al* (1985) on neonatal superior cervical ganglia SIF cells in culture has shown).

The histological preparations obtained by this study, have shown the nerve fibres of the major pelvic ganglion are all unmyelinated at birth, and the process of myelination appears to start during the second post-natal week. In the adult rat, work done by Hulsebosch and Coggeshall (1982) shows that all the post-ganglionic fibres are unmyelinated, and that the myelinated fibres are either afferent (sensory) or efferent pre-ganglionic. Therefore, the findings of this study show that during the second post-natal week the sensory and preganglionic fibres acquire a greater speed of conduction, and thus must contribute to a more efficient reflex.

As to the capsule, while it is only rudimentary at birth, it forms a complete and continuous lining of the ganglion during the second post-natal week. In this aspect, the

fibroblast capsule of the ganglion is similar to the glial capsule of the neuron: they both provide specialized microenvironments from the second post natal week.

Although not specifically investigated in this study, there is much literature on the importance of trophic factors from the target organ in the growth and survival of neurons. Work done on sympathetic neurons by amongst others Korsching and Thoenen (1988), Gorin and Johnson (1979), shows that endogenous Nerve Growth Factor (NGF) is retrogradely transported from the peripheral tissues. When this NGF is made unavailable to the neurons by treatment with anti-NGF antibodies the neurons die. Therefore, the growth and development of the pelvic ganglion neurons is supported by enlargement of the target tissues namely the bladder, rectum, vagina and uterus giving rise, presumably, to higher levels of growth factors.

4. MORPHOMETRIC STUDY OF TOTAL NUMBER OF NEURONS IN THE PELVIC GANGLION OF THE ADULT FEMALE SPRAGUE-DAWLEY RAT

The number of neurons present in the adult female Sprague-Dawley rat pelvic ganglion was studied using 3 different techniques: total reconstruction, the dissector method and, lastly, partial reconstruction.

4.1 TOTAL RECONSTRUCTION OF ADULT FEMALE MAJOR PELVIC GANGLION

In order to accurately count the total number of neurons present in the pelvic ganglion, each and every neuron was labelled and numbered on all the photomicrographs in which it appeared. The ganglion measured on average 0.213 mm^3 in volume and comprised about 7,800 neurons (Table 14). There was considerable variability: the largest of the three ganglia was 61% larger than the smallest, and it contained 71% more neurons.

Table 14. Total number of neurons present in the right pelvic ganglion of adult female Sprague-Dawley

Animal	Ganglion Volume ($10^6 \mu m^3$)	Ganglion length (μm)	Number of Neurons
S-D.01	259.0	1,708	10,332
S-D.02	218.7	1,400	7,143
S-D.03	161.3	978	6,037
Average	**213.0**	**1,362**	**7,837**

4.2 THE DISSECTOR METHOD FOR DETERMINATION OF NUMBER OF NEURONS IN ADULT FEMALE SPRAGUE-DAWLEY RATS

On the sections produced for the total reconstruction, the Disector Method (Sterio, 1984) which is designed to produce an unbiased estimation of cell numbers was applied. The basic principle of the disector method for particle counting is to determine their number per unit volume (numerical density); this is then multiplied by the total volume of the structure giving the cell number estimate.

This method is described in detail in section 2.3.3.5 above.

Disector pairs were taken at 100μm intervals throughout the entire length of the ganglion, and the height of the dissector was 8μm.

Along with the disector pair comparisons undertaken at each of the 100μm intervals, the section area was also measured. The average of these cross-sectional areas was calculated and this multiplied by the length of the ganglion to calculate its volume.

Pairs of sections, 8μm apart selected every 100μm along the length of the ganglion, were used. The number of tops per dissector pair in each ganglion is recorded in Table 15. The summation of the number of tops (Table 16) was divided by the summation of the disector volumes (Table 16). This value was multiplied by the ganglion volume (Table 14) to obtain an estimate of the total number of neurons (Table 16). In each ganglion, the difference from the total number obtained by total reconstruction was an underestimate of between 12-18%.

Table 15. Number of tops per disector pair in 8μm disector.

Ani-mal	A	B	C	D	E	F	G	H	I	J	K	L	M	N
S-D.01	19	28	24	29	35	36	52	61	66	59	66	57	34	29
S-D.02	13	14	16	21	34	29	29	50	53	71	41			
S-D.03	15	20	25	30	57	50	55	62	44					

Table 16. 8 μm disector estimation

Animal	Total Number Of Tops	Total Disector Volume ($10^6\mu m^3$)	Estimate of Neuronal Number	% difference compared with Table 14
S-D.01	595	17.4	8807	-14.8
S-D. 02	371	13.6	5886	-17.6
S-D. 03	358	10.8	5321	-11.9

4.3 DETERMINATION OF GANGLION NEURONAL NUMBERS BY PARTIAL RECONSTRUCTION

In each ganglion three equidistant 'short series' of 200μm were selected and the total number of neurons in each was counted (Table 17). The profile area of the ganglion at each short series, multiplied by the thickness of the short series (200 μm), gave the volume of the short series (Table 17), from which the total number of neurons per ganglion was calculated on the basis of its volume (Table 18). The figures thus obtained were compared, for each ganglion, with those based on total reconstruction: the difference ranged between +6.5% and -10.5% (Table 18).

Table 17. Number of neurons (top line in bold) present in a 200μm slice (short series) and slice volume (10^6 μm^3) (bottom line).

Animal	Slice A	Slice B	Slice C
S-D. 01	**714** 20.7	**1428** 23.8	**833** 37.8
S-D. 02	**625** 24.2	**1000** 31.6	**975** 37.3
S-D. 03	**1667** 36.9	**1600** 44.1	**1250** 29.1

Table 18. Total number of neurons extrapolated from the neuronal density in the three slices.

Animal	Sample A	Sample B	Sample C	Average	% Difference compared with Table 14
S-D. 01	8,947	15,541	5,715	10,067	- 2.6
S-D. 02	5,648	6,925	5,717	6,097	-10.5
S-D. 03	7,288	5,850	6,927	6,688	+ 6.5

Figure 4.1

Three 1-μm-thick serial sections of a pelvic ganglion (A-C), the sections are 4μm apart.

The photomicrograph shows; capsule, c; blood vessels, v; binucleate neurons, b; axonal processes in longitudinal section, p; axons (some myelinated), a.

Magnification x 220.

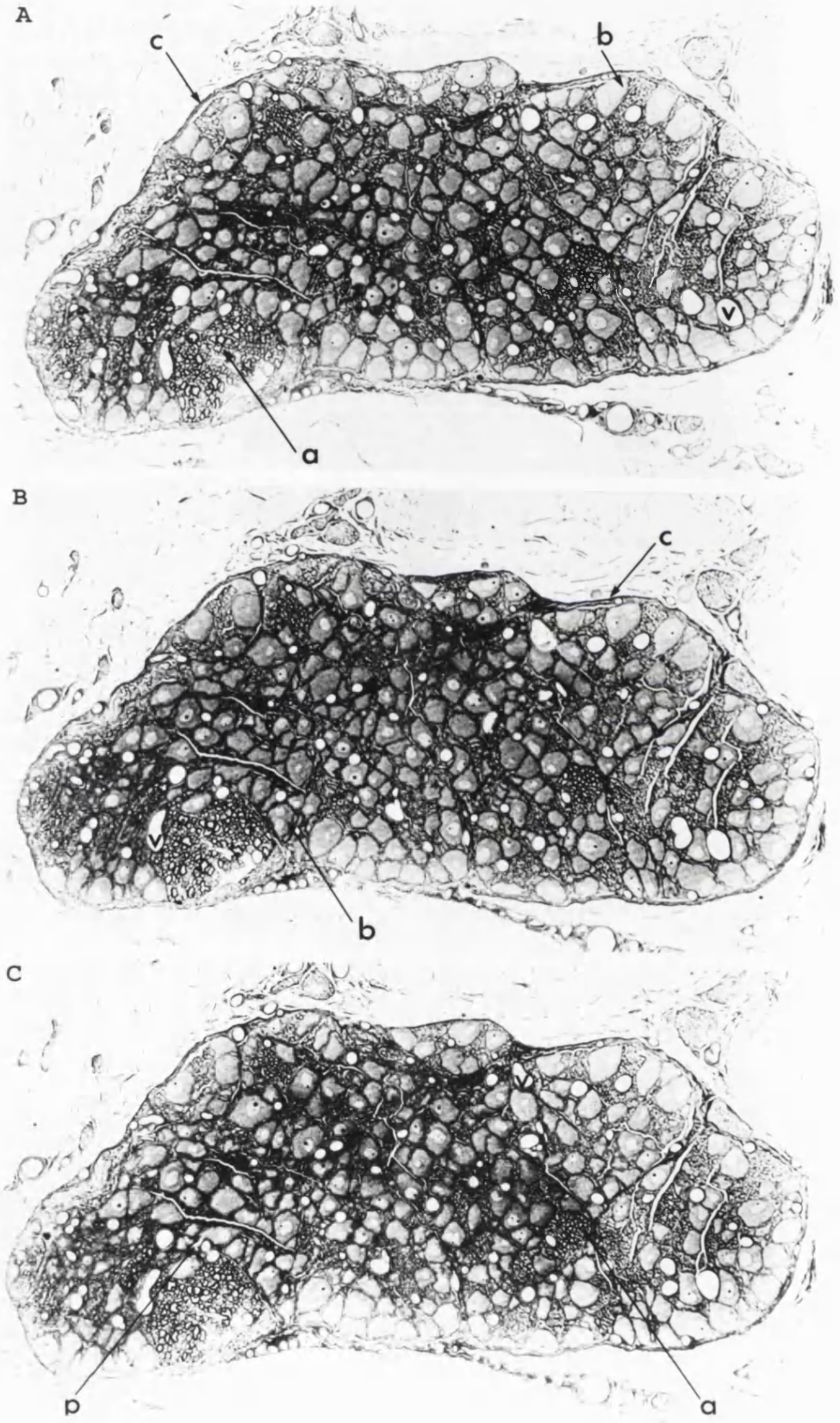

FIGURE 4.1

Figure 4.2

A series of 9 light micrographs of a binucleate vacuolated neuron.

All the sections are 1 μm thick, the sections within each row

are 8 μm apart, while the rows are 16 μm apart.

The profile of one of the nuclei appears in micrograph 4, while the

profile of the second nucleus appears in micrograph 7.

The nucleus of the neuronal glial cell is visible in micrograph 7.

Granular bodies are seen in some of the vacuoles (b) of micrograph 2.

Magnification x 730.

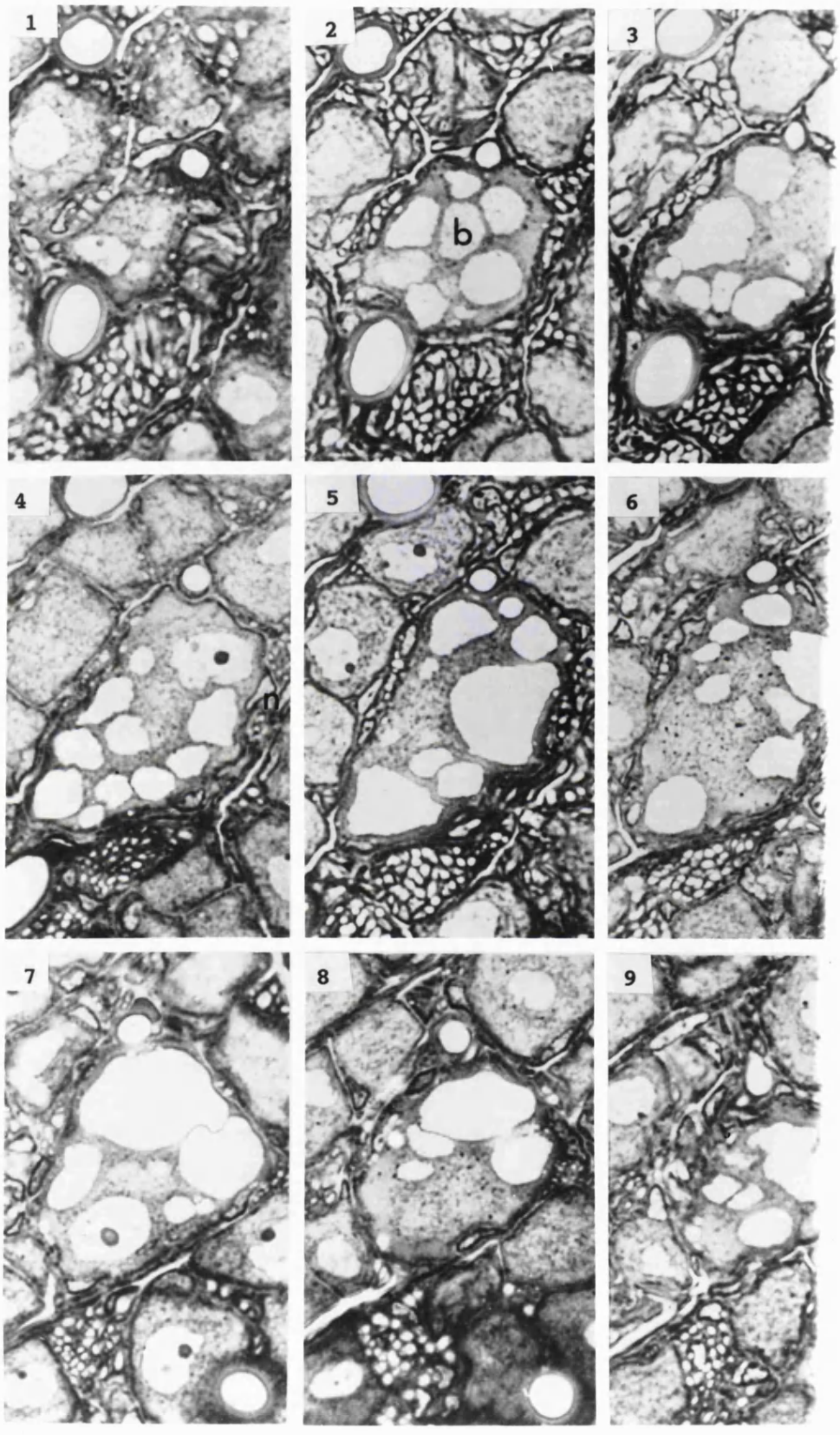

FIGURE 4.2

4.4 DISCUSSION

Total reconstruction of the major pelvic ganglion, although time consuming, gave a reference by which the methods of estimation of neuronal number could be evaluated. The total reconstruction also gave firm evidence of inter-individual variability, for the results showed a 60% difference in neuron number between the smallest and the largest ganglia.

In the evaluation of the number of ganglion neurons, the total reconstruction produces results that are free of assumptions and do not involve sampling. In this study, the method was combined with plastic embedding and very thin sections, so that a high resolution by light microscopy was achieved. There was very little uncertainty in the interpretation of the images. Furthermore, the sections collected in this study can in the future be used for other measurements and collection of structural data on the ganglion and its components.

To test the accuracy of a sampling-based approach, a method of partial reconstruction was applied to the same ganglia as used in the full reconstruction simply by taking into consideration only a fraction of the sections available. The results obtained by partial reconstruction showed a trend towards an underestimation of the true value (i.e. the value obtained by total reconstruction) by about 10%. The pelvic ganglion does not have an entirely uniform neuronal distribution, because the neuronal density varies; in some areas there are fewer neurons and more tracts containing axons or SIF cells, while in other areas the neurons are more densely packed. These two reasons make it necessary to sample more than one region of the ganglion. However, when choosing the regions to be sampled, it was found that the poles of the ganglion should not be used as

these tend to give misleading figures due to their small cross-sectional area and high neuropil-to-neuron ratio.

The main advantage of this method over other classical estimating methods is that the counts are carried out directly on the neuronal cell bodies. In other classical estimating methods, for example the 'empirical method' used by Pover and Coggeshall (1991), the counts are carried out on nuclei or nucleoli. Direct counting of the neuronal cell bodies removes errors that may occur due to ambiguous identification of the nucleolus and variations in the number of nucleoli per nucleus. As a result of the direct counts on neuronal cell bodies, the partial reconstruction does not involve the use of correctional factors as are used for example in the empirical method, and therefore can be viewed as more accurate than these methods. The principal advantage of partial reconstruction over total reconstruction is that partial reconstruction is less time-consuming and expensive than total reconstruction.

However, the method has limitations. It would be inappropriate for very short ganglia (length less than 700 μm) and/or very narrow ganglia. As one needs at least 3 slices with volumes of no less than 20 million μm^3 in order to make an accurate estimate, slices with volumes less than this will significantly lower the accuracy of the method.

The disector method too was applied to the same ganglia as used in the full reconstruction. An underestimate of 15% of the true number of neurons (i.e. the value obtained by total reconstruction), was produced by the disector method. The approximate 85% level of accuracy is lower than that recorded by Pover and Coggeshall (1991) who, although using wax embedded tissue, achieved an accuracy of between 97-102%. However, the underestimate in this work is consistent in all the ganglia studied and it may, therefore, be assumed that it is a shortcoming of the method.

Investigations into the disector technique employing a mathematical model where particles being counted are perfect spherical objects randomly spread throughout the body, reveal that it is in essence an accurate estimating technique. By contrast, the pelvic ganglion presents a more complex structure: the 'particles' (neurons) are heterogeneous in size, in some areas they are densely packed one on top of one another, and they are ovoid or only very approximately spherical, their long axis lying in many cases oblique to the line of sectioning.

The underestimation of the neuron number may stem from the difficulty in counting the number of tops in each section pair. The number of tops in each disector is often less than 60, even in the sections through the largest region, and small numbers of tops added or overlooked may have significant effects. The problem in top identification is a visual one. Although contrast in the prints produced is as high as possible, it is often difficult to differentiate between a top and the surrounding neuropil.

The process of top counting is also made difficult by section thickness which affects the clarity of the micrograph and imparts a 'depth' to each micrograph. The sections used in this work were 1μm thick, cut from resin embedded tissue, and giving a high resolution. This quality may sometimes be counter-productive as a great deal of fine details become visible and the risk of error in labelling tops increases. In less clear preparations (e.g. thicker, wax embedded sections) the presence or not of a stained neuronal profile is the only option available as little other cytological details are visible.

Other situations that may affect top counting are due to the characteristics of the ganglion itself. One such situation occurs when a second neuron is present soon after the previous one and in practically the same spatial position as the first, or when neurons lie obliquely to the plane of section. In the first case a top would be missed, while in the second case a top would be incorrectly recorded.

The outcome would be no better if nuclei had been selected as the 'particles' to be investigated rather than the perikarya. In numerous sections throughout each of the three ganglia, despite the nuclear material staining a lighter hue than the rest of the cell, many cases of indistinct termination of the nuclear body occurred, thus bringing about the same errors as previously described.

As can be seen from the above possible sources of error, the disector is not entirely a trouble free estimating technique. Although there is no doubt that in certain tissues the disector estimating technique is a valuable tool, it is apparent that, as is seen with most mathematical estimating techniques, the further away one gets from an ideal mathematical model (i.e. the more the biological variation is observed) the more inaccurate the estimating tool becomes. However, the underestimation observed is consistent enough to allow the calculation of a correctional factor which could be used to compensate for this small error.

5. ELECTRON MICROSCOPY OF PELVIC GANGLION AT BIRTH

The ultrastructure of the pelvic ganglion of the newborn rat was studied in the transmission electron microscope after dissection, fixation, embedding, sectioning and subsequent staining as described in section 2.4 above.

5.1 CAPSULE

The pelvic ganglion of the newborn rat was surrounded by a condensation of connective tissue referred to as the ganglion capsule. The capsule consisted of a layer of one to three flattened cells, presumably fibroblasts, with collagen fibrils between them. The fibroblasts of the capsule lay parallel to each other and at some points were very close to each other, but no tight junctions were observed between them. The fibroblasts had electron dense nuclei and only a rim of cytoplasm which continued into laminar processes. The cytoplasm contained all the usual cell organelles: mitochondria, Golgi apparatus, rough and smooth endoplasmic reticulum.

Occasionally a small blood vessel was seen running between the fibroblasts that formed the capsule (figure 5.12).

5.2 INTRAGANGLIONIC CONNECTIVE TISSUE

The cellular components of the newborn pelvic ganglion were tightly packed together, and there was very little connective tissue around and between the cells. The main element of connective tissue was collagen fibrils. The fibrils measured 25 nanometres in diameter and were grouped into small bundles, which were located in the interstices between neurons, along blood vessels (figure 5.12) and around axonal bundles (figure

5.3). The amount of fibrils was very small. The bundles were small and never formed proper laminae spread around or between neurons. Overall, the collagen was poorly developed in contrast with the large amounts of collagen found in adult ganglia.

5.3 NEURONS

The neurons, measuring up to 16 μm in diameter, had a smooth surface and a round or oval profile. Their nucleus was large pale and spherical. In contrast, the glial nuclei were distinguished by their small size and their electron dense appearance (figure 5.6). The most conspicuous components of the neuronal cytoplasm were mitochondria, Golgi apparatus, granular endoplasmic reticulum and ribosomes (figure 5.5).

Mitochondria. Mitochondria were spread throughout the cytoplasm. They were rod-like or round, with clearly defined cristae, and measured 0.2 -0.6μm.

Golgi apparatus. The Golgi complex was situated approximately one third of the distance from the nuclear membrane to the cell membrane. It appeared as groups of flattened smooth cisternae located closely together and surrounded by numerous small vesicles.

Rough (granular) Endoplasmic Reticulum. Rough endoplasmic reticulum consisted of flat cisternae, usually about 0.5 μm wide, which were studded with ribosomes. These cisternae appeared unrelated with each other and did not form stacks or parallel arrangements. Between the cisternae there were rosettes of ribosomes.

Smooth Endoplasmic Reticulum. Smooth endoplasmic reticulum were observed as smooth surfaced cisternae and tubules at the periphery of Golgi complexes.

Lysosomes. In many perikarya some lysosomes were observed; they were circular, electron dense and about 0.3 μm in diameter.

Microtubules. Microtubules, a cytoplasmic component that is well developed in the mature ganglion neurons, were very sparsely represented at this stage.

The cell membrane of the ganglion neurons was smooth except at the points of emergence of processes and displayed little specialization. As regards the relation of the perikaryal membrane with the surrounding structures, there were four different configurations. In some areas the neurons were in direct membrane-to-membrane contact with one another (figure 5.5), the distance between to two cell membranes being about 10 nanometres. Along these regions the cell membranes were parallel, straight, devoid of specialized junctions; often there was some condensation of organelles such as endoplasmic reticulum and mitochondria (figure 5.7), but there was no cytoplasmic continuity or bridges between the cells. Some areas of direct contact bordered with regions where the neurons were separated by a wedge-shaped space occupied by collagen fibrils (figure 5.9); here the neuronal membranes were lined by a basal lamina.

In other areas, neurons had direct membrane-to-membrane contact with SIF cells (figure 5.5). Some neurons were in direct membrane-to-membrane contact with glial cells (figure 5.6); at the point of contact with a neuron the glial cells did not have a basement membrane. Some of the neuronal profiles were associated with more than one glial cell (figures 5.6, 5.11). There was little or no collagen between the glial cells and the neurons, and some neurons did not have any glial cell association at all. Lastly, there were areas were the neuron was in synaptic contact with axons of other neurons.

5.3.1 Neuronal nuclei

The nucleus of the newborn rat ganglion neuron was generally located centrally or paracentrally, although in some cases it was seen at the edge of the neuronal cell body. The nucleus was surrounded by a well-defined continuous double membrane called the neurolemma or nuclear envelope. Within the nucleus were grains of chromatin, more

concentrated at the neurolemma than in the center of the nucleus and one or two prominent nucleoli.

In sectional area, the ratio of the nucleus to the cytoplasm was an average of 0.47 (Table 19, n = 24).

Table 19 Ratio of Nuclear Area to Cytoplasm Area in Neuronal Cell Profiles.

Neuron	Nucleus Area in μm^2	Cytoplasm Area in μm^2	Ratio
1	58	185	0.31
2	51	86	0.59
3	45	89	0.51
4	24	79	0.30
5	91	172	0.53
6	79	126	0.56
7	80	121	0.66
8	39	90	0.43
9	66	194	0.34
10	61	113	0.54
11	93	164	0.57
12	43	71	0.61
13	69	120	0.58
14	69	182	0.38
15	55	134	0.41
16	60	94	0.64
17	59	118	0.50
18	68	160	0.43
19	46	164	0.28
20	56	140	0.40
21	55	149	0.37
22	39	140	0.28
23	55	95	0.58
24	66	131	0.50
Total	**1427**	**2977**	**11.30**
Average	**59.5**	**124.0**	**0.47**

5.3.2 Glial cells

Cells located close to neurons, with electron dense nuclei 6 - 8 μm wide and a thin rim of cytoplasm were identified as glial cells. Their frequency was variable; some neuronal profiles showed none (figure 5.1), others had up to four (figure 5.10) and were seen in some cases sending processes along the borders of the neurons. However; none of the neurons had a complete glial capsule. Occasionally the intercellular distance between the glial cells and the neurons was as little as 15 nm and there was no basement membrane in between the two cells.

5.3.3 Neuronal processes

Small neuronal profiles containing mitochondria and endoplasmic reticulum lay near neurons and were identified as dendrites. Although several processes of this type lay around neurons, their actual continuity with the perikaryon was documented only very occasionally. Some of these dendrites had synapses on them (figure 5.11).

5.4 Synapses

Nerve endings, approximately circular and 0.5 - 1.0 μm in diameter, abutted onto perikarya and dendrites, forming axosomatic and axodendritic (figure 5.11) synapses. The dense area of the synapse was shorter than the area of apposition of the pre- and post-synaptic membranes. The nerve endings forming the presynaptic component of the synapse contained numerous clear small vesicles, the average diameter of which was 50 nm.

5.5 SIF Cells

The pelvic ganglion of the newborn rat contained a population of cells with small electron dense nuclei and a thin rim of cytoplasm containing granular vesicles, which were found either in groups or as single cells and tended to be located at the periphery of the ganglion or around the small blood vessels. These cells were identified as SIF (Small Intensely Fluorescent) cells. These cells had abundant mitochondria, granules and vacuoles in their cytoplasm.

The newborn rat SIF cells were found to have processes (figure 5.6), some of which extended to neighboring SIF cells.

Some of the SIF cells had extensive membrane-to-membrane contact with other SIF cells, and some SIF cells were seen in membrane-to-membrane contact with neurons.

It must be noted that in some instances (when nucleus was less electron-dense and there were few cytoplasmic vacuoles) these cells resemble neurons, in which cases it was only possible to differentiate them from neurons by the scarcity of their cytoplasm.

5.6 Nerve Fibres

The ganglion of the newborn rat had several clearly defined nerve fibres running through it. The bundles of fibres varied in shape from almost circular to elliptical, and varied in diameter from 20 μm to one μm and contained only 3-4 axons. The nerve fibres were covered by a thin, continuous, capsule of connective tissue laid down by flattened cells (presumably fibroblasts). The nerve fibres generally contained one or two peripherally placed Schwann cell nuclei, axons and very small amounts of collagen. The axons were occasionally divided into groups by septa of Schwann cell cytoplasm, but individual axons were not covered by Schwann cell cytoplasm and were therefore in direct contact with one another. All the axons seen in the nerves of the pelvic ganglion at birth were unmyelinated; no myelinated axons were seen in any of the preparations.

The nerves of the newborn rat ganglion had only a modest amount of collagen fibres, all of which were located near the capsule of the nerve fibre; no collagen was seen in between the axons of the nerve fibre (figure 5.3).

5.7 Blood vessels

The pelvic ganglion at birth had several small blood vessels distributed evenly through it, and occasionally some of them where intracapsular. These blood vessels when fixed by perfusion, appeared oval or circular in cross section, a fact implying that they ran parallel to the sides of the ganglion, and therefore ran dorso-ventrally in relation to the body of the rat.

The blood vessels of the newborn rat pelvic ganglion were lined by flattened endothelial cells 0.2 - 0.5 μm thick, the nucleus of these cells was small not centrally placed. The lining of the blood vessels appeared continuous with the cells having tight intercellular junctions (figure 5.2), no fenestrations or open intercellular junctions were seen. Occasionally, blood vessels with a layer of smooth muscle cells around them were seen and they were identified as arterioles. The vast majority of the blood vessels did no have a muscular coat; the smaller blood vessels of this group were identified as capillaries and the larger were identified as venules.

5.8 APOPTOTIC CELLS

In every preparation studied there were a few cells showing signs of cell death such as ruptured nuclear membranes and fragments of organelles in their cytoplasm; these were identified as apoptotic cells.

Figure 5.01

Electron micrograph of a pelvic ganglion neuron from a rat at birth.

This neuron is not associated with a sheath of glial cells.

The micrograph shows: N, nucleus; n, nucleolus; C, cytoplasm;

m, cell membrane, which outlines the already complex shape

of the neuron. Magnification x 9250.

Scale bar = 1 μm.

Figure 5.02

Electron micrograph of major pelvic ganglion at birth.

The micrograph shows: N, neuronal nucleus; B, blood vessel; T,

tight junction between to endothelial cells; S, axo-dendritic synapse.

Magnification x 9250

Scale bar = 1 μm

5.01

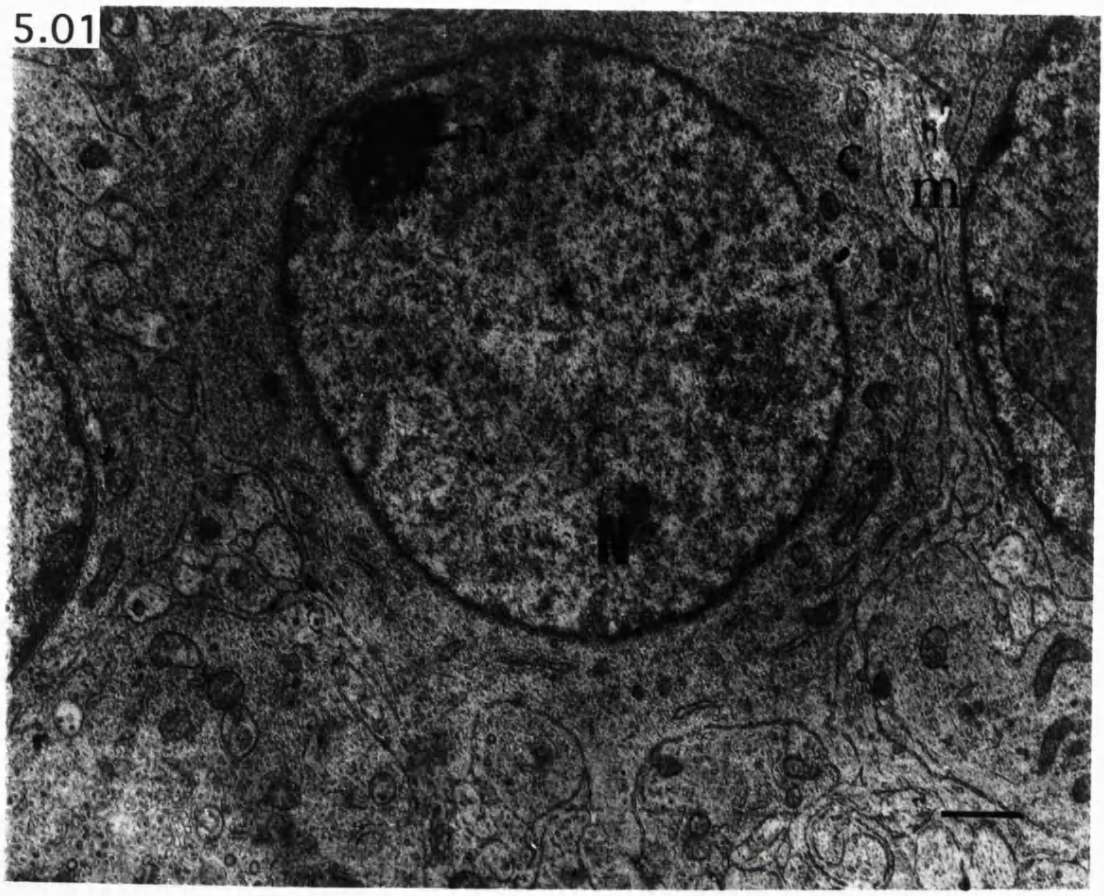

5.02

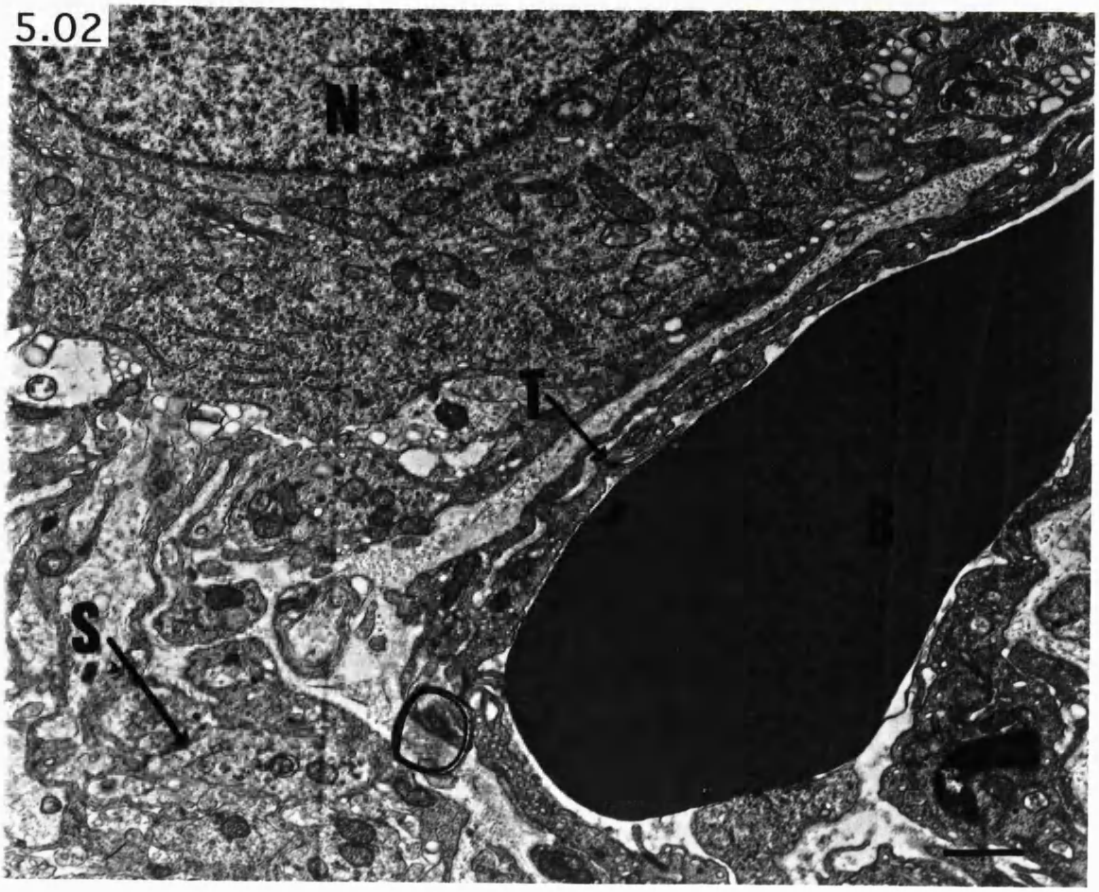

Figure 5.03

Electron micrograph of major pelvic ganglion at birth showing an intraganglionic nerve bundle, with unmyelinated axons (a) and two peripherally placed Schwann cell nuclei (S), surrounded by collagen fibrils (c). Magnification x 9250

Scale bar = 1 μm

Figure 5.04

Electron micrograph of Major pelvic ganglion at birth showing; a neuron (N) with; M, mitochondria; r, ribosomes; g, golgi apparatus an axodendritic synapse (S). Magnification x 9250

Scale bar = 1 μm.

5.03

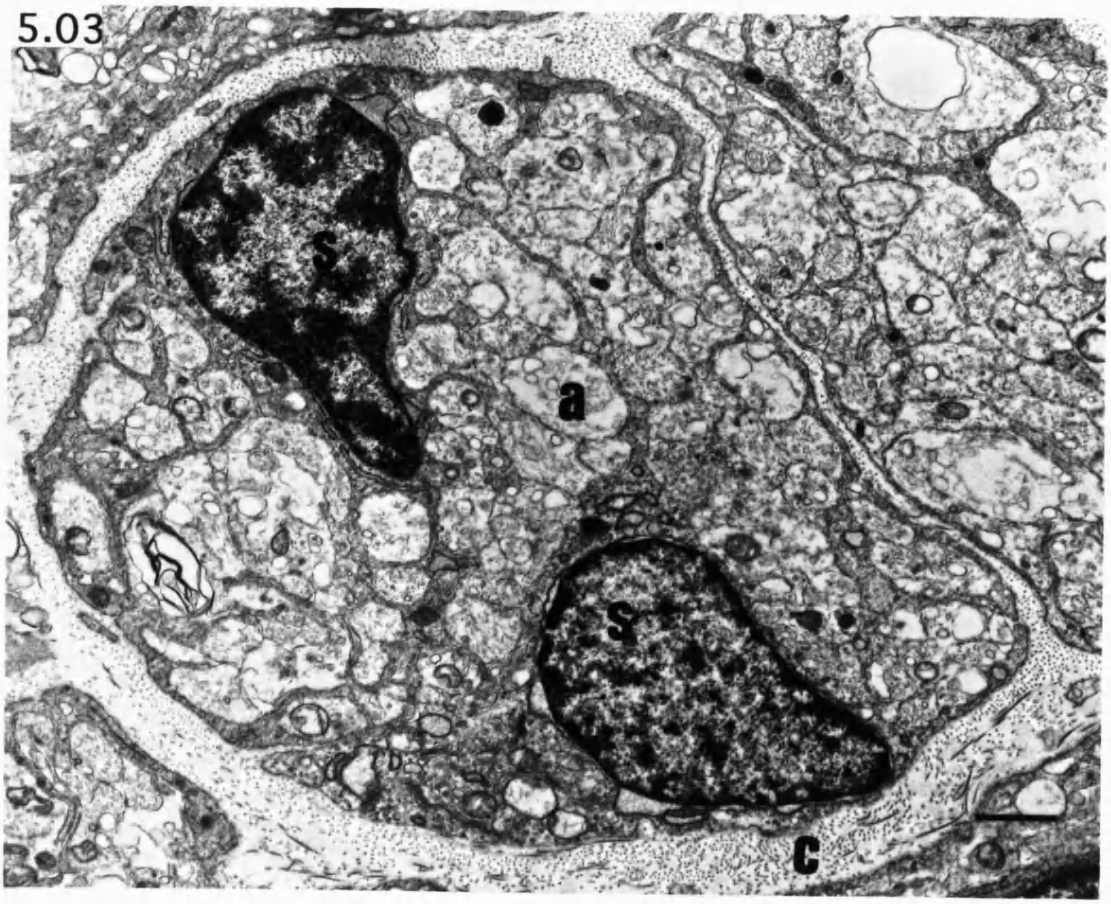

5.04

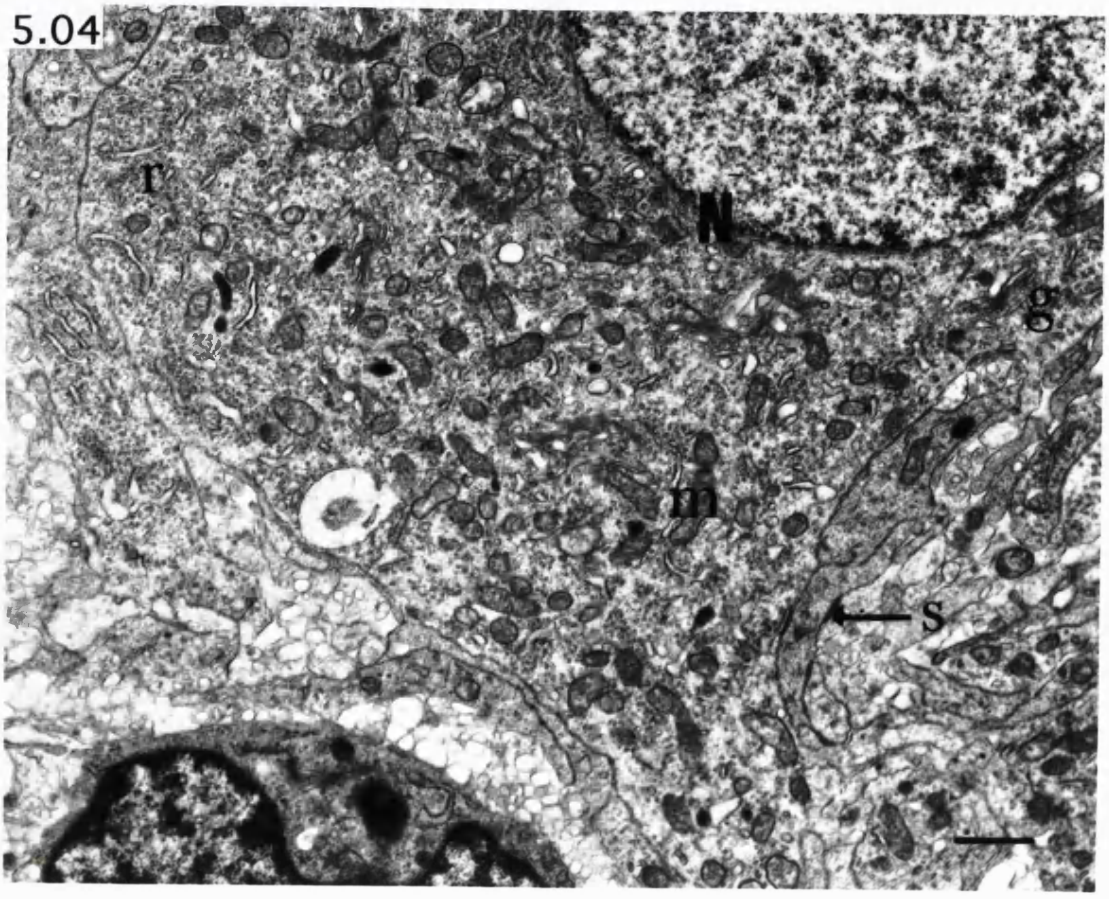

Figure 5.05

Electron micrograph of Major pelvic ganglion at birth showing two neurons (N1) and (N2) which have a large area of direct contact with each other with cell membranes less than 10 nm apart. The neurons show the following organelles: m, mitochondria; r, ribosomes; g, Golgi apparatus; R, rough endoplasmic reticulum; sr, smooth endoplasmic reticulum; L, lysosomes. S, Glial cell nucleus.

Magnification x 20000

Scale bar = 1 μm.

5.05

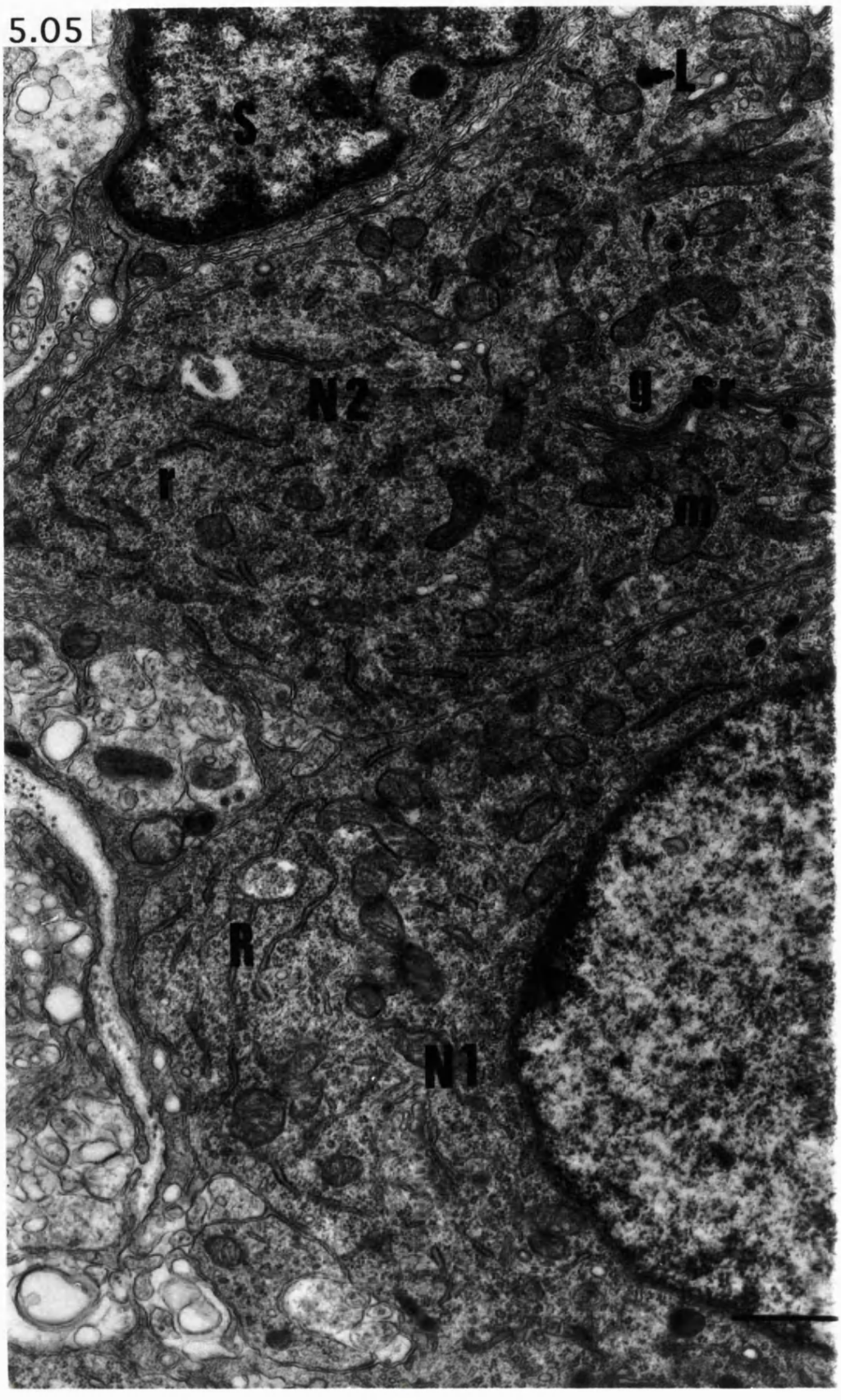

Figure 5.6

Electron micrograph of major pelvic ganglion at birth, showing a nucleated neuronal profile (N) and two nucleated glial cell profiles (G). SIF cell (S), and SIF cell processes (p). Magnification x 9250 Scale bar = 1 μm.

5.6

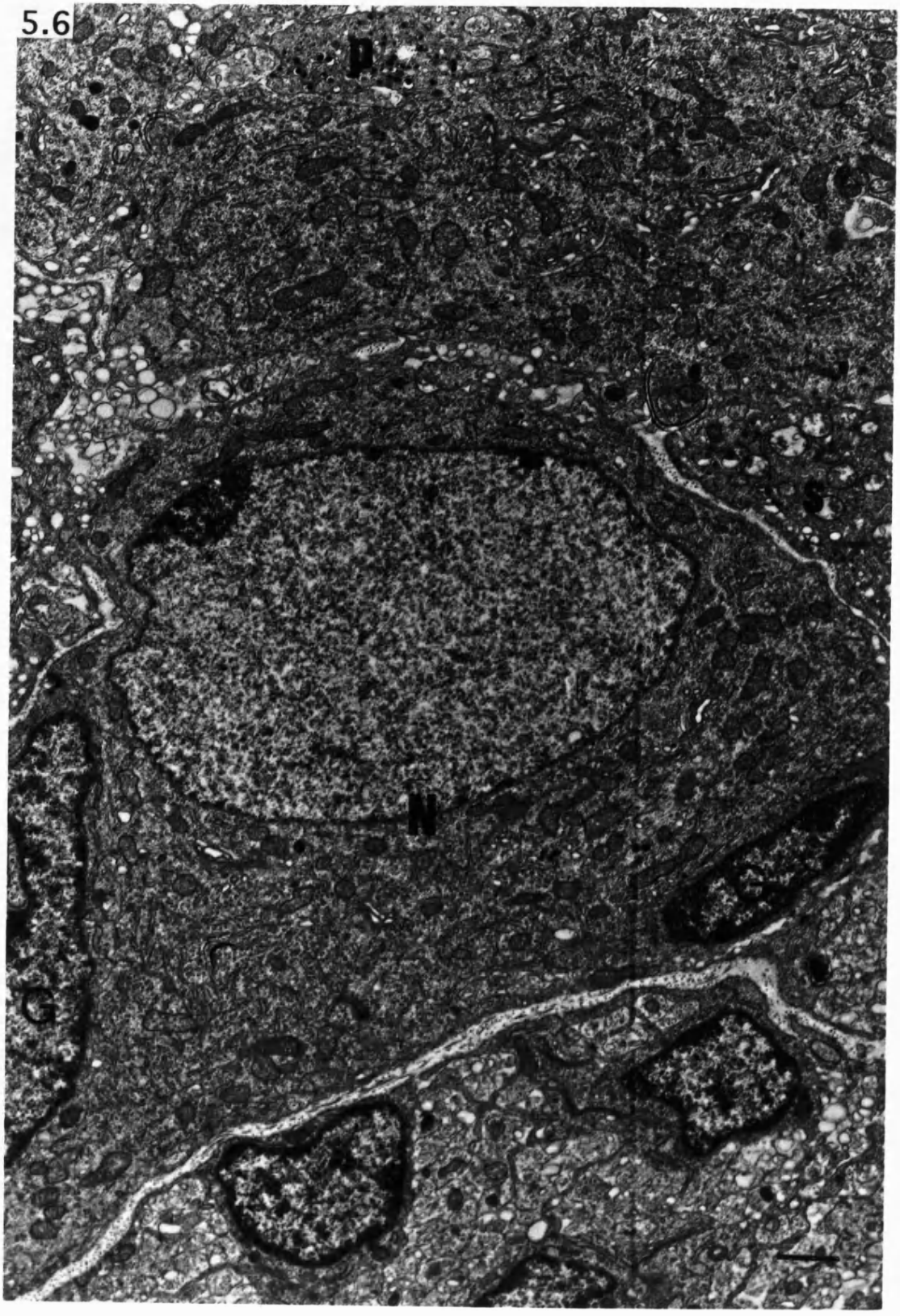

Figure 5.07

Electron micrograph of Major pelvic ganglion at birth showing two neurons (N1 and N2), with their cell membranes close together, and a condensation of organelles in their cytoplasm beneath the cell membranes. The organelles seen are; m, mitochondria; G, Golgi apparatus; L, lysosomes;R, rough endoplasmic reticulum; S, smooth endoplasmic reticulum; r, ribosomes.

Magnification x 20,000

Scale bar = 1 μm.

Figure 5.08

Electron micrograph of Major pelvic ganglion at birth showing; A neuron (N) with a process (P) with an axo-dendritic synapse (S) containing numerous small granules (v), and an axon (A).

Magnification x 20,000

Scale bar = 1 μm.

5.07

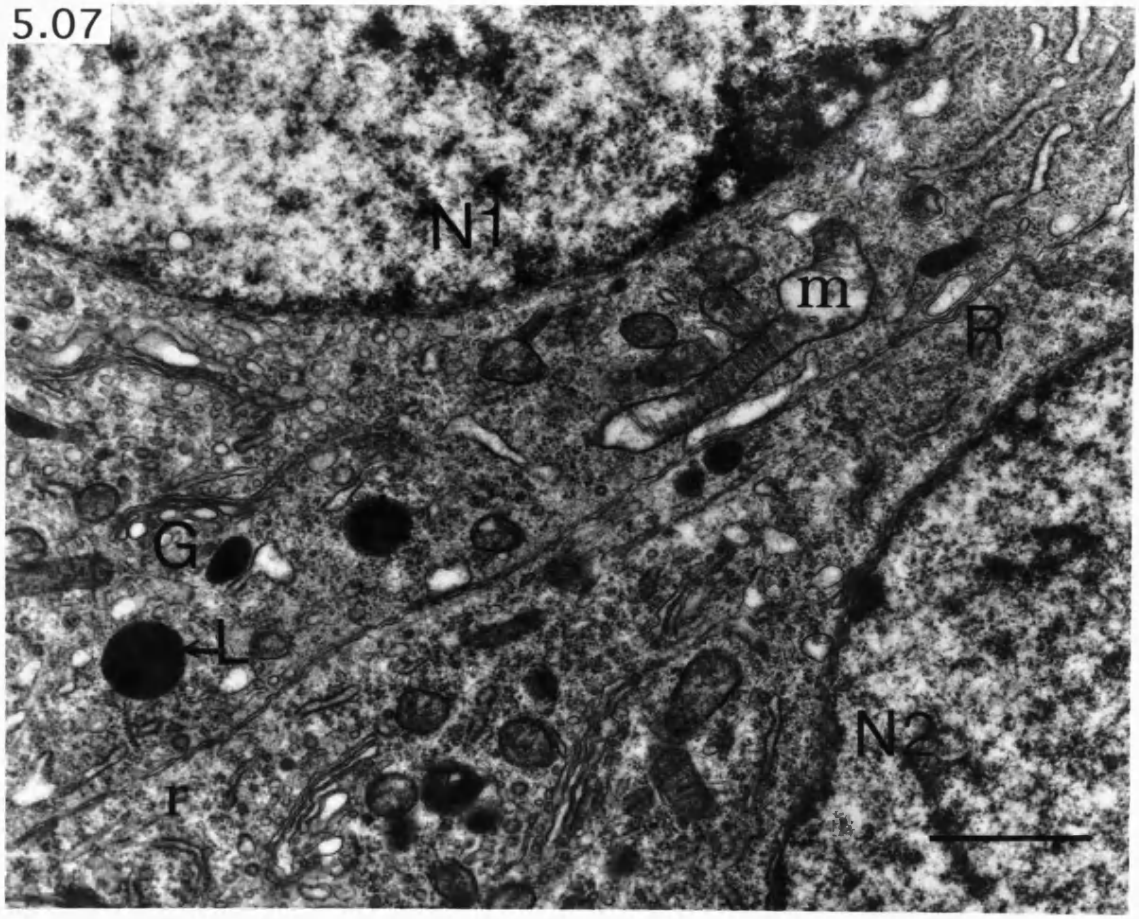

5.08

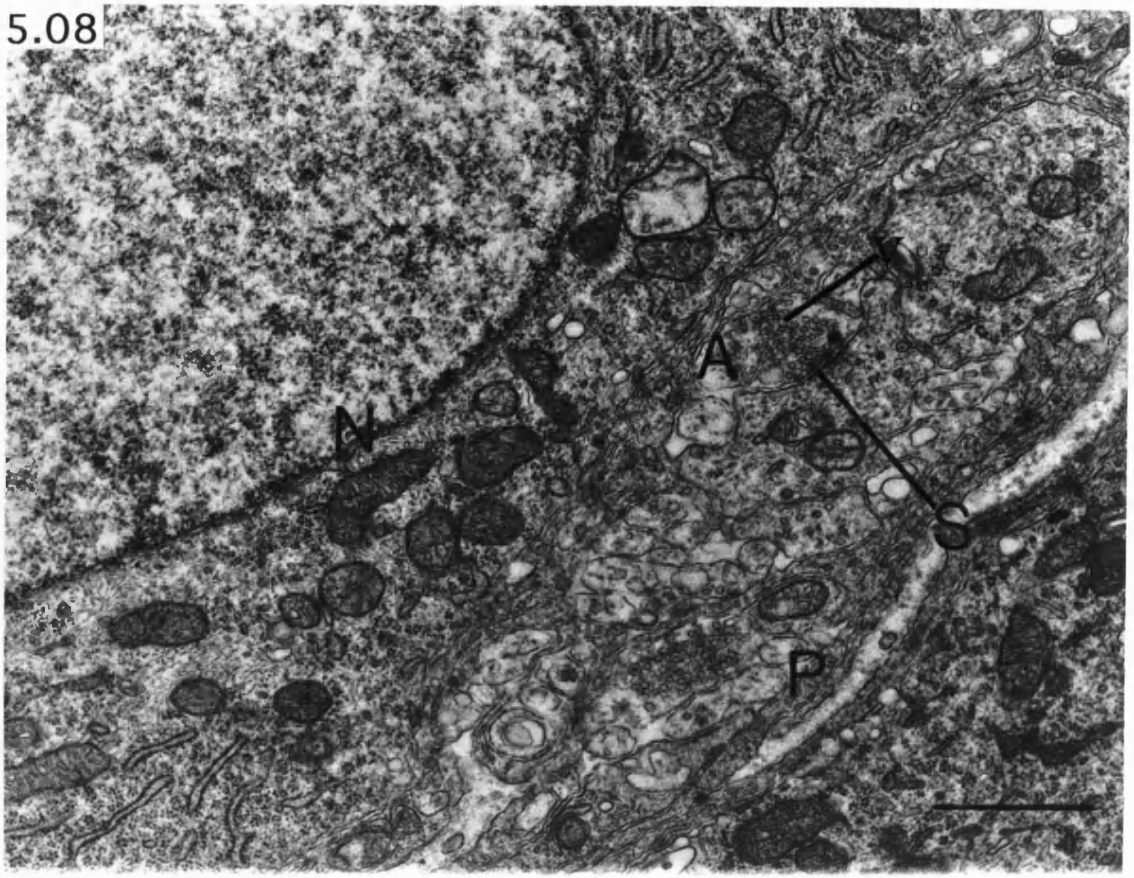

Figure 5.09

Electron micrograph of Major pelvic ganglion at birth showing two neurons (N1 and N2) with an area of direct membrane to membrane contact, and an adjacent area where they are separated by a wedge of collagen (c) and basement membrane. Neuron (N2) is also in direct membrane to membrane contact with a glial cell (G1).

Magnification x 20,000

Scale bar = 1 μm.

5.09

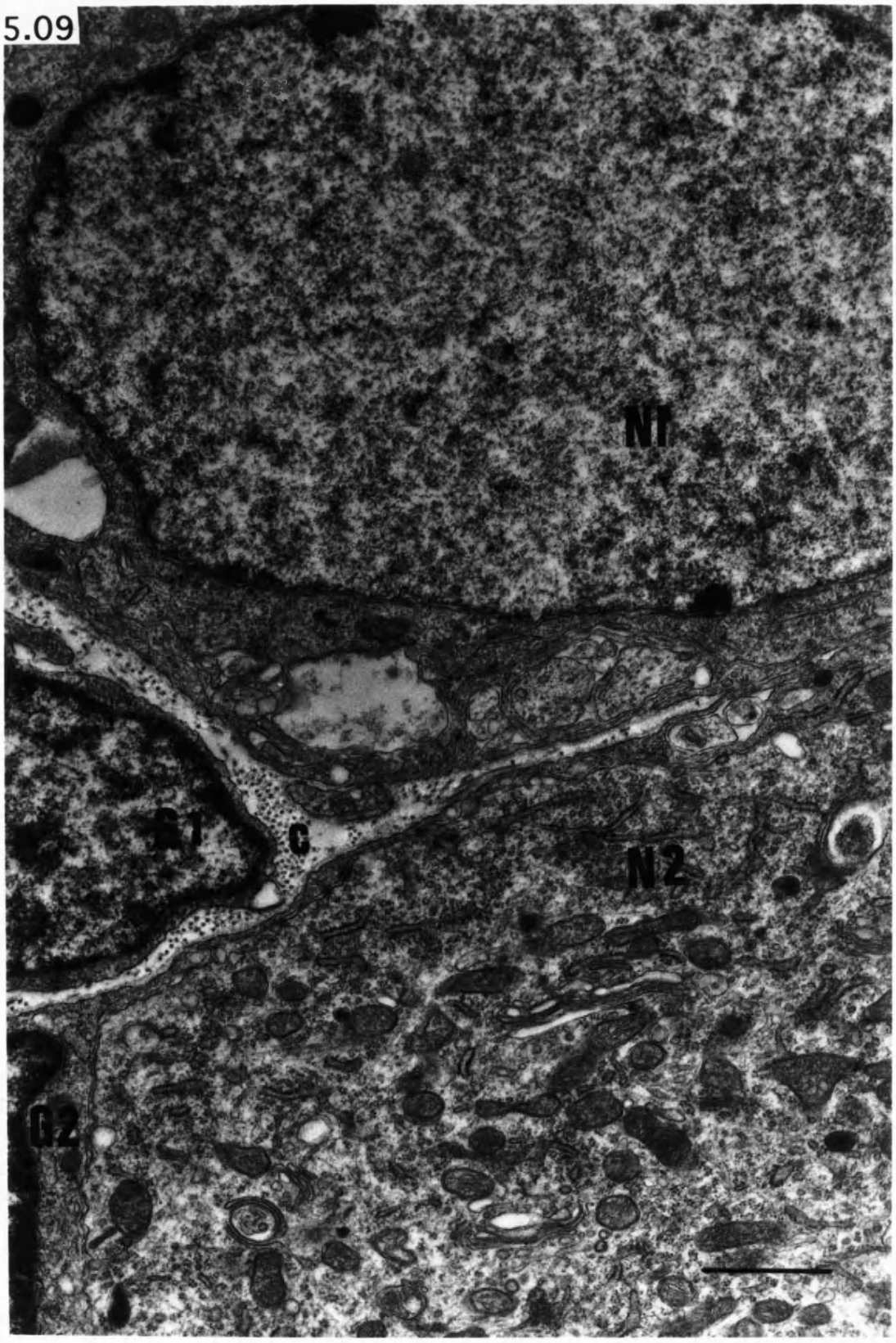

Figure 5.10

Electron micrograph of Major pelvic ganglion at birth showing

a neuron (N) associated with 4 glial cells.

Magnification x 9,250

Scale bar = 1 μm.

5.10

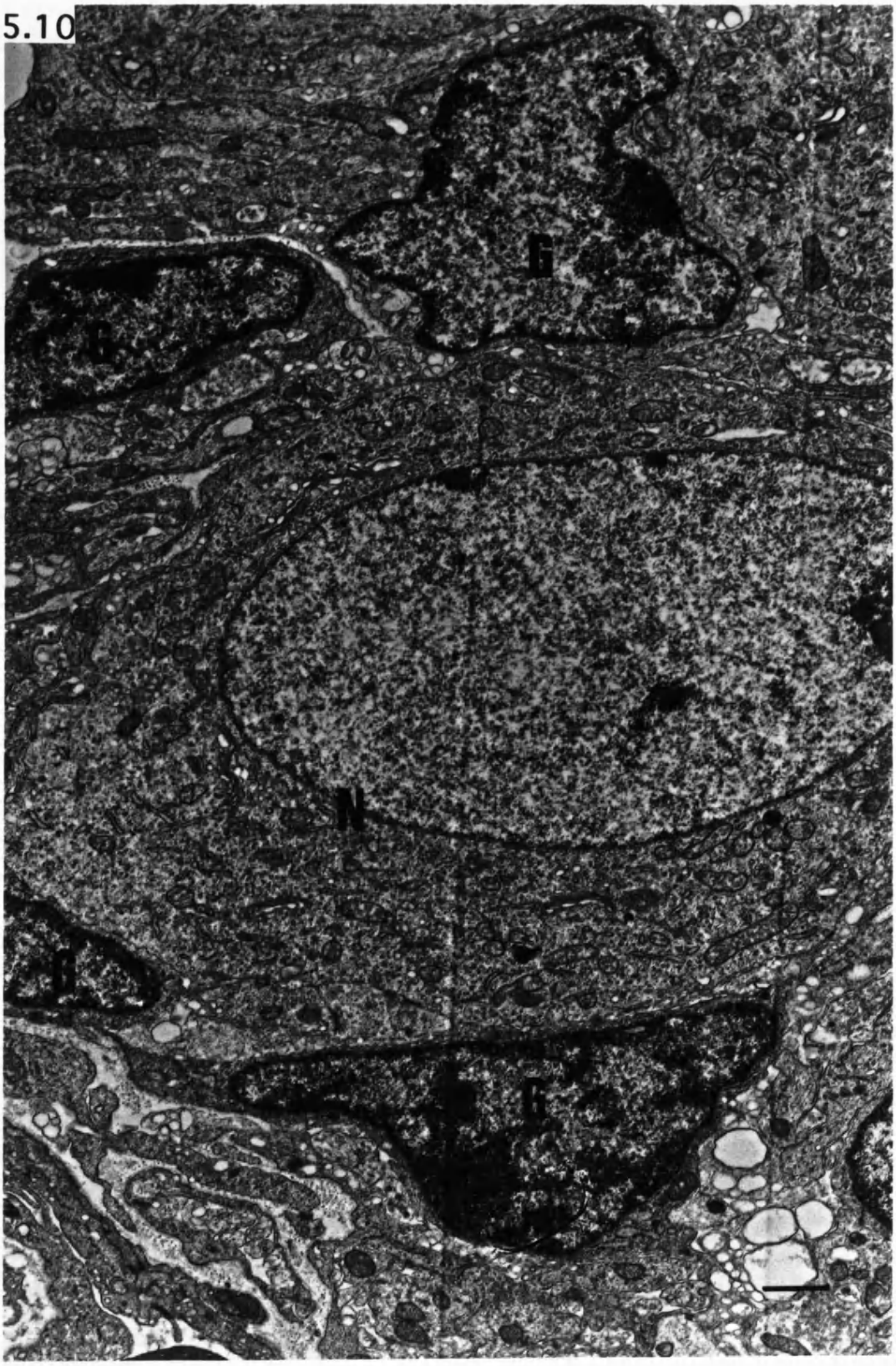

Figure 5.11

Electron micrograph of Major pelvic ganglion at birth

showing three axons (a), exhibiting a total of four axodendritic

synapses (S) filled with numerous small vesicles (v).

There is also an intercellular junction (T).

Magnification x 20,000

Scale bar = 1 μm.

Figure 5.12

Electron micrograph of the capsule of the pelvic ganglion at

birth showing F, fibroblast nuclei; FC, fibroblast cytoplasm;

B, blood vessel; c, collagen fibrils.

Magnification x 9,250

Scale bar = 1 μm.

5.11

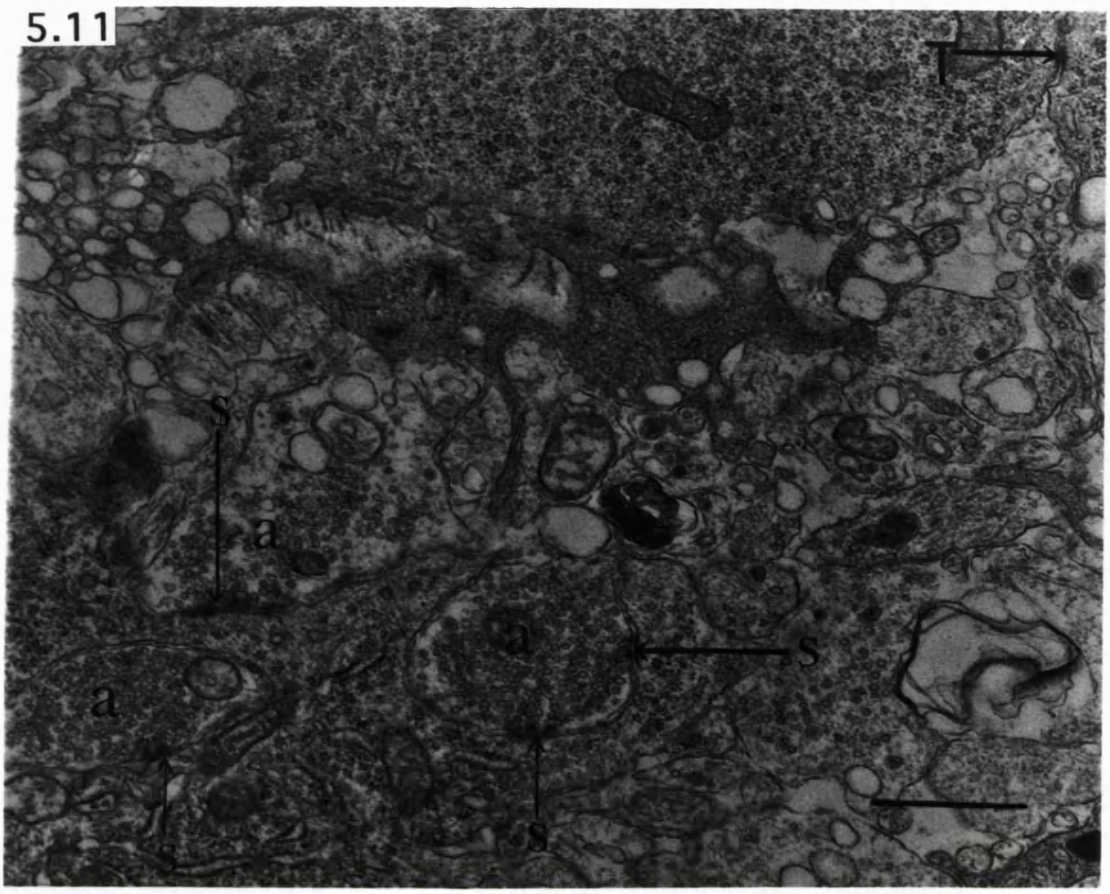

5.12

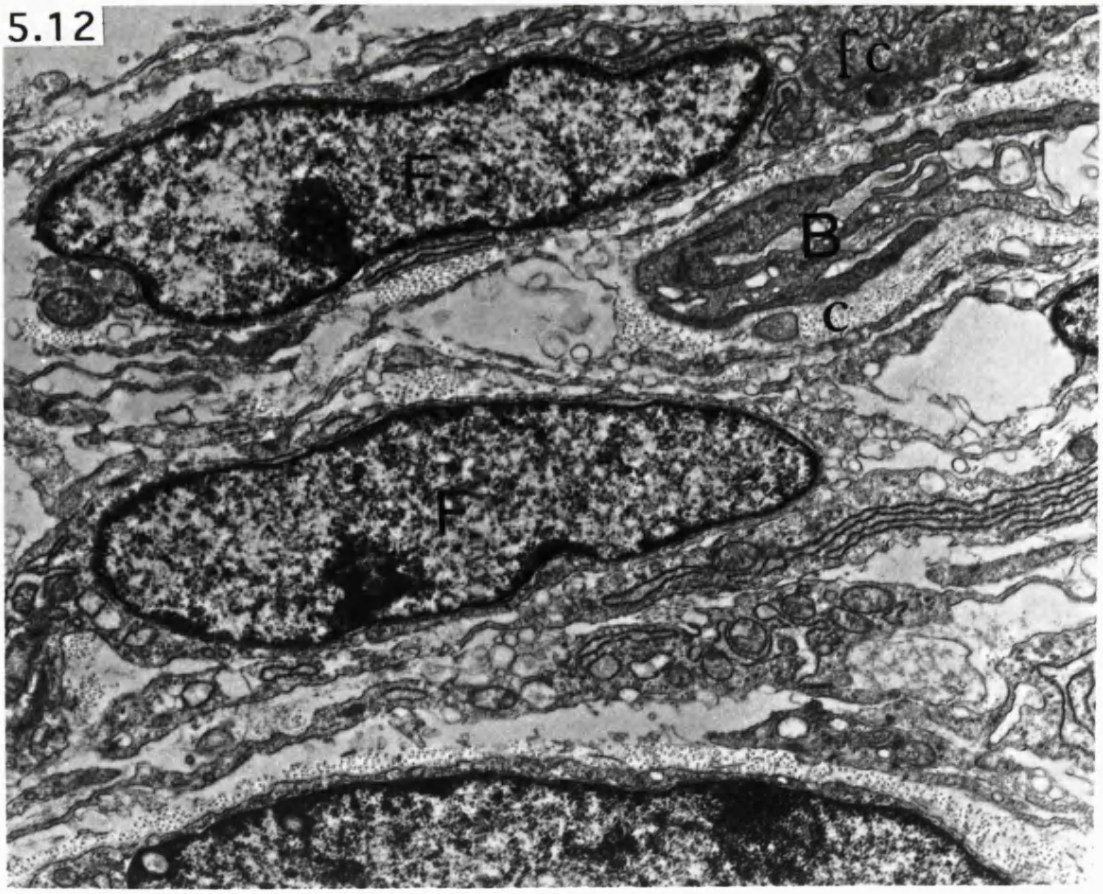

Figure 5.13

Electron micrograph of Major pelvic ganglion at birth showing;

A neuron (N) with a process (P) with an axo-dendritic synapse (S)

containing numerous small granules (v), and an axon (A).

Magnification x 40,000

Scale bar = 1 μm.

5.13

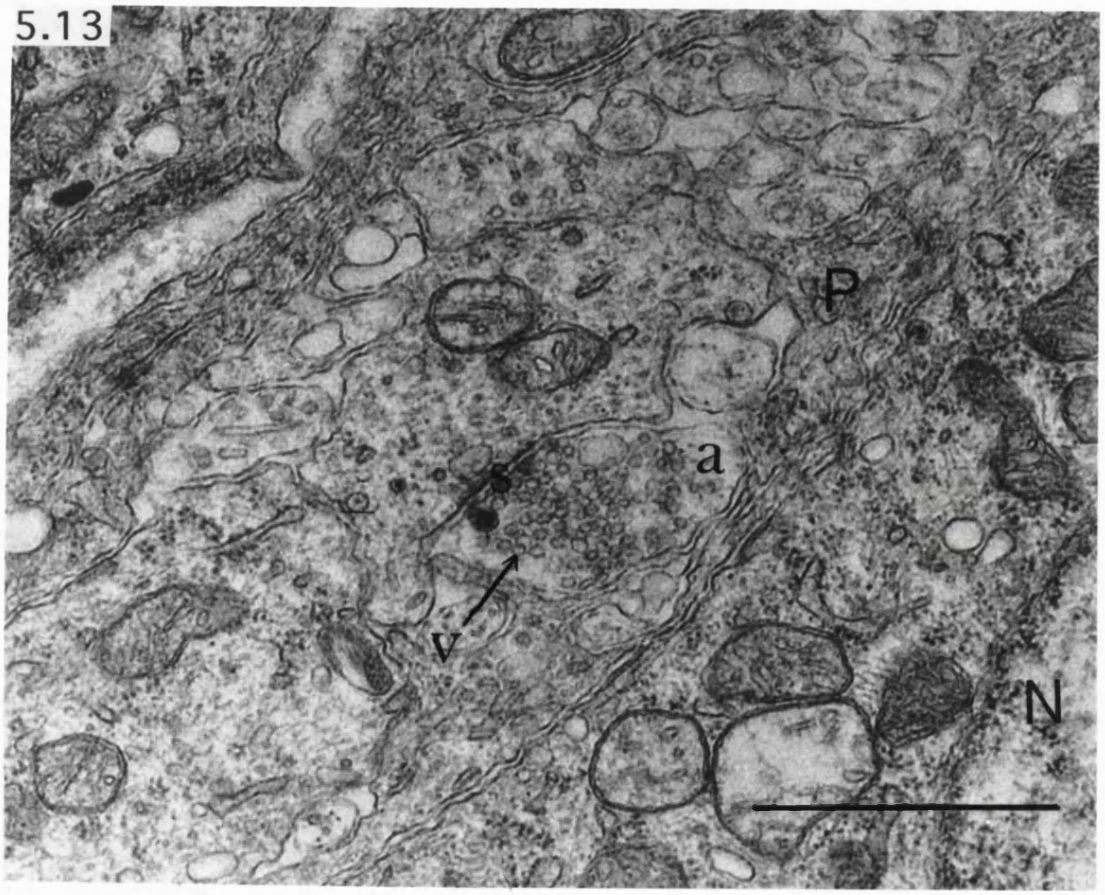

5.9 DISCUSSION

This study has showed that all the basic cell types seen in the adult ganglion are present at birth. However, there are differences in the size, complexity, location and fine structure of the ganglion components seen at birth as opposed to those in the adult.

One difference between the ganglion at birth and that in the adult is that, whereas there is a multi-layered capsule in the adult, in the newborn the capsule is rudimentary and incomplete. In addition in the newborn ganglion there are no septa of connective tissue between groups of neurons, whereas in the adult septa are common and connect up with the main capsule.

The cells that form the rudimentary capsule at birth have only loose intercellular connections. Only later in life and only fully in the adult are there complex intercellular junctions including tight junctions, as reported in other sympathetic and parasympathetic ganglia (Jacobs *et al.*,1976; Jacobs, 1977; Arvidson, 1979). The precursor of the cells that form the capsule of autonomic ganglia has only recently been confirmed. Previously two possible precursors were suggested: fibroblasts and Schwann cells. The capsule cells are similar to Schwann cells as they possess a basement membrane (unlike fibroblasts) and are similar to fibroblasts because they are able to synthesis fibronectin, an extracellular matrix protein. However, they differ from both fibroblasts and Schwann cells because they possess abundant caveolae and tight intercellular junctions. Bunge *et al.,* (1989) have shown by use of a histochemically detectable reporter gene (introduced by a retrovirus into both progenitor fibroblasts and Schwann cells) which enabled them to study the fate of dividing precursor cells, that capsular cells originate from fibroblasts.

In peripheral nerves epineurium, perineurium and endoneurium form distinct layers. In autonomic ganglia these layers are not as distinct as in peripheral nerves and at birth they are even less distinct.

The collagen content and distribution in the newborn pelvic ganglion differ from that reported in the adult. Not only are the collagen fibrils in the newborn smaller than those in the adult, but there is very little collagen seen in the newborn ganglion and it does not form laminae around neurons as reported in the adult.

As to the neurons, the most striking difference between them and those of the adult is the ratio of the size of their nucleus to their cytoplasm, in sectional profile the nucleus occupy half the area of the cytoplasm. In the adult, the nucleus in sectional profile occupies much less than half the area of the neuronal cytoplasm, implying that the neuronal cytoplasm grows more than the nucleus. The cytoplasm of the newborn rat neuron like that of the adult contains granular, filamentous and membranous organelles arranged concentrically round the nucleus. Mitochondria, granular endoplasmic reticulum, smooth endoplasmic reticulum, and Golgi complexes are all present in size and quantity very similar to the adult neuronal cytoplasm. However, lysosomes which are common in autonomic ganglia and in the central nervous system (Peters *et al.,* 1976) are not as frequently observed as in adult pelvic ganglion neurons. This finding agrees with the work of Pick (1970), who reported that lysosomes increase in number with age.

Newborn major pelvic ganglion neurons, in spite of their small size had processes (believed to be dendrites) which are few in number (because they were rarely observed in individual sections). In this respect the newborn pelvic ganglion neuron is similar to the adult where William Tabatabai *et al.,* (1986) reported an average of 1.5 dendrites per neuron (with a maximum of 4).

Both somata and processes are abutted by axons, and at the these points there were all the characteristics of a differentiated synapse, thickening of pre- and post-synaptic

membrane, narrow (10 nm) synaptic gap and numerous small clear vesicles. This experiment did not investigate synaptic functionality, but since the animal at birth can void via a spinal cord reflex, it is assumed that there is transmission through the ganglion and the synaptic junctions observed were the structural correlate of this.

Glial cells rarely spread fully over the surface of the neuron and do not form a capsule round the neurons, which allows the occurrence of two things not seen in the adult. Firstly, the occurrence of large areas of perikaryal membrane directly exposed to the extracellular matrix. Secondly, the occurrence of large areas of direct apposition of neurons. These two aspects of neuronal glial relations are probably of considerable functional significance; the amount of contact between the neuron and the glial cell is limited and this must limit the extent to which trophic support is provided to the neuron by the glial cell. Lack of a complete glial sheath exposes neurons to the extracellular environment, whereas in the adult the complete capsule with tight intercellular junctions completely insulates the neuron from the extracellular environment. Existence of membrane to membrane contact between neurons allows direct exchanges between neurons.

SIF cells, identified by their numerous dense granules, are numerous and resemble those in the adult; their prominence was stressed by some of them having direct membrane-to-membrane contact with neurons. Although there is a theory that SIF cells are more prevalent in pelvic ganglia of female animals (Keast, 1995) it was not possible to prove this as the male was not investigated. Kanerva and Hervonen in 1976 indicated that there appear to be higher quantities of noradrenaline in newborn rodents SIF cells than in adults. The newborn rat SIF cells possess processes as in the adult mouse and guinea-pig (Becker, 1972), and these extend to neighbouring SIF cells. Sites of synaptic contact between SIF cells and neuronal processes are rarely observed as in mouse and adult rat (Becker, 1972; Dail *et al.*, 1975).

Axon conduction velocity and interaction are very different from the adult, the axons are non-myelinated, unsheathed and smaller (approximately half the size) than those in the adult. Individual axons are in direct contact with one another, unlike the picture seen in the adult rat pelvic ganglion where each individual axon is insulated (Hulsebosch and Coggeshall, 1982).

The nerves have in general one or two peripherally placed Schwann cell nuclei in sectional profile. The nerves have only a modest amount of collagen fibers found near the capsule of the nerve and not between the axons.

This study showed that the intraganglionic blood supply of the major pelvic ganglion is already present at birth, and resembles that of the adult ganglion as described by Dail *et al.*, (1975); Kanerva and Hervonen, (1976); Gabella *et al.*, (1992). The blood vessels of the newborn rat pelvic ganglion, as in the adult are lined by endothelial cells which had tight intercellular junctions. In this aspect the blood supply of the pelvic ganglion at birth resembles that of autonomic and peripheral nerve trunks (Akert *et al.*, 1976) and that of the central nervous system (Jacobs, 1977). However, the lack of fenestrations or open intercellular junctions means that the blood supply of the ganglion at birth differs from that of the rat superior cervical, dorsal root and coeliac ganglia (Jacobs, 1977), as well as the pre- and paravertebral ganglia of the aged rat (Baker, *et al.*, 1989).

6. BLADDER AND PELVIC GANGLION IN BRATTLEBORO RATS WITH DIABETES INSIPIDUS

Brattleboro rats are a strain of Long-Evan's rats with hereditary hypothalamic diabetes insipidus. In this work female rats homozygous for diabetes insipidus were used and the control group were female Long-Evans non-diabetic rats.

6.1 ADULT FEMALE RATS

6.1.1 Long-Evans (control)

6.1.1.1 Bladder and kidneys

The bladder was ovoid in shape and had a diameter in the cranio-caudal axis of ~ 16 mm and in the transverse and dorso-ventral axes ~ 11 mm. The cranio-caudal diameter was 1.5 times the transverse and dorso-ventral diameters. When fully distended the bladder had an average capacity of 0.9 ml (Table 20). The emptied bladder weighed on average 117 mg (range 90 - 140; n = 3) (Table 20).

The serosa, smooth muscle layer, connective tissue, mucosa and numerous blood vessels, were all clearly observed by use of a light microscope on histological sections cut at a thickness of one micrometre through the bladder wall (figure 6.3). The wall of the bladder averaged 137 micrometres in thickness (range 126-149 micrometres; n = 3) (Table 20) when fully distended.

The average weight of the kidneys in the control animals ranged from 0.87-1.10 gm (Table 20).

Table 20. Adult Long-Evans rats. Kidney and bladder

Animal	Body weight (gm)	Bladder weight (mg)	Bladder wall thickness (μm)	Bladder capacity (ml)	Kidney weight (gm)
L.E.01	193	90	126	0.7	0.87
L.E.02	211	120	137	1.2	1.10
L.E.03	213	140	149	0.9	0.96
Average	**206**	**117**	**137**	**0.9**	**0.97**

6.1.1.2 Pelvic ganglion

The general histological characteristics of the pelvic ganglion of the Long-Evans rats were the same as in the Sprague-Dawley rats (see chapter 3) (figures 6.1 & 6.2).

By use of serial sections studied by light microscopy, the length and sectional area of the ganglion were estimated in 3 rats. The length ranged from 945 μm to 1071 μm (mean 962 μm) (Table 21; n=3). The average sectional area had values from 56,727 μm^2 to 70,783 μm^2 (mean 62,419 μm^2) (Table 21; n=3). From these two sets of values, the total volume of the ganglion was calculated as 59.9 million μm^3 on average.

Table 21. Adult Long-Evans rats Ganglion Volume

Animal	Ganglion length (μm)	Average sectional area of ganglion profiles (μm^2)	Ganglion volume (millions of μm^3)
L.E.01	1071	56,727	60.7
L.E.02	870	59,748	52.0
L.E.03	945	70,783	66.9
Average	**962**	**62,419**	**59.9**

6.1.1.3 Pelvic ganglion neurons

The maximum cross sectional areas of the pelvic ganglion neurons in the control animals ranged from 100 - 1050 μm^2 (graph 9) corresponding to a range in diameter of

11- 36 micrometres. The average maximal neuronal sectional area was 292 μm^2 (Table 22; n = 1000).

The average neuronal volume (assuming the neurons are spherical) was calculated as 3762 μm^3 (Table 22). Binucleate and vacuolated neurons were found in the proportion of less than 1%. (Figures 6.6 & 6.7).

Table 22. Adult Long-Evans rats. Body weight, bladder weight and neuronal size.

Animal	Body weight (gms)	Bladder weight (mg)	Average neuronal sectional area (μm^2)	Average neuronal volume (μm^3)
L.E.04	194	120	317	4,245.7
L.E.05	187	100	339	4,695.3
L.E.06	195	90	258	3,117.4
L.E.07	201	130	301	3,928.4
L.E.08	205	100	275	3,430.5
L.E.09	198	120	282	3,562.4
L.E.10	195	140	271	3,356.0
Average			**292**	**3,762.2**

6.1.2 Brattleboro strain

6.1.2.1 Bladder and kidneys

The bladder in rats with diabetes insipidus was visibly larger than that of the Long-Evans: the diameter in the cranio-caudal axis was on average 27 mm, the transverse and dorso-ventral axes measured on average 15 mm. The cranio-caudal diameter was 1.8 times larger than the transverse and dorso-ventral diameters.

The empty Brattleboro bladder was found to weigh 375-660 mg (average 486 mg; n = 3) (Table 23); this is four times heavier than the control bladder.

When studied by use of a low power light microscope (x16 and x 25 objectives) on histological sections cut at a thickness of one micrometre, the walls of the bladders of

animals with diabetes insipidus were histologically similar to the controls in that; the serosa, smooth muscle layer, connective tissue, mucosal surface and numerous blood vessels, were all clearly observed in the similar proportions to those in the control bladders (figures 6.3A & B). The walls of the Brattleboro bladders measured an average of 112 micrometres in thickness (table 23; n = 3) a value not significantly different from the control bladders. The main difference between the two strains was observed at high power (x40 objective) the Brattleboro muscle cells were visibly larger than those of the controls (figures 6.3 C & D).

The capacity of the Brattleboro bladders was 2.9 ml on average (Table 23; n = 3).

The kidneys of the Brattleboro rats had an average weight of 1.42 gm.

Table 23. Adult Brattleboro rats. Bladder, kidneys and bladder wall thickness.

Animal	Body weight (gm)	Bladder weight (mg)	Bladder capacity (ml)	Kidney weight (gm)	Bladder thickness (μm)
BRT.01	215	320	2.1	1.28	
BRT.07	209	660	3.9	1.61	
BRT.03	200	480	2.7	1.37	
BRT.11					106
BRT.12					119
BRT.13					110
Average	**208**	**486**	**2.9**	**1.42**	**112**

6.1.2.2 Pelvic ganglion

Enlargement of the bladder does not produce a significant displacement of the ganglion; it is still found following the description of Baljet and Drukker (1980) 'a flat triangular structure located lateral to the junction between uterus and vagina, caudal to the terminal segment of the ureter and close to the vaginal artery (or one of the vaginal arteries) branching off the internal iliac artery'.

The pelvic ganglia were visibly larger than the controls and therefore easier to dissect. The capsule was continuous (figure 6.4). Neurons, Schwann cells, nerve fibres (both myelinated and unmyelinated), SIF cells and numerous blood vessels were noted.

By use of serial sections studied by light microscopy, the length and sectional area of the ganglia were measured in 3 rats. The length ranged from 1,652 μm to 2,092 μm (mean 1,888μm) (Table 24), 96 % larger than the value for the Long-Evans ganglia. The average sectional area had a mean value of 79,470 μm^2 (range 68,121 μm^2 - 87,701 μm^2), 27 % larger than the control. From these values, the total volume of the ganglion for three animals was calculated as 151 million μm^3 on average (Table 24), 152 % larger than the control.

Table 24. Adult Brattleboro rats. Ganglion sizes

Animal	Ganglion length (μm)	Average sectional area of ganglion profiles (μm^2)	Ganglion volume (millions of μm^3)
BRT.01	2,092	82,590	172.7
BRT.02	1,652	68,121	112.5
BRT.03	1,920	87,701	168.3
Average	**1,888**	**79,470**	**151.2**

6.1.2.3 Pelvic ganglion neurons

The maximum cross sectional areas of the pelvic ganglion neurons in the Brattleboro animals ranged from 100 - 1300 μm^2 (graph 9) corresponding to a range in diameter of 11-41 micrometres. The average maximal neuronal sectional area was 503 μm^2 (Table 25; n = 1000). Assuming the neurons to be spherical the average neuronal volume was calculated as 8488 μm^3, a value which is 125 % larger than that of the control neurons.

Both binucleate (figure 6.8) and vacuolated neurons (figure 6.9) were observed and both formed less than 1 % of the total population of neurons.

Table 25. Adult Brattleboro rats. Body weight, bladder weight and neuronal size

Animal	Body weight (gms)	Bladder weight (mg)	Average neuronal sectional area (μm^2)	Average neuronal volume (μm^3)
BRT.04	211	490	548	9,650.2
BRT.05	190	375	449	7,157.0
BRT.06	193	480	485	8,034.8
BRT.07	208	660	512	8,715.0
BRT.08	188	590	502	8,461.0
BRT.09	203	470	509	8,638.5
BRT.10	193	620	514	8,766.1
Average			**503**	**8,488.9**

Graph 9

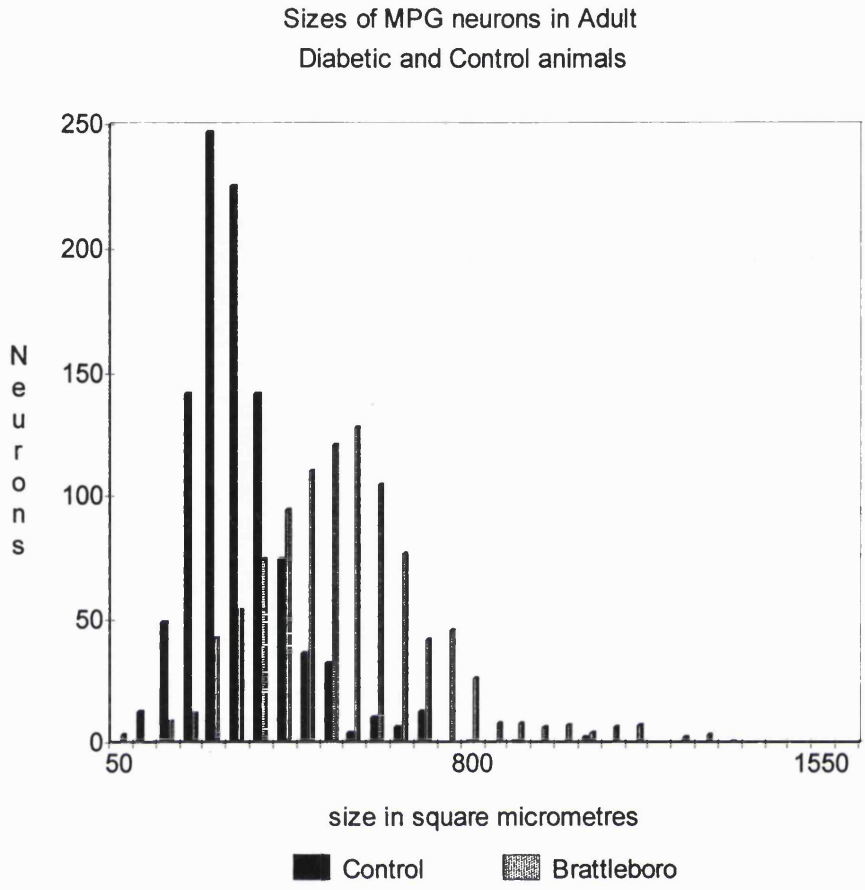

Y axis = number of neurons. X axis = Size of the largest sectional profile of a series of sections through the neuron.

6.2 14 DAY OLD FEMALE RATS

6.2.1 Long-Evans

6.2.1.1 Bladder and kidneys

At 14 days after birth the bladder averaged 65 mg in weight (Table 26; n = 6) approximately half the weight of the adult Long-Evans bladder.

The kidneys supplying the control bladders ranged in weight from 140-185 mg, the average kidney weight being 171 mg (Table 26).

Table 26. 14 day old Long-Evans rats. Body, bladder and kidney weights.

Animal	Body Weight (gm)	Bladder Weight (mg)	Kidney Weight (mg)
L.E.21	32	50	175
L.E.22	35	40	185
L.E.23	35	60	183
L.E.24	36	90	140
L.E.25	37	70	175
L.E.26	35	80	165
Average	**34**	**65**	**171**

6.2.1.2 Pelvic ganglion

The ganglia were positioned and orientated in the same manner as those in the adult. The ganglion had a continuous capsule and contained blood vessels, neurons, and glia (Figures 6.10 and 6.11) very similar to those seen in the 14 day old Sprague-Dawley rats (figures 3.10 and 3.11).

By use of serial sections studied by light microscopy, the length and sectional area of the ganglia were measured in three 14-day-old rats. The average length was 697 μm (range 655 - 745 μm) (Table 27). The average sectional area 85,146 μm^2 (range 76,564

- 97,153 μm) (table 27). From these values, the total volume of the ganglion was calculated as 59.4 million μm^3 on average.

Table 27. 14-day-old Long-Evans rats. Ganglion size.

Animal	Animal Weight (gms)	Ganglion length (μm)	Average Ganglion section area (μm^2)	Ganglion volume (millions of μm3)
L.E.21	32	655	76,564	50.2
L.E.22	35	690	97,153	67.0
L.E.23	35	745	81,721	60.9
Average	**34**	**697**	**85,146**	**59.4**

6.2.1.3 Pelvic ganglion neurons

The pelvic ganglion neurons at 14 days after birth appeared similar to those of the 14-day-old Sprague-Dawley (see chapter 3). They consistently had one or two glial cell nuclei placed close to them, though the glial sheath details were not seen clearly under the light microscope. The ganglion neurons generally, had a nucleus, with 1-2 nucleoli, placed towards the edge of the cell, with a rim of cytoplasm between it and the cell membrane.

The average neuronal sectional area was 241 μm^2 (Table 28), 17 % less than the adult control value. The average neuronal volume (assuming the neuron to be a sphere) was calculated to be 2,814 μm^3 (75% of adult control value) for the pelvic ganglion neurons of 3 rats.

Table 28. 14-day-old Long-Evans rats. Neuronal sizes.

Animal	Animal Weight (gms)	Average neuronal sectional area (μm^2)	Average Neuronal volume (μm^3)
L.E.21	32	217.8	2,417.96
L.E.22	35	243.1	2,851.29
L.E.23	35	262.1	3,192.00
Average	**34**	**241.0**	**2,814.42**

6.2.2 Brattleboro strain

6.2.2.1 Bladder and kidneys

The bladders of the 14-day-old Brattleboro rats weighed an average of 80 mg (Table 29; n = 6), this is 23 % more than the control bladders of the same age ($P<0.02$). The bladder of the 14-day-old Brattleboro rat was already 70 % of the weight of the adult control rat, but weighed only 15 % of the weight of the adult Brattleboro rat bladder.

The kidneys of the young Brattleboro rats averaged 208 mg in weight (table 29), 18 % heavier than the control kidneys of the same age, 21 % of the weight of the adult control rat kidneys, but only 15 % of the weight of the adult Brattleboro kidney.

Table 29. 14-day-old Brattleboro rats. Bladder and kidney weights.

Animal	Body Weight (gm)	Bladder Weight (mg)	Kidney Weight (mg)
BRT.21	36	60	225
BRT.22	35	40	215
BRT.23	35	70	200
BRT.24	38	100	190
BRT.25	37	120	205
BRT.26	39	90	210
Average	**35**	**80**	**208**

6.2.2.2 Pelvic ganglion

The ganglia of the 14-day-old Brattleboro animals were positioned and orientated in the same position as those in the Long-Evans animals and the adult Brattleboro animals.

The ganglia had a well developed continuous capsule, numerous blood vessels, and neuropil with both myelinated and unmyelinated fibres visible (Figures 6.12 and 6.13).

The ganglia ranged in length from 720 μm to 840 μm the average length being 778 μm (Table 30; n = 3). The sectional area of the ganglia ranged from 122,986 μm^2 to 142,717 μm^2 the average value being 131,795 μm^2 (Table 30).

The average ganglion volume (a product of its length and cross-sectional volume) was 102 million μm^3 (Table 30), this represents 67 % of the volume of an adult Brattleboro ganglion and is 42 % larger than the adult control ganglion.

Table 30. 14-day-old Brattleboro rats. Ganglion sizes.

Animal	Animal Weight (gms)	Ganglion length (μm)	Average Ganglion section area (μm^2)	Ganglion volume (millions of μm^3)
BRT.21	36	775	142,717	110.6
BRT.22	35	840	129,683	108.9
BRT.23	35	720	122,986	88.5
Average	**35**	**778**	**131,795**	**102.7**

6.2.2.3 Pelvic ganglion neurons

The neurons of the 14 day old Brattleboro rats (figures 6.12 and 6.13) appeared to be well developed and they had an average sectional area of 282 μm^2 (Table 31), a value which is 17 % bigger than that of the controls of the same age. At 14 days the Brattleboro pelvic ganglion neurons have grown to 97 % of the size of the adult control rats, but only 54 % of the size of the adult Brattleboro rat neurons.

Assuming the neurons to be spherical, the average neuronal volume was calculated to be 3564.25 μm^3 (table 31). This value is 26 % larger than the control neurons of the

same age, 5 % less than the volume of the adult control neurons and only 42 % of the value of the adult Brattleboro neurons.

Table 31. 14-day-old Brattleboro rats. Neuronal sizes.

Animal	Animal Weight (gms)	Average neuronal sectional area (μm^2)	Average Neuronal volume (μm^3)
BRT.21	36	285.2	3,623.16
BRT.22	35	290.0	3,715.01
BRT.23	35	271.1	3,357.83
Average	**35**	**282.1**	**3,564.25**

FIGURE 6.01

Photomicrograph of an adult Long-Evans ganglion

showing; capsule, c; ganglion neuron, N; blood vessel, B;

nerve bundle, n.

Magnification x 250

Scale bar = 100 μm

FIGURE 6.02

Photomicrograph of adult Long-Evans ganglion at high power

Showing; intraganglionic blood vessels, B; ganglion neurons, N;

nerve bundle, n; glial cell nucleus, g; nucleus of endothelial cell, e;

intracapsular blood vessel, b.

Magnification x 800.

Scale bar = 50 μm

6.01

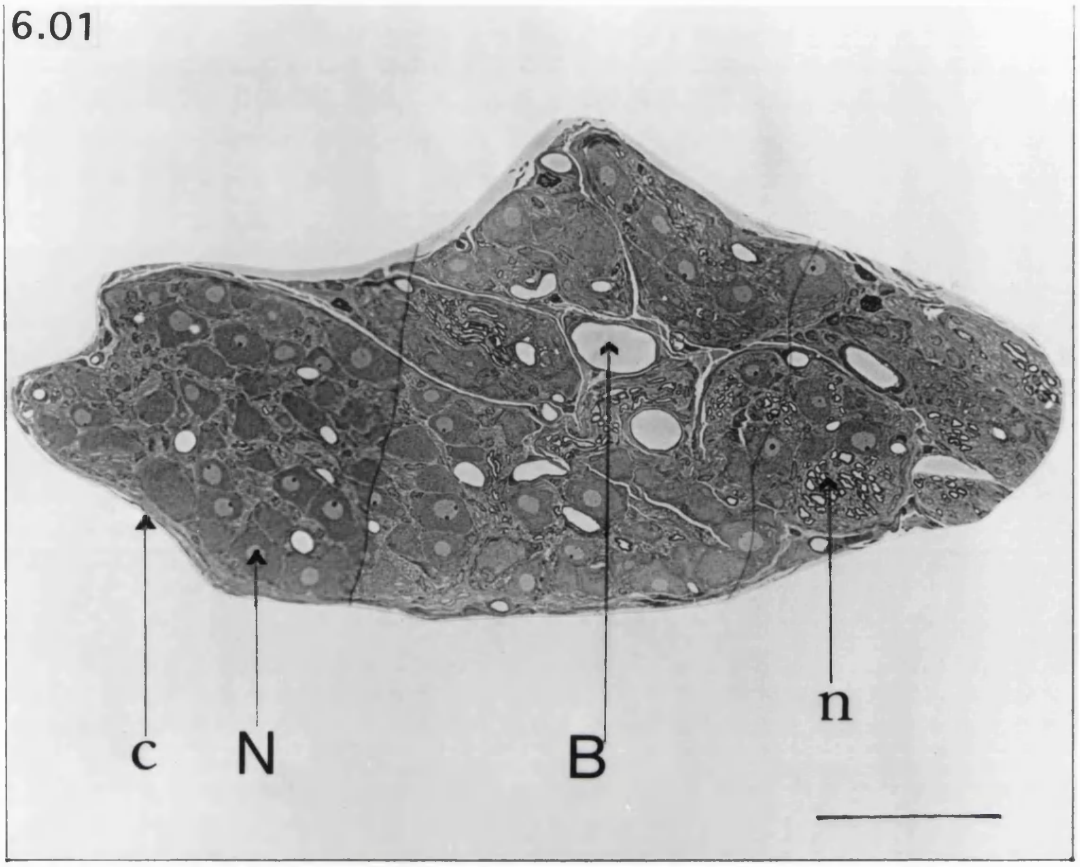

6.02

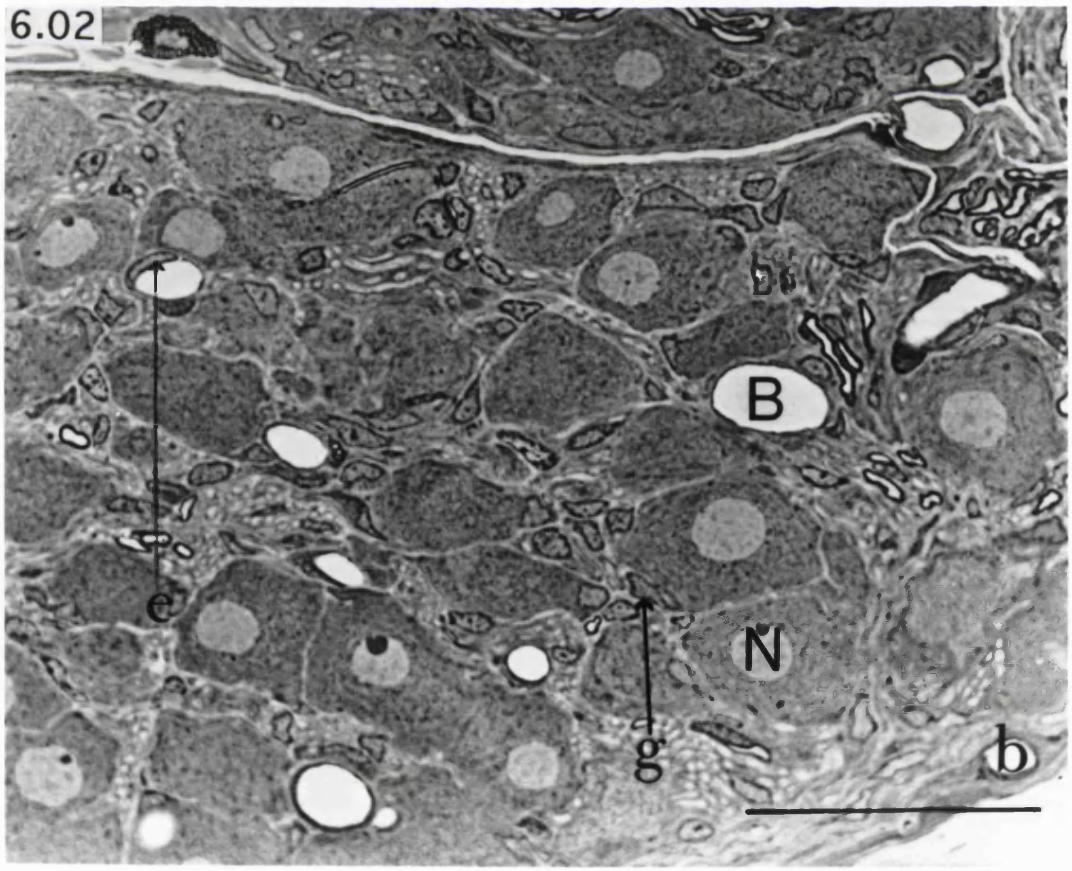

FIGURE 6.03

A) Photomicrograph of the bladder of the adult Long-Evans rat

Showing: epithelium, E; submucosa, m; smooth muscle, M;

serosal surface, S.

Magnification x 640.

Scale bar = 100 μm

B) Photomicrograph of the bladder of adult Brattleboro rat.

Showing: epithelium, E; submucosa, m; smooth muscle, M;

serosal surface, S; blood vessel , B.

Magnification x 640.

Scale bar = 100 μm

C) High power photomicrograph of adult Long-Evans rat

bladder showing: smooth muscle cells, M.

Magnification x 1,600

Scale bar = 10 μm

D) High power photomicrograph of the adult Brattleboro

Rat bladder showing: smooth muscle cells, M.

Magnification x 1,600

Scale bar = 10 μm

6.03

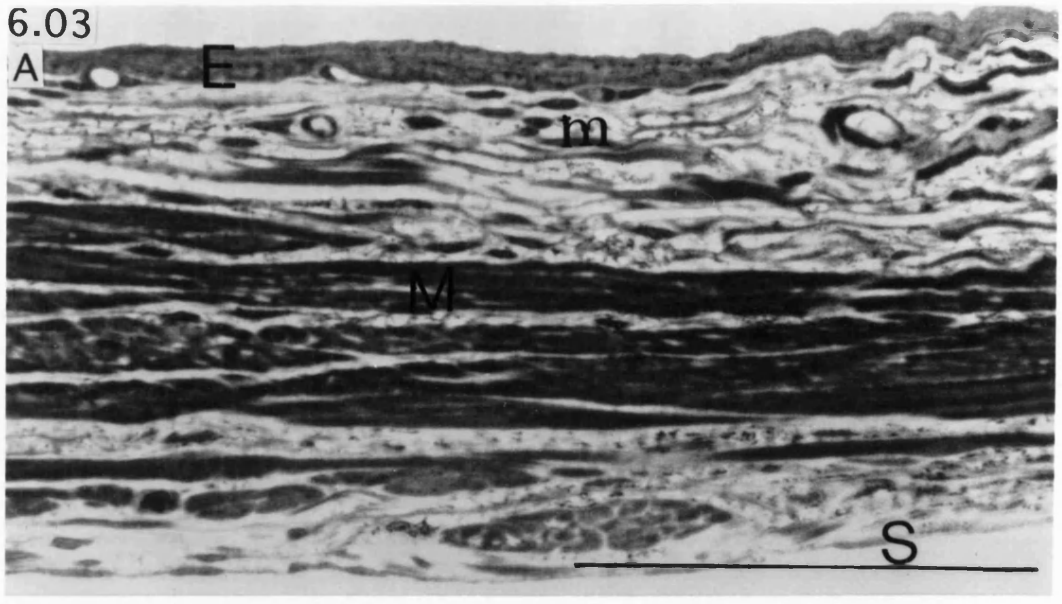

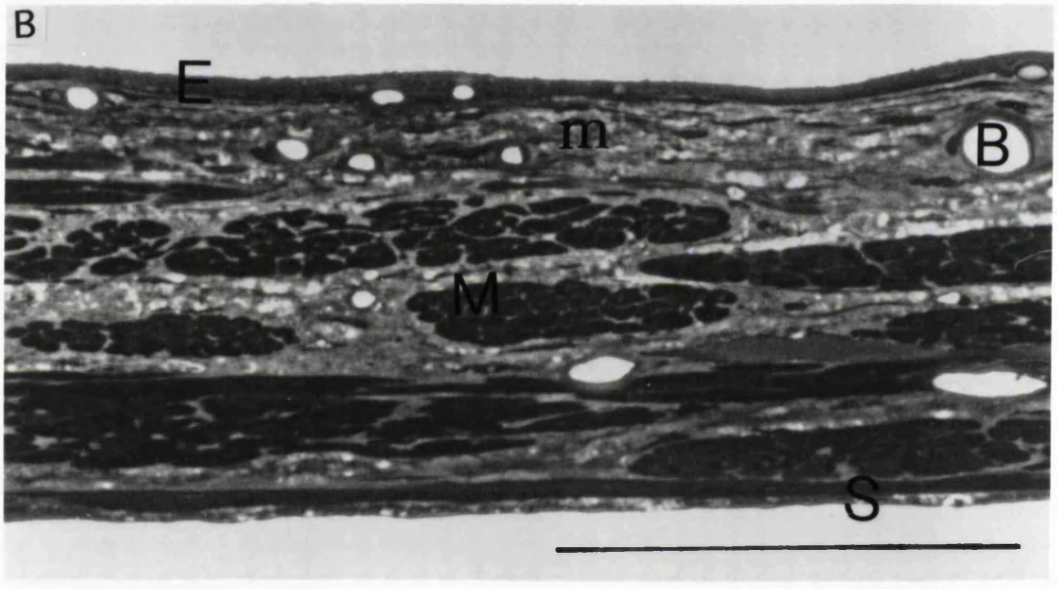

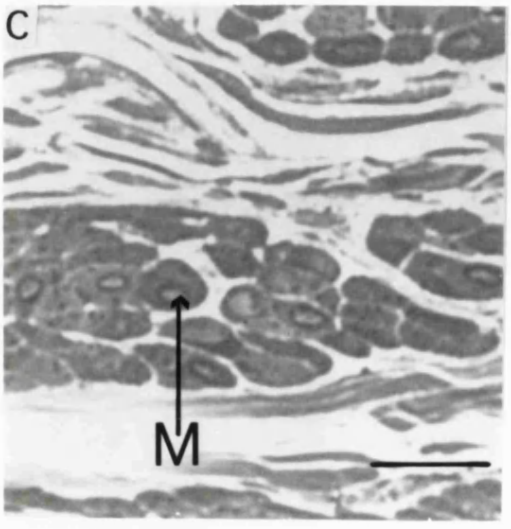

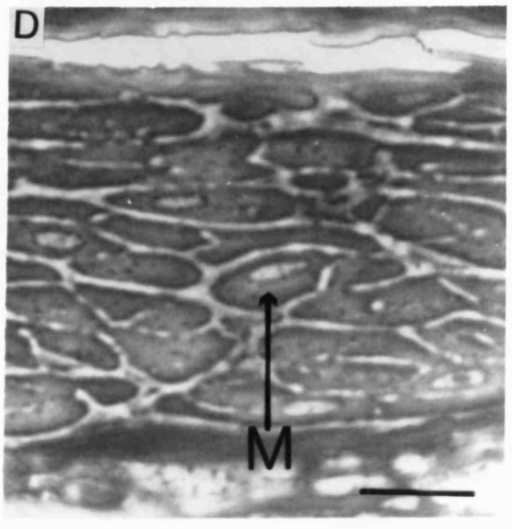

FIGURE 6.04

Photomicrograph of the adult Brattleboro rat pelvic ganglion

Showing: capsule, C; ganglion neuron, N; nerve bundle, n.

Magnification x 250

Scale bar = 100 μm

FIGURE 6.05

Photomicrograph of the adult Brattleboro rat pelvic ganglion

at high power showing: neuron, N; glial cell nucleus, g; myelinated

fibre, m; fibroblast nucleus, f; SIF cell, s.

Magnification x750

Scale bar = 50 μm

6.04

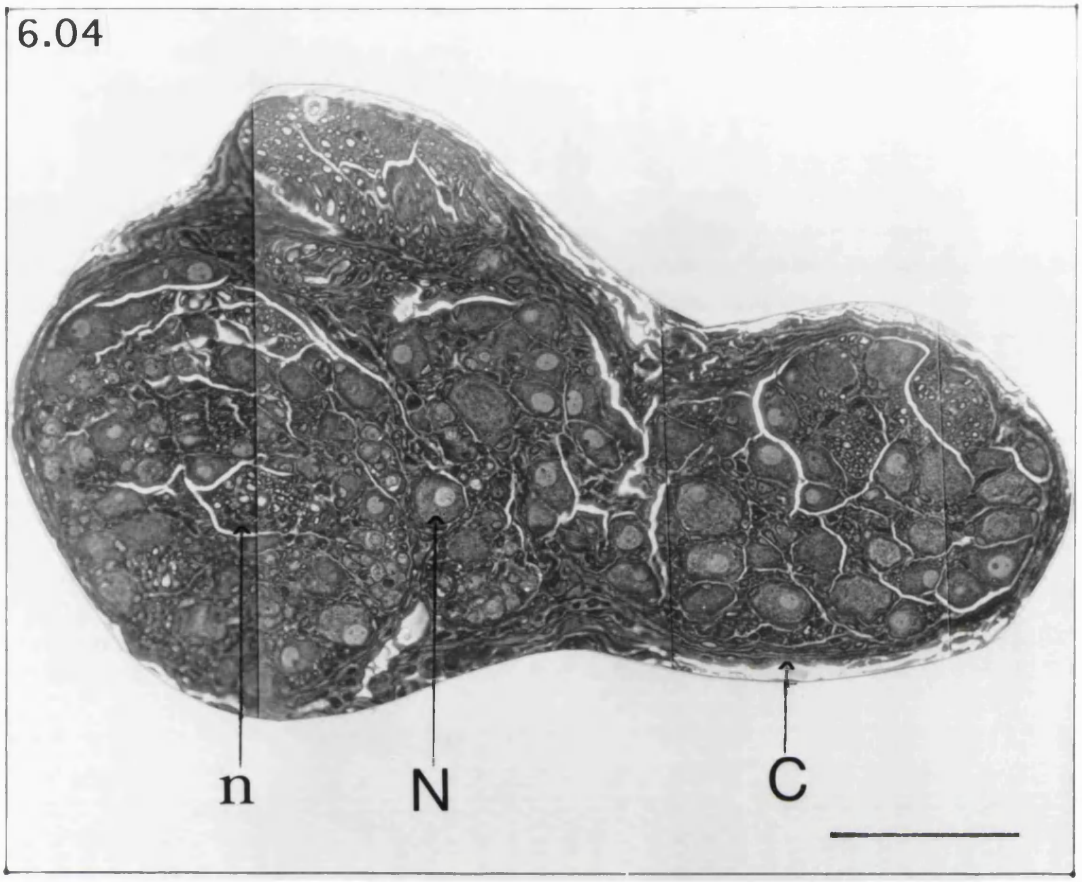

6.05

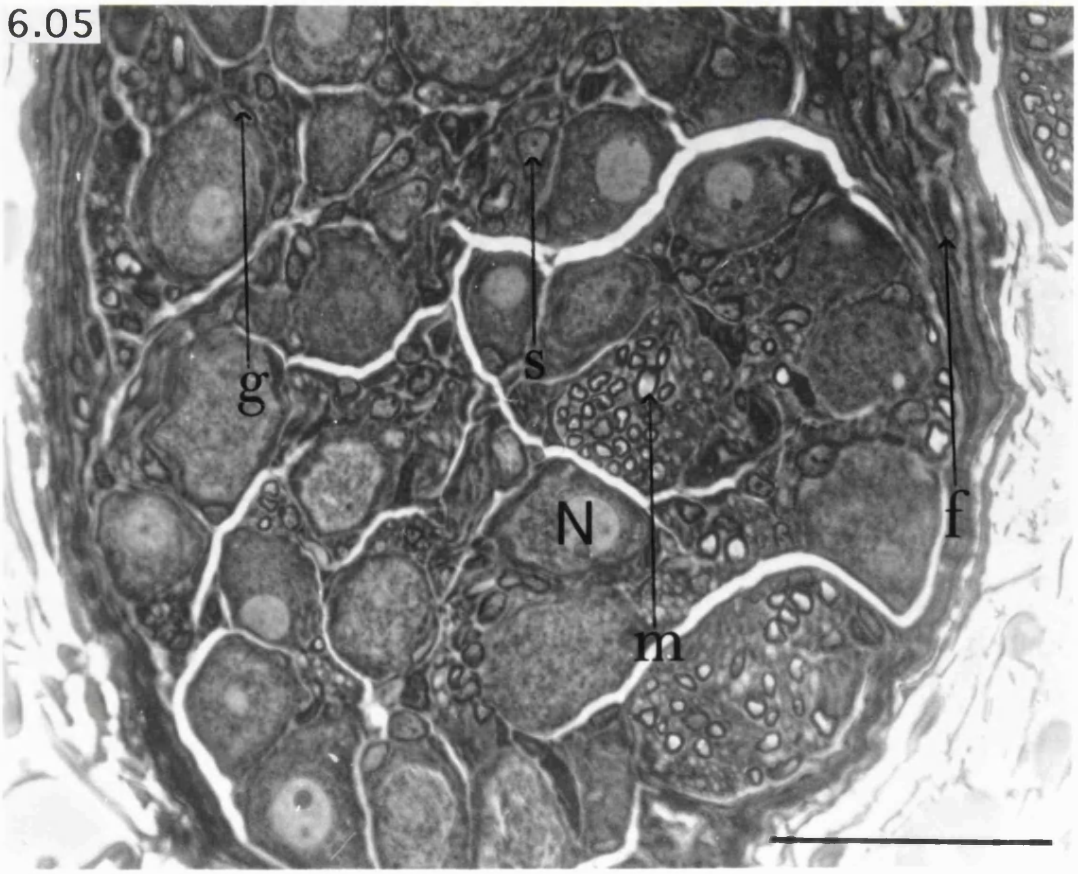

FIGURE 6.06

Photomicrograph of a binucleate neuron, B; from

the pelvic ganglion of an adult female Long-Evans rat.

Magnification x 800

Scale bar = 10 μm.

FIGURE 6.07

Photomicrograph of a vacuolated neuron, V from

the pelvic ganglion of an adult female Long-Evans rat.

Magnification x 500

Scale bar = 50 μm.

FIGURE 6.08

Photomicrograph of binucleate neuron, B from the

pelvic ganglion of an adult female Brattleboro rat.

Magnification x 800

Scale bar = 10μm

FIGURE 6.09

Photomicrograph of a vacuolated neuron, V from the

Pelvic ganglion of an adult female Brattleboro rat.

Magnification x 800

Scale bar = 10 μm

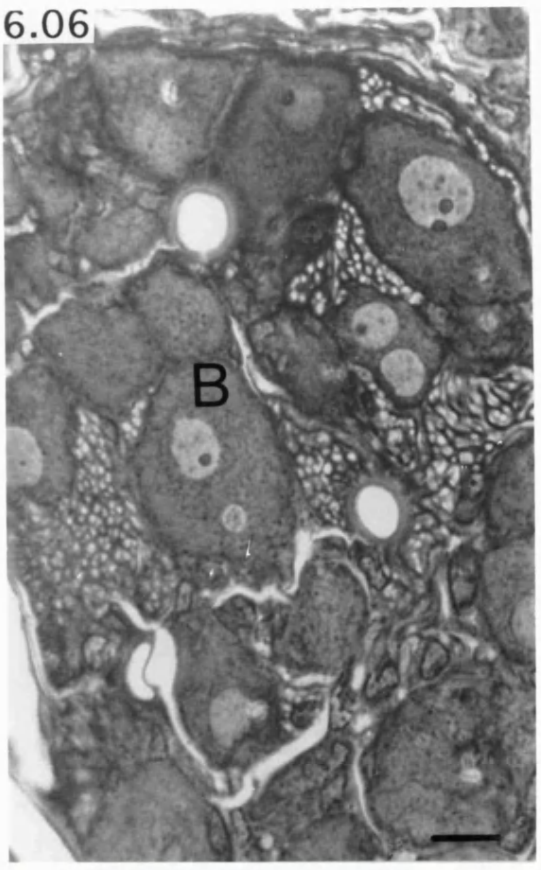
6.06
B

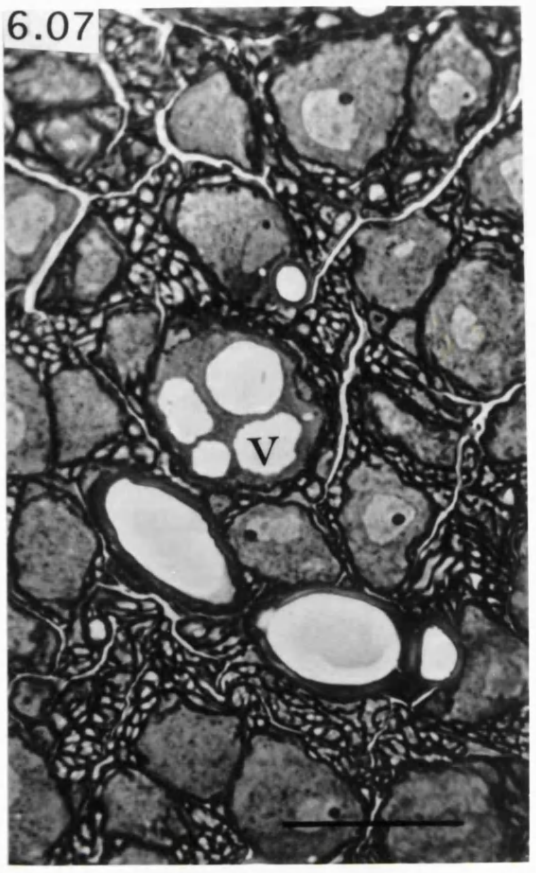
6.07
V

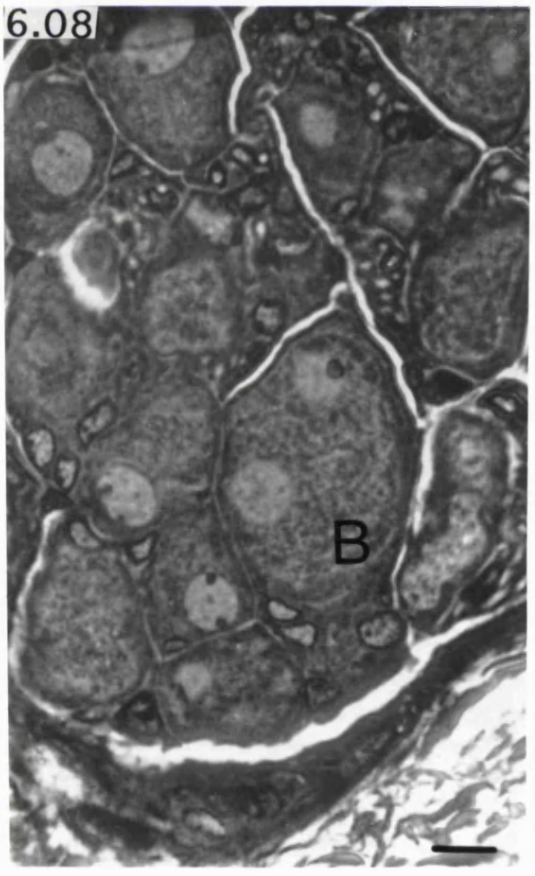
6.08
B


6.09
V

FIGURE 6.10

Photomicrograph of 14-day-old control ganglion

Showing: capsule, C; neuron, N.

Magnification x 250

Scale bar = 100 μm

FIGURE 6.11

Photomicrograph of 14-day-old control ganglion at high power

Showing, neuron, N; SIF cell, S; blood vessel, B; glial cell nucleus, g.

Magnification x 500

Scale bar = 50 μm

6.10

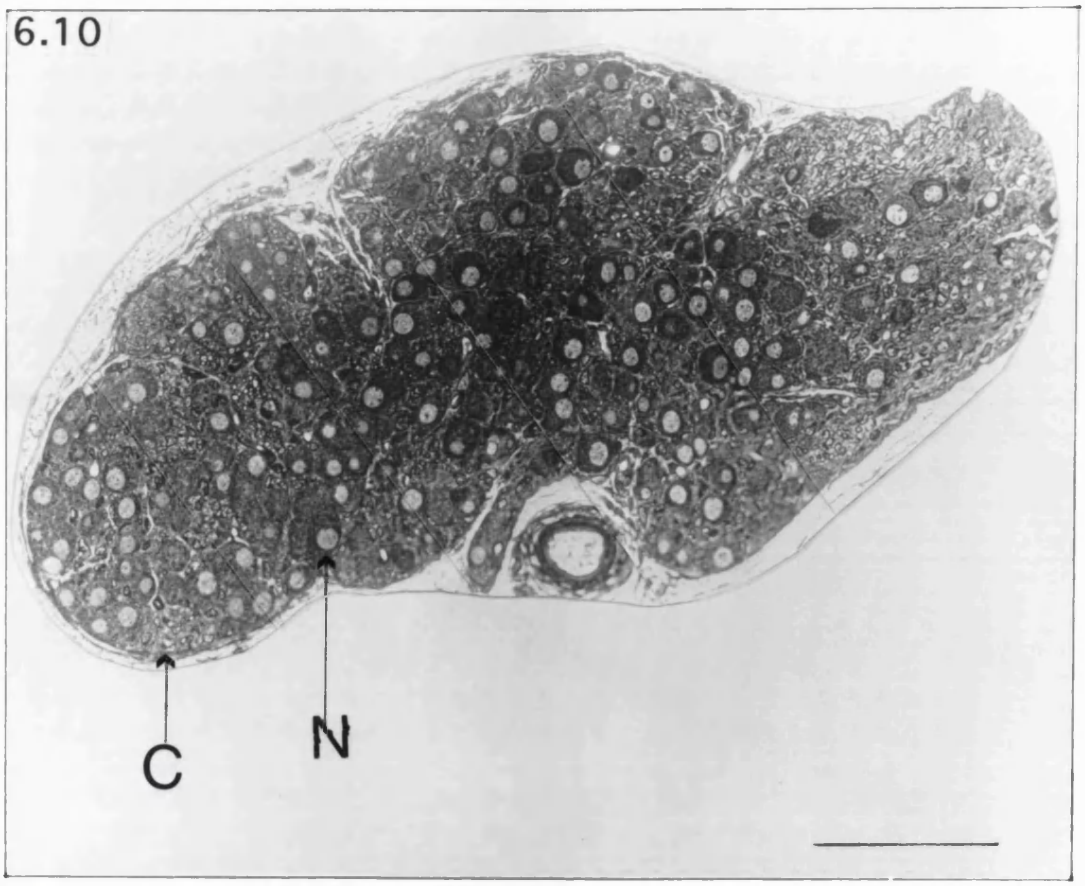

6.11

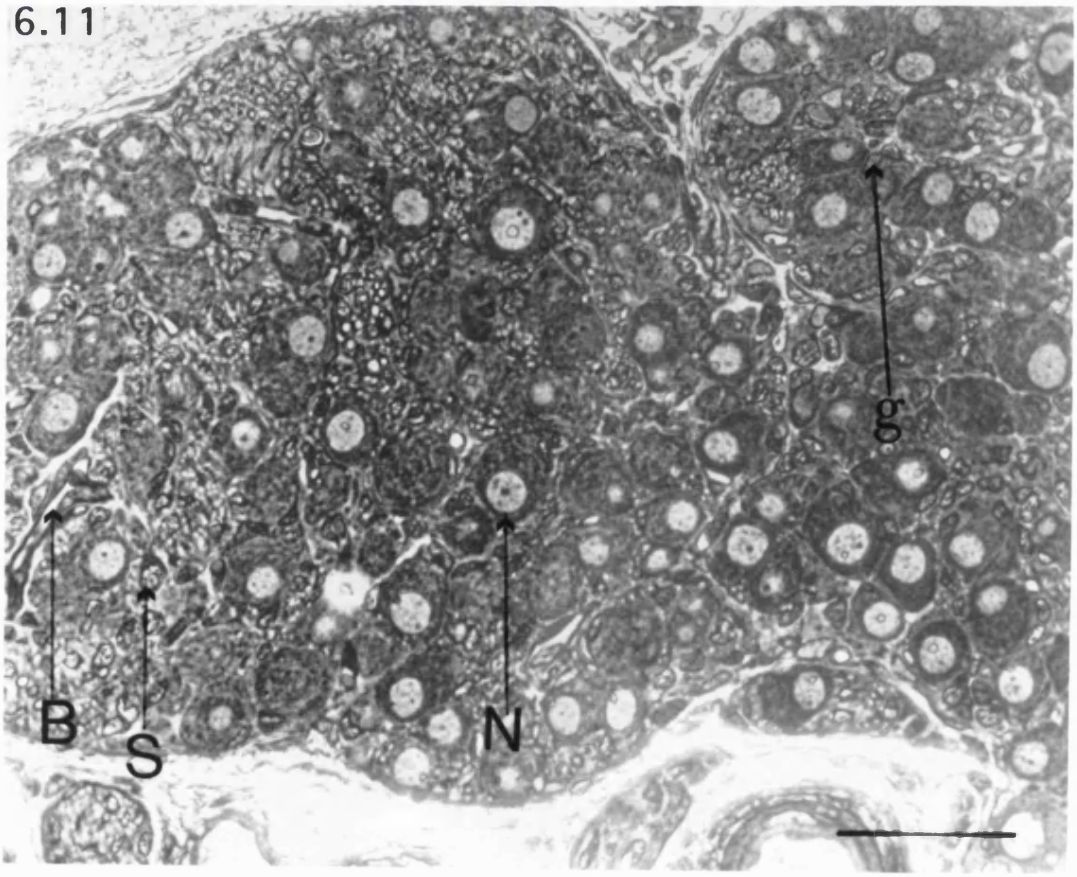

FIGURE 6.12

Photomicrograph of 14-day-old Brattleboro ganglion

Showing: capsule, C; neuron, N; extra-capsular

blood vessel, V.

Magnification x 250

Scale bar = 100μm

FIGURE 6.13

Photomicrograph of 14-day-old Brattleboro ganglion at high power.

Showing : neurons, N; nerve bundles, n; glial cell nucleus, g;

fibroblast nucleus, f; small intraganglionic blood vessel with

red blood cell, b.

Magnification x 500

Scale bar = 50 μm

6.12

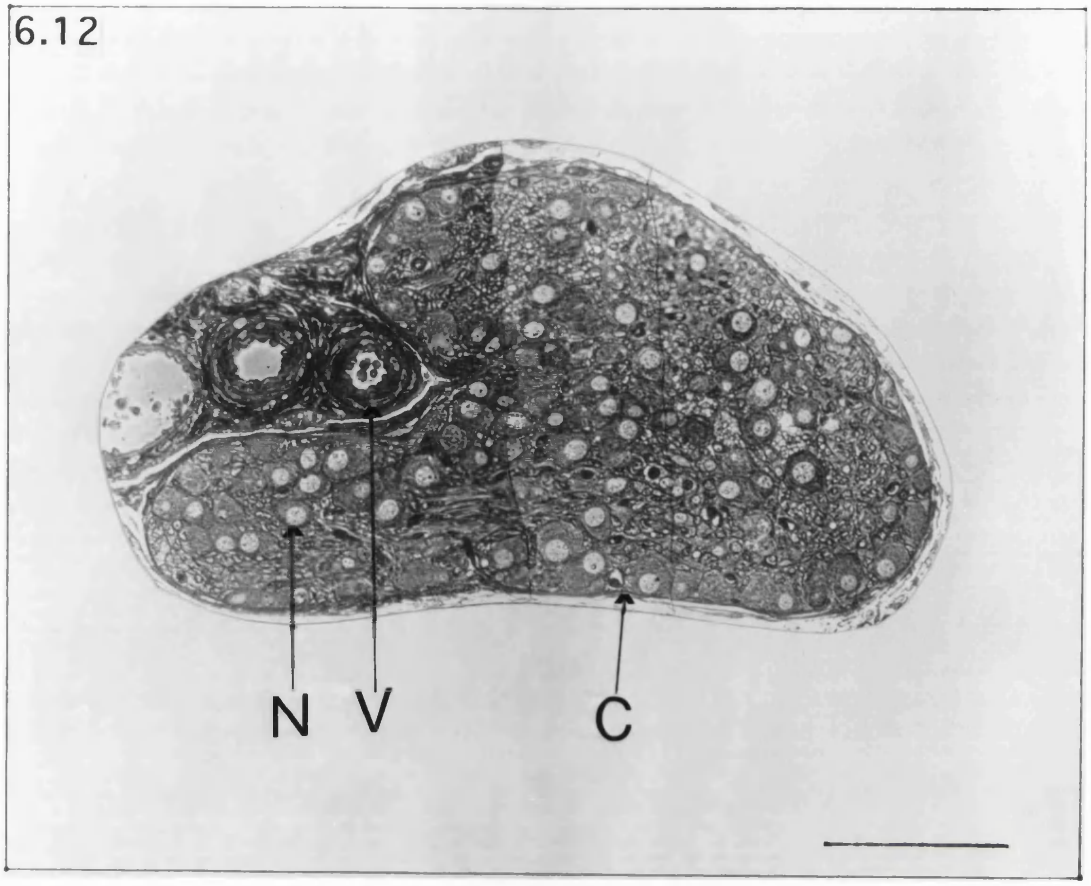

6.13

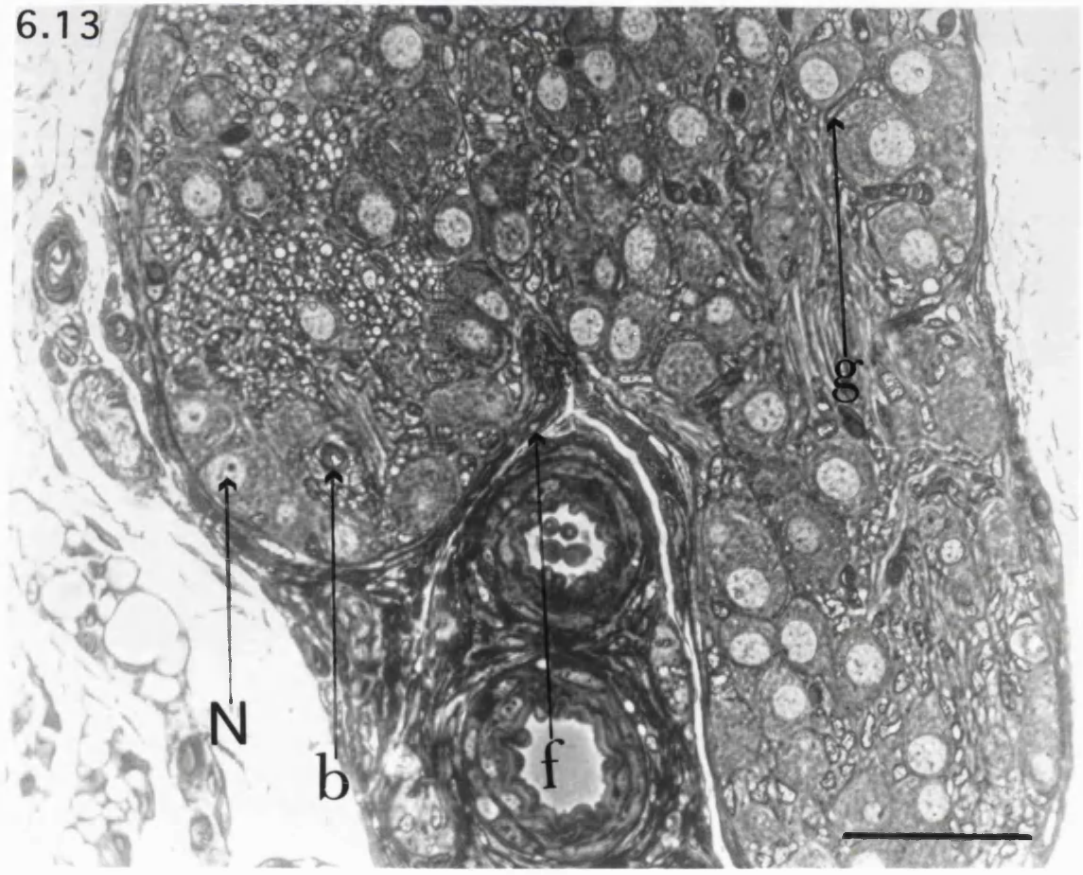

6.3 DISCUSSION

The Brattleboro rats, because of a base deletion in the vasopressin gene, express a vasopressin precursor which is unable to enter the secretory pathway. The resulting lack of the hormone vasopressin leads to an inability to reabsorb water in the distal tubuli of the kidneys and results in polyuria (Pickering *et al.,* 1982). The polyuria, which is the only abnormal feature found in these animals (Valtin and Schroeder, 1964), is most pronounced in animals homozygous for the condition (as were used in this study), but it is seen also, although to a lesser extent, in the heterozygous condition (Valtin *et al.,* 1965). The most striking effect of polyuria on the bladder of the adult Brattleboro rats is that the bladder capacity is about three times that of the Long-Evans rats (the control strain). There are other studies on the diabetic bladder Eika *et al* (1994) in a comparison of diabetes insipidus, diabetes mellitus and sucrose-induced diuresis, noted that, although all three conditions lead to an increase in bladder capacity, diabetes insipidus produced the greatest increase. Another study (Malmgren *et al.,* 1992) compared the changes between the bladders of rats homozygous and heterozygous for diabetes insipidus and found that the enlargement of the bladder was greater in the homozygous rats than in the heterozygous.

In addition, the enlarged bladder is somewhat different in shape from the controls. While in Long-Evans rats the long axis of the distended bladder is about 1.5 times the transverse or the sagital axis (a value which is similar to that observed by others in Sprague-Dawley rats [Gabella and Uvelius, 1990]), in the Brattleboro rat the corresponding value is 1.8. This indicates that, while enlarging in all directions, the bladder of the rats with diabetes insipidus grows proportionally more in length than in width. It is not known why the bladder of the rat is not a sphere but a prolate spheroid,

and it is also not known why the enlarged bladder of the Brattleboro rat is even more elongated, but it seems likely that the different constraints imposed by the surrounding organs and by the pelvic and abdominal walls are an important factor.

Along with the differences in capacity and shape, there is a difference in bladder weight. The weight of the bladder (bladder wall) is significantly greater in the Brattleboro rats than in the controls. Brattleboro bladders are on average four times as heavy as control bladders. The difference in weight observed is larger than the two-fold weight difference reported in experiments where the control animals were heterozygous for diabetes insipidus (Malmgren *et al.*, 1992).

Despite having greater weight and capacity than control bladders, the Brattleboro rat bladder has a wall thickness (measured in control standard conditions of full distension) similar to that of the control bladders. Histologically, the Brattleboro and control bladders have similar proportions of the various layers of their walls. This observation shows that the enlargement of the bladder with congenital diabetes insipidus is not a simple distension, but it involves additional growth of all the tissues of the wall to enable them to remain in similar proportion to those of the control bladder. The growth of the muscle layer is partly accounted for by an increase in the size of the muscle cell profiles. The growth of all the layers in the bladder wall (including their blood supply, i.e. an increase in the number of blood vessels), accompanied by an increase in the size of the muscle cell profiles is called hypertrophy.

The behavior of the muscle layer and its relationship to the rest of the bladder wall depends on the type of stimulus; in acute distension with urinary retention the wall of the bladder is thinned and there is no muscle growth. Usually, however, the bladder has a great capacity to undergo hypertrophic growth, especially when exposed to chronic stimuli. In addition to diabetes insipidus, another experimental condition producing bladder hypertrophy is a chronic outflow obstruction by surgical narrowing of the

urethra. Using this model workers including Speakman *et al.,* (1987), Gabella and Uvelius (1990), and Steers *et al.,* (1990), have showed that the bladder was up to fourteen times heavier than the control. In this case the stimulus for hypertrophy is not polyuria, but the resistance created by the narrower bladder outlet and the resulting increase in weight is much greater than that seen in diabetes insipidus. Secondly, the creation of short-term polyuria e.g. by administration of sucrose in the diet also makes the bladder hypertrophic. Using this model Nadelhaft *et al.,* (1992) reported a two-fold increase in bladder weight. Although the stimulus for hypertrophy in this method is polyuria, the amount of increase in bladder weight is less than that seen in diabetes insipidus. This difference may be due to the diabetes insipidus being present from birth, therefore stimulating the bladder for a longer period of time than the sucrose-induced polyuria. Thirdly, bladder hypertrophy develops after spinal cord injury leading to bladder sphincter dyssynergia. Kruse *et al.,* (1995) using this method reported a four-fold increase in bladder weight. In this case the stimulus for hypertrophy is increased outflow resistance caused by the bladder sphincter being unable to open normally. The amount of weight increase is similar to that seen in diabetes insipidus though the stimulus for hypertrophy is different.

From the results of this study and the literature on this topic, it can be seen that the bladder hypertrophy caused by polyuria is only modest by comparison with that accompanying partial urethral obstruction. This implies that polyuria alone, whether applied from birth or over a short period, is a weak stimulus for hypertrophy.

Interestingly, work done by Gabella *et al* (1992) has shown that, the bladder undergoes a reduction in the amount of hypertrophy present when the 'overload ' is removed, and as a result returns to near its original size. The relationship between how near the original size the bladder returns, appears to depend on the duration of the stimulus for hypertrophy. The administration of vasopressin to Brattleboro rats to assess

how reversible the long-term changes observed are, would be a line of further investigation for this work.

The ultrastructure of the Brattleboro bladder was not investigated in this study but by light microscopy it was possible to detect an increase in the size of the muscle cells. However, it remains unknown whether there are muscle cell divisions leading to an increase in the number of muscle cells. The innervation of the Brattleboro bladder, was not studied this in work, although it is expected that it grows, as has been shown with other forms of hypertrophy. It also remains unclear how the rest of the tissue of the bladder wall grows in order to maintain similar proportions to those of the control bladder.

Accompanying bladder hypertrophy in the Brattleboro rats, is a two-fold increase in the average volume of the pelvic ganglion and its neurons (i.e. neuronal hypertrophy). Neuronal hypertrophy following bladder hypertrophy is well documented in conditions such as partial urethral obstruction (Steers *et al.,* 1990; Gabella and Uvelius, 1990), or sucrose-induced polyuria (Nadelhaft *et al.,* 1993). In these conditions (including diabetes insipidus) the amount of neuronal hypertrophy is no more than two-fold. Pelvic ganglion neuron hypertrophy can also occur without bladder hypertrophy, as is seen in unilateral ganglionectomy where the amount of bladder supplied by the neurons is doubled without the volume of bladder muscle increasing (Gabella and Uvelius, 1992). However, a combination of bladder muscle hypertrophy (as caused by partial urethral obstruction) and contralateral ganglionectomy leads to the largest reported increase in the average size of pelvic ganglion neurons (Gabella and Uvelius, 1992).

These findings suggest that an important factor in determining the amount of neuronal hypertrophy is the amount of bladder muscle that the neurons have to innervate. It also suggests that the bladder muscle cells are able to produce factors that lead to the growth of the neurons that innervate them. This reasoning is in line with the

work of Steers *et al.,* (1991), who showed that hypertrophied bladders of rat and human contain significantly more nerve growth factor (NGF) than normal bladders. Steers *et al.,* (1991) also reported that autoimmunity to NGF abolished the hypertrophy of NGF-sensitive bladder neurons in the pelvic ganglion after partial bladder obstruction. However, it must be pointed out that the neuronal hypertrophy seen in diabetes insipidus and partial urethral obstruction is similar, though the bladder in the obstructed animals is much larger than that of those with diabetes insipidus. Therefore, there are factors other than the amount of muscle being innervated that determine the amount of neuronal hypertrophy.

The pelvic ganglion neurons also show 'plasticity'; in cases of neuronal hypertrophy following urethral obstruction (and subsequent bladder hypertrophy), the neuronal hypertrophy is reversed to a significant degree if the obstruction is removed within 8 weeks of it being initiated (Gabella *et al.,* 1992). An interesting line of further investigation for this work would be the administration of vasopressin to adult Brattleboro rats, and the study of its effect on the size of the pelvic ganglion neurons which have been stimulated from birth.

As regards the development of the Brattleboro rats in the present study only the stage of fourteen days of age was studied, and the results show that the bladder was larger than that of the controls and the pelvic ganglion too was correspondingly larger. These results show that additional growth can be superimposed on normal development.

7. SUMMARY AND CONCLUSION

The major pelvic ganglion of the female rat is the main source of autonomic innervation to the bladder, vagina, uterus, and rectum. The results of this thesis have shown that the ganglion grows in volume and undergoes changes in its structure between birth and three months of age. However, at birth the basic anatomical relationships and nervous connections seen in the adult are already present.

The growth (increase in volume) of the ganglion during the first three months of life (four-fold) is half that of its neurons (eight-fold). This discrepancy is most probably due to changes in the total number of neurons. This study revealed that the total number of neurons present in the ganglion of the adult female rat is on average 7800, whereas other workers have found approximately 12000 in the ganglion of the newborn female rat. These two figures suggest that there is substantial post-natal reduction in the number of pelvic neurons in the female rat.

Histologically, all the basic cell types seen in the adult ganglion are present at birth. However, there are differences in the size, complexity, location and fine structure of the ganglion components seen at birth as opposed to those in the adult. As an example of this, the neurons of the pelvic ganglion undergo not only an increase in volume, but also changes in the nucleo-cytoplasmic ratio, and changes in their relation with the supporting glial cells: during post-natal development the source of trophic support of the neurons changes from the extracellular environment, to a specialized microenvironment provided by a complete glial cell capsule.

Study of the nerve fibres of the major pelvic ganglion revealed that the process of myelination begins during the second post-natal week. This gives rise to the hypothesis that the sensory and preganglionic fibres (i.e. those which, in part, undergo myelination)

acquire a greater speed of conduction, and are thus able to contribute to a more efficient reflex.

The present study has shown that the ganglion capsule and connective tissue are present at birth only in a rudimentary form. The capsule becomes complete during the second post-natal week, while the collagen content in the ganglion increases more gradually and its distribution changes until eventually in the adult it forms laminae between all the neurons.

Electron microscopy of the newborn major pelvic ganglion revealed that the neurons (like those of the adult) contain organelles arranged concentrically around the nucleus and have short and long processes. Both somata and dendrites are abutted by axons, and at these points there are junctions with all the characteristics of a differentiated synapse.

Next, an attempt was made to investigate the effect of polyuria from birth on the bladder and pelvic ganglion of the female rat. Rats homozygous for congenital diabetes insipidus (Brattleboro) were used as the group with polyuria, and Long-Evans rats were used as controls. The results showed that in the bladder of the adult Brattleboro rats there was a three-fold increase in capacity, an increase in weight and a change in shape compared with the control group. However, the wall thickness and the proportion of the various layers the bladder wall of the Brattleboro and Long-Evans rats were similar. These results lead to the hypothesis that the enlargement of the bladder with congenital diabetes insipidus is not a simple distension of the bladder, but it involves additional growth of all the tissues of the wall.

Accompanying this bladder hypertrophy in the adult Brattleboro rats there was a two-fold increase in the average volume of the pelvic ganglion and its neurons (i.e. neuronal hypertrophy). The results of this study confirm the reports in the literature that neuronal hypertrophy follows bladder hypertrophy; however, it is still not possible to determine a direct relationship between the amounts of neuronal and bladder hypertrophy.

As regards the development of the Brattleboro rats this study was limited to fourteen days of age, and the results show that the bladder was larger than that of the controls and the pelvic ganglion was correspondingly larger.

In conclusion, the rat major pelvic ganglion undergoes increase in volume, and changes in the complexity and spatial distribution of its cellular components during normal development. In addition, it is capable of undergoing extra growth when the bladder it innervates hypertrophies.

8. REFERENCES

AKERT, K., SANDRI, C., WEIBEL, E., PEPER, K. and MOOR, H. (1976). The fine structure of the perineural endothelium. *Cell and Tissue Research* **165,** 281-295.

ALIAN, M. and GABELLA, G. (1996). Decrease and disappearance of intramural neurons in the rat bladder during post-natal development. *Neuroscience Letters* **218,** 103-106.

ANDREW, A. (1971). The origin of intramural ganglia. IV. The origin of enteric ganglia: A critical review and discussion of the present state of the problem. *Journal of Anatomy* **108,** 169-184.

ARVIDSON, B. (1979). A study of the demonstration of the perineurial diffusion barrier of a peripheral ganglion. *Acta Neuropathologica (Berlin)* **46,** 139-144.

BAKER, H. A., BURKE, J. P., BHATNAGER, R. K., VAN ORDEN, D. E. and HARTMAN, B. K. (1977). Histochemical and biochemical characterization of the rat paracervical ganglion. *Brain Research* **132,** 393-405.

BAKER , D. G., MACDONALD, D. M., BASBAUM, C. B. and MITCHELL, R. A. (1986). The architecture of nerves and ganglia of the ferret trachea as revealed by acetylcholinesterase histochemistry. *Journal of Comparative Neurology* **246,** 513-526.

BAKER, D., SANTER, R. and BLAGGAN, A. (1989). Morphometric studies on the microvasculature of pre- and paravertebral sympathetic ganglia in the adult and aged rat by light and electron microscopy. *Journal of Neurocytology* **18,** 647-660.

BALJET, B. and DRUKKER, J. (1980). The extrinsic innervation of the pelvic organs in the female rat. *Acta Anatomica* **107,** 241 - 67.

BALUK, P. and GABELLA, G. (1989). Innervation of the guinea pig trachea: quantitative morphological study of intrinsic neurons and extrinsic nerves. *Journal of Comparative Neurology* **285**, 117-132.

BANKS, B. E. C. and WALTER, S. J. (1977). The effects of postganglionic axotomy and nerve growth factor on the superior cervical ganglia of developing mice. *Journal of Neurocytology* **6, 287-297.**

BECKER, K. (1968). Uber die vakuolenhaltigen Nervwnzellen im Ganglion Cervicale Uteri der Ratte. *Zeitschrift für Zellforschung und mikroskopische Anatomie* **88**, 318-339.

BECKER, K. (1972). Paraganglienzellen im Ganglion cervicale uteri der Maus. *Zeitschrift für Zellforschung und mikroskopische Anatomie* **130**, 249-261.

BLISS, E. R. C. (1997). Sexual dimorphism and change in number of neurons in the pelvic ganglion of the rat. *Phd Thesis,* University of London.

BLOOM, W. and FAWCETT, D. W. (1975). *A Textbook of Histology.* Tenth Edition. Saunders. Philadelphia.

BUNGE, M., WOOD, P., TYNAN, L., BATES, M. and SANES, J. (1989). Perineurium originates from fibroblasts: demonstration in vitro with a retroviral marker. *Science* **243,** 229-231.

COOK, R. D. and BURNSTOCK, G. (1976). The ultrastructure of Auerbach's plexus. I. Neuronal elements. *Journal of Neurocytology* **5,** 171-194.

COSTA, M. and FURNESS, J. B. (1973). The origins of the adrenergic fibres which innervate the internal anal sphincter, rectum and other tissues of the pelvic region of the guinea-pig. *Zeitschrift für Anatomie und Entwicklungsgeschichte* **140,** 129-142.

DAIL, W. G. and DZIURZYNSKI, R. (1985). Substance P immunoreactivity in the major pelvic ganglion of the rat. *Anatomical Record* **212,** 103-109.

DAIL, W. G., EVAN, A. P. and EASON, H. R. (1975). The major pelvic ganglion in the pelvic plexus of the male rat; a histochemical and ultrastructural study. *Cell and Tissue Research* **159,** 49-62.

DAIL, W. G., TRUJILLO, D., de la ROSA, D. and WALTON, G. (1989). Autonomic innervation of reproductive organs: Analysis of the neurons whose axons project in the main penile nerve in the pelvic plexus of the rat. *Anatomical Record* **224,** 94-101.

DE LOMOS, C. and PICK, J. (1966). The fine structure of the thoracic sympathetic neurons in the adult rat. *Zeitschrift für Zellforschung und mikroskopische Anatomie* **71,** 189-206.

DETWILER, S. R. (1937). Does the developing medulla influence cellular proliferation within the spinal cord ? *Journal of Experimental Zoology* **77,** 109-122.

DIBNER, M. D. and MYTILINEOU, C. and BLACK, I. B. (1977). Target organ regulation of sympathetic neuron development. *Brain Research* **123,** 301-310.

DIXON, J. S. and GOSLING, J. A. (1974). The distribution of noradrenergic nerves and small intensely fluorescent (SIF) cells in the cat urinary bladder. A light and electron microscope study. *Cell and Tissue Research* **150,** 147-159.

DÖFFLER-MELLY, J. and NEUHUBER, W. L. (1988). Retrospinal neurons : Evidence for a direct projection from the enteric to the central nervous system in the rat. *Neuroscience Letters* **92,** 21-25.

DOUPE, A. J., PATTERSON, P. H. and LANDIS, S. C. (1985). Small intensely fluorescent cell in culture, role of glucocorticoids and growth factors in their development and interconversions with other neural crest derivatives. *Journal of Neuroscience* **5,** 2143-2160.

ECCLES, J. C. (1959). The development of ideas on the synapse. *The Historical Development of Physiological Thought* Edited by C Brooks, Hafner, New York.

ECCLES, J. C. (1964). *The Physiology of Synapses.* Springer-Verlag, Berlin.

EHINGER, B., SUNDLER, F. and UDDMAN, R. (1983). Functional morphology in two parasympathetic ganglia: the ciliary and the pterygopalatine. *Autonomic Ganglia*. Edited by L. G. Elfvin. p. 97-123. Chichester: John Wiley and Sons.

EIKA, B., LEVIN, R. and LONGHURST, P. (1994). Comparison of urinary function in rats with hereditary diabetes insipidus, streptozotocin-induced diabetes mellitus and non-diabetic osmotic diuresis. *Journal of Urology* **151,** 496-502.

EMERY, D. G., FOREMAN, R. D. and COGGESHALL, R. E. (1976). Fiber analysis of the feline inferior cardiac sympathetic nerve. *Journal of Comparative Neurology* **166,** 457-468.

ELBADAWI, A. and SCHENK, E. A. (1966). Dual innervation of the mammalian urinary bladder. A histochemical study of the distribution of cholinergic and adrenergic nerves. *American Journal of Anatomy* **119,** 405-428.

ERÄNKÖ. O. and HÄRKÖNEN. M. (1963). Histochemical demonstration of fluorogenic amines in the cytoplasm of sympathetic ganglion cells of the rat. *Acta Physiologica Scandinavica* **63,** 511-512.

FLEMING, A. (1928). The peripheral innervation of the uterus. *Transactions of the Royal Society (Edinburgh)* **15,** 507-529.

FOREHAND, C. (1985). Density of somatic innervation on mammalian autonomic ganglion cells is inversely related to dendritic complexity and preganglionic convergence. *Journal of Neuroscience* **5,** 3403-3408.

FOROGLOU, C. and WINKLER, G. (1973). Characteristiques du plexus hypogastrique inferieur (pelvien) chez la rat. *Bulletin de l'Association des Anastomistes, Paris* **57,** 853-857.

FUKAI, K. and FUKUDA, H. (1984). The intramural pelvic nerves in the colon of dogs. *Journal of Physiology* **354,** 89-98.

FURSHPAN, E. J. and POTTER, D. D. (1957). Mechanism of nerve-impulse transmission at a crayfish synapse. *Nature* **180,** 342-343.

FURNESS. J. B. and COSTA, M. (1980). Types of nerves in the enteric nervous system. *Neuroscience* **5,** 1-20.

GABELLA, G. (1979). Innervation of the gastrointestinal tract. *International Review of Cytology* **59,** 129-193.

GABELLA, G. (1990). Hypertrophy of visceral smooth muscle. *Anatomy and Embryology* **182,** 409-424.

GABELLA, G. (1995 a). The structural relations between the nerve fibres and muscle cells in the urinary bladder of the rat. *Journal of Neurocytology* **24,** 159-187.

GABELLA, G. (1995 b). Autonomic nervous system. *The Rat Nervous System (Second Edition)* 81-103. Edited by G. Paxinos. San Diego. Academic press.

GABELLA, G. and UVELIUS, B. (1990). Urinary bladder of rat : Fine structure of normal and hypertrophic musculature. *Cell Tissue and Research* **262,** 67-79.

GABELLA, G. and UVELIUS, B. (1992). Effect of decentralization or contralateral ganglionectomy on obstruction-induced hypertrophy of the rat urinary bladder muscle and pelvic ganglion. *Journal of Neurocytology* **22,** 827-834.

GABELLA, G., BERGGREN, T. and UVELIUS, B. (1992). Hypertrophy and reversal of hypertrophy in rat pelvic ganglion neurons. *Journal of Neurocytology* **21,** 649-662.

GERSHON, M. D. (1981). The enteric nervous system. *Annual Reviews of Neuroscience* **4,** 227-272.

GIBBINS, I. L. (1990).Peripheral autonomic nervous system. *In the Human Nervous System,* Edited by G. Paxinos pp. 3-123. San Diego. Academic Press.

GILPIN, S. A., GOSLING, J. A. and BARNARD, R. J. (1985). Morphological and morphometric studies of the human obstructed trabeculated urinary bladder. *British Journal of Urology* **57,** 525-529.

GOEDERT, M., OTTEN, U. and THOENEN, H. (1978). Biochemical effects of antibodies against NGF on developing and differentiating sympathetic ganglia. *Brain Research* **148,** 264-268.

GORIN , D. G. and JOHNSON, E. M. (1979). Experimental autoimmune model of nerve growth factor deprivation. Effects on the developing peripheral sympathetic and sensory neurons. *Proceedings of the National Academy of Sciences* **76,** 5382-5387.

GREENE, E. C. (1963). *Anatomy of the Rat.* Hafner. New York.

HALL, A. K. and LANDIS, S. C. (1991). Principal neurons and small intensely fluorescent cells in the rat superior cervical ganglion have distinct developmental histories. *Journal of Neuroscience* **11,** 472-484.

HAMER , D. W. and SANTER, R. M. (1981). Anatomy and blood supply of the coeliac-superior mesenteric ganglion complex of the rat. *Anatomy and Embryology* **162,** 353-362.

HARDEBO, J. E., SUZUKI, N., EKBLAD, E., and OWAN, C. (1992). Vasoactive intestinal polypeptide and acetylcholine coexist with neuropeptide Y, dopamine-beta-hydroxylase, tyrosine hydroxylase, substance P or calcitonin gene-related peptide in neuronal subpopulations in cranial parasympathetic ganglia of the rat. *Cell and Tissue Research* **267,** 291-300.

HEDGER, J. and WEBBER, R. (1976). Anatomical study of the cervical sympathetic trunk and ganglia in the albino rat (*Mus norvegicus albinus*). *Acta Anatomica* **96,** 206-217.

HENDRY, I. A. (1977). Cell division in the developing sympathetic nervous system. *Journal of Neurocytology* **6,** 299-309.

HENDRY, I. A. and CAMPBELL, J. (1976).Morphometric analysis of rat superior cervical ganglion after axotomy and NGF treatments. *Journal of Neurocytology* **5,** 351-366.

HICKS, R. M. (1975). The mammalian urinary bladder : an accommodating organ. *Biological Reviews of the Cambridge Philosophic Society.* **50,** 215-246.

HICKS, R. M. and KETTERER, B. (1970). Isolation of the plasma membrane of the luminal surface of the rat bladder epithelium, and the occurrence of a hexagonal lattice of subunits both in negatively stained whole-mounts and in sectional membranes. *Journal of Cell Biology* **45,** 542.

HULSEBOSCH, C. E. and COGGESHALL, R. E. (1982). An analysis of the axon populations in the nerves to the pelvic viscera in the rat. *Journal of Comparative Neurology* **211,** 1-10.

INOUE, T. and GABELLA, G. (1990). A vascular network closely linked to the epithelium of the urinary bladder of the rat. *Cell and Tissue Research* **263,** 137-143.

ISOMURA, G., IWATA, S., CHIBA, M. and SHIMUZI, N. (1985). Constitution of the greater splanchnic nerve in the rat. *Anatomischer Anzeiger* **159,** 159-171.

JACOBS, J. M. (1977) Penetration of systemically injected horseradish peroxidase into ganglia and nerves of the autonomic nervous system. *Journal of Neurocytology* **6,** 607-618.

JACOBS, J. M., MACFARLANE, R. and CAVANAGH, J. (1976). Vascular leakage in the dorsal root ganglia of the rat studied with horseradish peroxidase. *Journal of Neurological Sciences* **29,** 95-107.

JACOBSON, M. (1991). *Developmental Neurobiology 3rd edition.* Plenum Press. New York.

KANERVA, L. (1971). Postnatal development of monamines and cholinesterases in the paracervical ganglion of the rat uterus. *Progress in Brain Research* **34,** 433-444.

KANERVA, L. and TERÄVÄINEN, H. (1972). Electron microscopy of the paracervical (Frankenhäuser) ganglion of the adult rat. *Zeitschrift für Zellforschung und mikroskopische Anatomie* **129**, 161-177.

KANERVA, L. and HERVONEN, A. (1976). SIF cells, short adrenergic neurons and vacuolated nerve cells of paracervical (Frankenhauser) ganglion. SIF cells. Structure and function of the small, intensely fluorescent sympathetic cells. *Fogarty International Center Proceedings* **30,** 19-34.

KARNOVSKI, M. and ROOTS, L. (1964). A 'direct coloring' thiocholine method for cholinesterases. *Journal of Histochemistry and Cytochemistry* **12,** 219-221.

KAWATANI, M., SHIODA, S., NAKAI, Y., TAKA, C. and DE GROAT, W. C. (1989). Ultrastructural analysis of enkephalinergic terminals in parasympathetic ganglia innervating the urinary bladder of the cat. *Journal of Comparative Neurology* **288,** 81-91.

KEAST, J. R., KAWATANI, M. and DE GROAT, W. C. (1989). Cholecystokinin has excitatory effects on transmission in vesical ganglia and on bladder contractility in cats. *Proceedings of the Society for Neuroscience* **15,** 630.

KEAST, J. R., BOOTH, A. M. and DE GROAT, W. C.(1989). Distribution of neurons in the major pelvic ganglion of the rat which supply the bladder, colon, or penis. *Cell and Tissue Research* **256,** 105-112.

KEAST, J. R. (1995). Pelvic ganglia. In: *Autonomic Ganglia.* edited by E M Mclachlan p. 445-479.

KING, T. S. and COAKLEY, J. B. (1958). The intrinsic nerve cells of the cardiac atria of mammals and man. *Journal of Anatomy* **92,** 353-376.

KORSCHING, S. and THOENEN, H. (1988). Developmental changes of nerve growth factor levels in sympathetic ganglia and their target organs. *Developmental Biology* **26,** 40-46.

KRUSE, M. N., BRAY, L. A. and DE-GROAT, W. C. (1995) Influence of spinal cord injury on the morphology of bladder afferent and efferent neurons. *Journal of the Autonomic Nervous System* **54,** 215-24.

KURAMOTO, H. and FURNESS, J. B. (1989). Distribution of enteric nerve cells that project from the small intestine to the coeliac ganglion in the guinea-pig. *Journal of the Autonomic Nervous System* **27,** 241-248.

LANDIS, S. C. and FREDIEU, J. R. (1986). Coexistence of calcitonin gene-related peptide and vasoactive intestinal polypeptide in cholinergic innervation of rat sweat glands. *Brain Research* **377,** 177-18.

LANGLEY, J. N. and ANDERSON, H. K. (1895). On the innervation of the pelvic and adjoining viscera. I. The lower portion of the intestine. *Journal of Physiology* **18,** 67-105.

LANGLEY, J. N. and ANDERSON, H. K. (1895). On the innervation of the pelvic and adjoining viscera. II. The bladder. *Journal of Physiology* **19,** 71-84.

LANGLEY, J. N. and ANDERSON, H. K. (1895). On the innervation of the pelvic and adjoining viscera. VII. Anatomical observations. *Journal of Physiology* **20,** 372-406.

LANGLEY, J. N. (1921). *The Autonomic Nervous System,* Part 1. W Heffer and Sons. Cambridge.

LANGWORTHY, O. R. (1965). Innervation of the pelvic organs of the rat. *Investigative Urology* **2,** 491-498.

LE DOUARIN, N. M. and TEILLET, M. A. (1973). The migration of neural crest cells to the wall of the digestive tract in avian embryos. *Journal of Embryology and Experimental Morphology* **30,** 31-48.

LE DOUARIN, N. M. and TEILLET, M. A. (1974). Experimental analysis of the migration of neuroblasts of the autonomic nervous system and of the neuroectodermal mesenchymal derivatives, using a biological marking technique. *Developmental Biology* **41,** 162-184.

LE DOUARIN, N. M., TEILLET, M. A., ZILLER, C. and SMITH, J. (1978). Adrenergic differentiation of cells of the cholinergic ciliary and Remak ganglia in the avian embryo after in vivo transplantation. *Proceedings of the National Academy of Sciences* **75,** 2030-2034.

LE DOUARIN, N. M. (1982). *The Neural Crest.* Cambridge University Press. Cambridge.

LEHMANN, H. J. and STANGE, H. H. (1953). Uber das Vorkommen vakuolenhaltiger Ganglienzellen in Ganglion Cervicale Uteri trachtiger und nichttrantiger Ratten. *Zeitschrift für Zellforschung und mikroskopische Anatomie* **38,** 230-236.

LEVI-MONTALCINI, R. (1964). Growth control of nerve cells by protein factor and its antiserum. *Science* **231,** 105-110.

LEVI-MONTALCINI, R. and BOOKER, B. (1960). Excessive growth of the sympathetic ganglia evoked by a protein isolated from mouse salivary glands. *Proceedings of the National Academy of Sciences* **46,** 373-384.

LICHTMAN, J. W. (1977) The reorganization of synaptic connections in the rat submandibular ganglion during post-natal development. *Journal of Physiology* **273,** 155-177.

MALMGREN, A., UVELIUS, B., ANDERSSON, K. and ANDERSSON, P. (1992). Urinary bladder function in rats with hereditary diabetes insipidus; A cystometrical and in vitro evaluation. *Journal of Urology* **148,** 930-934.

NADELHAFT, I., VERA, P. and STEINBACHER, B. (1993). Hypertrophic neurons innervating the bladder and colon of the streptozotocin-diabetic rat. *Brain Research* **609,** 277-283.

NAWAR, G. (1956). Experimental analysis of the origin of the autonomic ganglia in the chick embryo. *American Journal of Anatomy* **99,** 473-506.

NG, Y.K., WONG, W. C. and LING, E. A. (1992). The intraglandular submandibular ganglion of postnatal and adult rats. II. A morphometric and quantitative study. *Journal of Anatomy* **181,** 249-258.

NORBERG, K. A., RITZEN, M. and UNGERSTEDT, U. (1966). Histochemical studies on a special catecholamine-containing cell type in sympathetic ganglia. *Acta Physiologica Scandinavica* **67,** 260-270.

PAKKENBERG, B. and GUNDERSON, H. J. G. (1988). New steriological method for obtaining unbiased and efficient estimates of total nerve cell number in human brain areas. *Acta Pathologica Microbiologica Immunologica Scandinavica* **97,** 677-681.

PAPKA, R. E. (1990). Some nerve endings in the rat pelvic paracervical autonomic ganglia and varicosities contain calcitonin gene-related peptide and originate from dorsal root ganglia. *Neuroscience* **39,** 459-470.

PAPKA, R. E. and MCNEILL, D. L.(1993). Light and electron microscopic study of synaptic connections in the paracervical ganglion of the female rat: special reference to calcitonin gene-related peptide-, galanin- and tachykinin (substance P and neurokinin A)-immunoreactive nerve fibres and terminals. *Cell and Tissue Research* **271,** 417-428.

PARDINI, B. J., PATEL, K. P., SCHMID, P. G. and LUND, D. D. (1987). Location, distribution and projections of intracardiac ganglion cells in the rat. *Journal of the Autonomic Nervous System* **20,** 91-101.

PATTERSON, P. H. (1978). Environmental determination of autonomic neurotransmitter functions. *Annual Reviews of Neuroscience* **1,** 1-17.

PAWLIKOWSKI, M. (1961). The occurrence of vacuoles in the nerve cells of autonomic ganglia as a sign of neurosecretion. *Polish Medical Science History Bulletin* **4,** 110-112.

PETERS, A., PALAY, S. and WEBSTER, H. D. (1976). The fine structure of the nervous system. *Philadelphia:* W.B. SANDERS.

PICK, J. (1970). *The Autonomic Nervous System* Philadelphia: J.B.Lippincott and Co

PICKERING, B. T., and NORTH, W. G. (1982). Biochemical and functional aspects of magnocellular neurons and hypothalamic diabetes insipidus. *Annals of New York Academy of Science.* **394,** 72-81.

POVER, C. M. and COGGESHALL, R. E. (1991). Verification of the Disector method for counting neurones, with comments on the empirical method. *Anatomical Record* **231,** 573-578.

PURINTON, P. T., FLETCHER, T. F. and BRADLEY, W. E. (1973). Gross and light microscopic features of the pelvic plexus in the rat. *Anatomical Record* **175,** 697-706.

PURVES, D. and HUME, R. I. (1981). The relation of postsynaptic geometry to the number of presynaptic axons that innervate autonomic ganglion cells. *Journal of Neuroscience* **1,** 441-452.

PURVES, D. and LICHTMAN, J. W. (1983). Specific connections between nerve cells. *Annual Reviews of Physiology* **45,** 553-565.

RAEZER, D. M., WEIN, A. J., JACOBOWITZ, D. and CORRIERE, J. N. Jr. (1973). Autonomic innervation of canine urinary bladder: cholinergic and adrenergic contributions and interaction of sympathetic and parasympathetic nervous systems in bladder function. *Urology* **2,** 211-221.

ROBERTSON, J. D. (1953). Ultrastructure of two invertebrate synapses. *Proceedings of the Societies for Experimental Biology and Medicine* **82,** 219-223.

ROGERS, H., KENNEDY, C. and HENDERSON, G. (1990). Characterization of the neurons of the mouse hypogastric ganglion: morphology and electrophysiology. *Journal of the Autonomic Nervous System* **29,** 255-270.

RUBIN, E. (1985 a). Development of the rat superior cervical ganglion: Ganglion cell maturation. *Journal of Neuroscience* **5,** 673-684.

RUBIN, E. (1985 b). Development of the rat superior cervical ganglion: Growth of preganglionic axons. *Journal of Neuroscience* **5,** 685-696.

RUBIN, E. (1985 c). Development of the rat superior cervical ganglion: Initial stages of synapse formation. *Journal of Neuroscience* **5,** 697-704.

SANTER, R. M. and SYMONS, D. (1993). Distribution of NADPH-diaphorase activity in the rat paravertebral, prevertebral and pelvic sympathetic ganglia. *Cell and Tissue Research* **271,** 115-121.

SCHAFFER, T., SCHWAB, M. E. and THOENEN, H. (1983). Increased formation of preganglionic synapses and axons due to retrograde trans-synaptic action of nerve growth factor in the rat sympathetic nervous system. *Journal of Neuroscience* **3,** 1501-1510.

SCHULMAN, C. C., DUARTE-ESCALANTE, O. and BOYARSKY, S. (1972). The ueterovesical innervation: a new concept based on a histochemical study. *British Journal of Urology* **44,** 698-712.

SCHULTZBERG, M.,HOKFELT, T., NILSSON, G., TERENIUS, L., RECHFELD, J. R., BROWN, M., ELDE, R., GOLDSTEIN, M. and SAID, S. (1980). Distribution of peptide and catecholamine containing neurons in the gastrointestinal tract of rat and guinea-pig: Immunohistochemical studies with antisera to substance P, vasoactive intestinal poly-peptide, enkephalins, somatostatin, gastrin/ cholecystokinin, neurotensin, and dopamine- hydroxylase. *Neuroscience* **5,** 689-744.

SENBA, E. and TOHYAMA, M. (1989). Calcitonin gene-related peptide containing autonomic efferent pathways to the pelvic ganglia of the rat. *Brain Research* **449,** 386-390.

SHERRINGTON, C. S. (1906). *The Integrative Action of the Nervous System.* Yale University Press. New Haven.

SMOLEN, A. J. and BEASTON-WIMMER, P. (1986). Dendritic development in rat superior cervical ganglion. *Brain Research* **394,** 245-252.

SMOLEN, A. J. and RAISMAN, G. (1980). Synapse formation in the rat superior cervical ganglion during normal development and after neonatal deafferentation. *Brain Research* **181,** 315-323.

SNELL, R. S. (1958). The histochemical appearances of cholinesterase in the parasympathetic nerve supplying the submandibular and sublingual salivary glands of the rat. *Journal of Anatomy* **92,** 534-543.

SNELL, R. S. (1987). *Clinical Neuroanatomy for Medical Students (2nd Edition).* Little, Brown and Company. New York.

SNIDER, W. D. (1988). Nerve growth factor enhances dendritic arborization of sympathetic ganglion cells in developing mammals. *Journal of Neuroscience* **8,** 2628-2634.

SOKOL, H.W. and VALTIN, H. (1982). Homozygous Brattleboro rats lack normal nephron heterogeneity as a consequence of their urine concentrating defect. *Annals of the New York Academy of Science.* **394,** 1-828.

SONNEMANS, M. S., EVANS, D. A., BURBACH, J. P. and VAN-LEEUWEN, F.W. (1996). Immunocytochemical evidence for the presence of vasopressin in inidentified asiate sized neurosecretory granules of solitary neurohypophyseal terminals in the homozygous Brattleboro rat. *Neuroscience* **72,** 225-31.

SPEAKMAN, M. J., BRADING, A. F., GILPIN, C. J., DIXON, J. S., GILPIN, S. A. and GOSLING, J. A. (1987). Bladder outflow obstruction – a cause of denervation super-sensitivity. *Journal of Urology* **138,** 1461-1466.

STEERS, W. D., KOLBECK, S., CREEDON, D. and TUTTLE, J. B. (1991). Nerve growth factor in the urinary bladder of the adult regulates neuronal form and function. *Journal of Clinical Investigation* **88,** 1709-15

STEERS, W. D., CIAMBOTTI, J., ERDMAN, S. and DE GROAT, W. C. (1990). Morphological plasticity in efferent pathways to the urinary bladder of the rat following urethra obstruction. *Journal of Neuroscience* **10,**1943-53.

STERIO, D. C. (1984). The unbiased estimation of number and sizes of arbitrary particles using the Disector. *Journal of Microscopy* **134,** 127-136.

SUZUKI, N. and HARDEBO, J. E. (1991). The pathway of parasympathetic nerve fibres to the cerebral vessels from the otic ganglion in the rat. *Journal of the Autonomic Nervous System* **36,** 39-46.

SUZUKI, N., HARDEBO, J. E. and OWMAN, C. (1988). Origins and pathways of cerebrovascular vasoactive intestinal polypeptide-positive nerves in the rat. *Journal of Cerebral Blood Flow and Metabolism* **8,** 697-712.

TABATABAI, M., BOOTH, A. M. and DE GROAT, W. C. (1986). Morphology and electrophysiological properties of pelvic ganglion cells in the rat. *Brain Research* **382,** 61-70.

TELLO, J. F. (1925). Sur la formatiom des chaines primaries et secondaries du grand sympathique dans l'embryon de poulet. *Trabajos del Laboratorio de Investigaciones Biologicas de la Universidad de Madrid* **23,** 1-28.

VALTIN, H. and SCHROEDER, H. A. (1964). Familial hypothalamic diabetes insipidus in rats (Brattleboro strain). *American Journal of Physiology* **206,** 425-430.

VALTIN, H., SAWYER, W. and SOKOL, H. (1965). Neurohypophysial principles in rats homozygous and heterozygous for hypothalamic diabetes insipidus (Brattleboro strain). *Endocrinology* **77,** 701 -706.

VALTIN, H., NORTH, W., La ROCHELLE, F., SOKOL, H. and MORRIS, J. (1978). Enzymatic interconversions of neurophysins. The nature of enzyme(s) with in neurosecretory granules of the neurohypophysis. *Proceedings of the 7th International Congress of Nephrology Basel.* 43-52. (Karger, Basel 1978).

VAN CAMPENHOUT, E. (1930 a). Historical survey of the development of the sympathetic nervous system. *Quarterly Review of Biology* **5,** 23-50; 217-234.

VAN CAMPENHOUT, E. (1930 b). Contributions to the problem of the development of the sympathetic nervous system. *Journal of Experimental Zoology* **56,** 295-320.

VAN CAMPENHOUT, E. (1931). Le developpement du systeme nerveux sympathique chez le poulet. *Archives de Biologie (Paris)* **42,** 479-507.

VAN DRIEL, C. and DRUKKER, J. (1973). A contribution to the study of the architecture of the autonomic nervous system of the digestive tract of the rat. *Journal of Neural Transmission* **34,** 301-320.

VOYVODIC, J. (1987). Development and regulation of dendrites in the rat superior cervical ganglion. *Journal of Neuroscience* **71,** 904-917.

WANG, B. R., SENBA, E. and TOHYAMA, M. (1990). Met^{5}-enkephalin-Arg^{6}-Gly^{7}-Leu^{8}- like immunoreactivity in the pelvic ganglion of the male rat: a light and electron microscopic study. *Journal of Comparative Neurology* **293,** 26-38.

WOOD, J. D. (1981). Physiology of the enteric nervous system. *In "Physiology of the Gastrointestinal Tract"* pp 1-37, Edited by L. R. Johnson. Raven. New York.

WIGSTON, D. J. (1983). Maintenance of cholinergic neurons and synapses in the ciliary ganglion of aged rats. *Journal of Physiology* **344,** 223-231.

WRIGHT, L. L. (1995). Development and sexual differentiation of sympathetic ganglia. In: *Autonomic Ganglia.* Edited by E McLachlan.

WRIGHT, L. L., CUNNINGHAM, T. J. and SMOLEN, A. J. (1983). Developmental neuronal death in the rat superior cervical ganglion. Cell counts and ultrastructure. *Journal of Neurocytology* **1,** 739-750.

YAMAUCHI, A. and LEVER, J. D. (1971) Correlations between formol fluorescence and acetylcholinesterase (AChE) staining in the superior cervical ganglion of normal rat, pig and sheep. *Journal of Anatomy* **110,** 435-443.

YNTEMA, C. L. and HAMMOND, W. S. (1947). The development of the autonomic nervous system. *Biological Review* **22,** 344-359.